VOLUME 117 NUMBER 2

THE ASTROPHYSICAL JOURNAL

AN INTERNATIONAL REVIEW OF SPECTROSCOPY AND ASTRONOMICAL PHYSICS

Founded in 1895 by GEORGE E. HALE *and* JAMES E. KEELER

Edited by

S. CHANDRASEKHAR
Managing Editor

GERARD P. KUIPER
Associate Editor

Yerkes Observatory of the University of Chicago

H. W. BABCOCK (1953-57)
Mount Wilson Observatory of the Carnegie Institution of Washington

FRED L. WHIPPLE (1952-54)
Harvard College Observatory

G. HERZBERG (1952-56)
National Research Council, Ottawa

C. D. SHANE (1952-55)
Lick Observatory, University of California

LYMAN SPITZER, JR. (1952-53)
Princeton University Observatory

MARCH 1953

SPECTRAL CLASSIFICATION OF THE HIGH-VELOCITY STARS . . . *Philip C. Keenan and Geoffrey Keller* 241

EXPANDING MOTIONS IN THE LACERTA AGGREGATE . . . *A. Blaauw and W. W. Morgan* 256

SOME REMARKS ON THE SPATIAL AND KINEMATIC STRUCTURE OF THE PLANETARY NEBULA IC 418 . . . *O. C. Wilson* 264

A PECULIARITY OF THE SPECTRUM OF PI PEGASI . . . *Jesse L. Greenstein* 269

A NEW DETERMINATION OF THE SPECTROGRAPHIC ORBIT OF CAPELLA . . . *Otto Struve and Ruth F. Kilby* 272

THE SPECTRA OF NOVAE NEAR MINIMUM . . . *Dean B. McLaughlin* 279

ERUPTIVE PROMINENCE ASSOCIATED WITH LIMB FLARE OF MAY 8, 1951 . . . *Thomas J. Bartlett, Bruno Witte, and Walter Orr Roberts* 292

COMPTON SCATTERING BY ELECTRONS WITH A MAXWELLIAN DISTRIBUTION OF THERMAL VELOCITIES . . . *Frank N. Edmonds, Jr.* 298

CONVECTIVE CORES IN STARS . . . *Peter Naur and Donald E. Osterbrock* 306

ON THE SUN'S INTERIOR . . . *I. Epstein and L. Metz* 311

THE UNIVERSITY OF CHICAGO PRESS
CHICAGO, ILLINOIS, U.S.A.

March 1953 Vol. 117, No. 2

THE ASTROPHYSICAL JOURNAL

AN INTERNATIONAL REVIEW OF SPECTROSCOPY AND ASTRONOMICAL PHYSICS

Published in Collaboration with the American Astronomical Society

S. CHANDRASEKHAR
Managing Editor

GERARD P. KUIPER
Associate Editor

Yerkes Observatory of the University of Chicago

EDITORIAL BOARD

H. W. BABCOCK (1953-57)
Mount Wilson Observatory of the Carnegie Institution of Washington

G. HERZBERG (1952-56)
National Research Council, Ottawa

FRED L. WHIPPLE (1952-54)
Harvard College Observatory

C. D. SHANE (1952-55)
Lick Observatory, University of California

LYMAN SPITZER, JR. (1952-53)
Princeton University Observatory

The Astrophysical Journal is published bimonthly by the University of Chicago at the University of Chicago Press, 5750 Ellis Avenue, Chicago 37, Illinois, during January, March, May, July, September, and November. ¶Two volumes are published per year, one beginning with the January issue and the other beginning with the July issue. The subscription price is $6.00 per volume or $12.00 per year; the price of single copies is $3.00. (Orders for service of less than a volume will be charged at the single copy rate.) ¶Postage is prepaid by the publishers on all orders from the United States and its possessions. No extra charge is made for postage to countries in the Pan American Postal Union. ¶Postage is charged extra as follows: for Canada, 20 cents per volume, 40 cents per year (total $6.20 per volume, $12.40 per year); on single copies 5 cents (total $3.05); for all other countries in the Postal Union, 40 cents per volume, 75 cents per year (total $6.40 per volume, $12.75 per year), on single copies 10 cents (total $3.10). ¶Subscriptions are payable in advance. Please make all remittances payable to The University of Chicago Press, in United States currency or its equivalent by postal or express money orders or bank drafts.

The following is an authorized agent:

For the British Empire, except North America and Australasia: The Cambridge University Press, Bentley House, 200 Euston Road, London, N.W. 1, England. Prices of yearly subscriptions and of single copies may be had on application.

Claims for missing numbers should be made within the month following the regular month of publication. The publishers expect to supply missing numbers free only when losses have been sustained in transit, and when the reserve stock will permit.

Business correspondence should be addressed to The University of Chicago Press, Chicago 37, Illinois.

Communications for the editors and manuscripts should be addressed to: S. Chandrasekhar, Editor of THE ASTROPHYSICAL JOURNAL, Yerkes Observatory, Williams Bay, Wisconsin.

Line drawings and photographs should be made by the author, and all marginal notes such as co-ordinates, wave lengths, etc., should be included in the cuts. It will not be possible to set up such material in type.

One copy of the corrected galley proof should be returned as soon as possible to the editor, Yerkes Observatory, Williams Bay, Wisconsin. Authors should take notice that the manuscript will not be sent to them with the proof.

The cable address is "Observatory, Williamsbay, Wisconsin."

The articles in this journal are indexed in the *International Index to Periodicals*, New York, N.Y.

Applications for permission to quote from this journal should be addressed to The University of Chicago Press, and will be freely granted.

Microfilms of complete journal volumes are available to regular subscribers only and may be obtained at the end of the year. Orders and inquiries should be addressed to University Microfilms, 313 North First Street, Ann Arbor, Michigan.

Notice to subscribers: If you change your address, please notify us and your local postmaster immediately.

Entered as second-class matter, July 31, 1940, at the Post-Office at Chicago, Ill., under the Act of March 3, 1879.
Acceptance for mailing at special rate of postage provided for in United States Postal Act of October 3, 1917, Section 1103, amended February 28, 1925.

[PRINTED IN U.S.A.]

THE ASTROPHYSICAL JOURNAL

AN INTERNATIONAL REVIEW OF SPECTROSCOPY AND ASTRONOMICAL PHYSICS

VOLUME 117 MARCH 1953 NUMBER 2

SPECTRAL CLASSIFICATION OF THE HIGH-VELOCITY STARS*

PHILIP C. KEENAN AND GEOFFREY KELLER
Perkins Observatory
Received October 1, 1952

ABSTRACT

Spectral types and absolute magnitudes are determined for 108 suspected high-velocity stars; 83 of these are accepted as probable members of the high-velocity group defined by a minimum space motion of 85 km/sec.

In their distribution over the spectrum-luminosity diagram, these stars appear to be intermediate between normal low-velocity stars and the stars which are members of globular clusters.

For stars of types G and K the spectral peculiarities associated with high velocity are termed the "cyanogen discrepancy" for convenience and are evaluated by several criteria, of which the most sensitive is the line ratio 4172/4216 in the range from G6 to K4. Stars of a given type and luminosity show a considerable range of values of the cyanogen discrepancy, which accordingly appears as an additional variable of classification.

I. THE PROBLEM OF CLASSIFICATION

The construction of a spectrum-luminosity diagram for the stars with high space velocities involves difficulties peculiar to these objects. In the first place, the course of the giant branch cannot be directly established by trigonometric parallaxes, for in the entire northern sky there are only about five giants and subgiants which have both accurately known parallaxes and large space velocities. At the same time, the very definition of the high-velocity group rules out most of the usual statistical methods of finding mean distances by the use of radial or tangential velocities. Such methods assume that the peculiar motions have small dispersion and (usually) random distribution—conditions which are known to be violated when the stars are selected by their high speeds.

For these reasons the present investigation attacks the problem by direct spectroscopic estimates of the luminosities of stars belonging to the group. This method is also open to objection, for the spectra of the high-velocity stars are known to exhibit peculiarities in the strengths of some of the features which are normally used as criteria of classification. The more serious effects are the general weakening of the lines of hydrogen and the metals in spectra of types F5–G5,[1] and the marked weakening of the bands of

* *Contributions of the Perkins Observatory*, No. 34.

[1] N. G. Roman, *Ap. J.*, **112**, 554, 1950.

CN in types G8–K3.[2] The change in absorption within the λ 4216 band affects the intensities of most of the metallic lines between 4143 A and 4216 A.

The essential question is whether criteria can be found in which the effects of the high-velocity peculiarities are either very slight or tend to counterbalance one another. Examination of the spectra of the near-by standard stars of high velocity (listed in Table 1) showed that these requirements are met by the following spectral features:

1. Ratios *Hδ*/*Ca* 4226, *Hγ*/4325, and strength of the G band. Useful for assigning types in the range F5–K0. In stars later than G5 some weight is given also to the absolute intensities of the metallic lines.

2. Ratios *Cr* 4254/*Fe* 4250 and *Fe* 4260. Useful for assigning types in the range G8–K5.

3. Absolute intensities of the *TiO* bands. Define subdivisions of type M.

4. Ratios *Sr* II 4077/*Fe* 4045, *Fe* 4063, and *Fe* 4071. Useful for estimating luminosities in the range F5–M5.

TABLE 1

HIGH-VELOCITY STARS AT KNOWN DISTANCES

Star	m_v	Parallax (ρ)	Source of Parallax	M_v	Type	Space Velocity (Km/Sec)
μ Cas	5.26	0".136	Trig.	+5.9	G5 V+	145
γ Leo A	2.61	.017	Trig.+dyn.	−1.2	K0 III−	113
γ Leo B	3.80	.017	Trig.+dyn.	0.0	G7 III+	113
HR 4550	6.46	.116	Trig.	+6.8	G7 V+	290
α Boo	0.24	.090	Trig.	0.0	K1 III	103
HD 135204	7.5	.056	Trig.	+6.2	G8 V	108
31 Aql	5.23	.059	Trig.	+4.1	G8 IV	120
η Cep	3.59	.071	Trig.	+2.7	K0 IV	87
61 Cyg A	5.57	0.292	Trig.	+7.9	K5 V	88

5. Ratio 4172/4185. Each of these two absorption features is a blend of several atomic lines and lies within the area affected by the 4216 *CN* bands. Nevertheless, their ratio remains a useful criterion of luminosity in the range G5–K2. In using this criterion, correction must be made for the slightly enhanced intensity of 4172 in the high-velocity stars.

The first four of the above criteria are well known and are generally employed in the classification of normal stars. It should always be remembered that all these criteria were chosen for their applicability to spectrograms with scales ≈ 100 A/mm. If one wishes to classify high-velocity stars on plates differing greatly from this moderately low dispersion, the criteria must be re-examined.

II. OBSERVATIONAL MATERIAL

The spectrograms employed in this investigation were taken with the two-prism spectrograph on the 69-inch reflector during the period July, 1948, to August, 1952. About 25 per cent of the spectrograms were made with the P*β* camera, which gives a scale of 54 A/mm at *Hγ*; but, after it was found that the images obtained with the new PG*γ* camera (scale 104 A/mm at *Hγ*) were very satisfactory for classification, the remainder of the program was carried out with this camera. For the great majority of the suspected high-velocity stars on the program, at least two good spectrograms of each were obtained. Altogether, more than 240 spectrograms of the program stars were judged

[2] Morgan, Keenan, and Kellman, *An Atlas of Stellar Spectra* (Chicago: University of Chicago Press, 1943), Pl. 45.

satisfactory for classification and were compared with several hundred comparison spectrograms of standard stars with either MKK types from the *Atlas of Stellar Spectra* or additional types on the same system.

The observing list for the high-velocity group was made up chiefly of stars with estimated space motions in Miczaika's catalogue[3] exceeding 80 km/sec, or with radial velocities exceeding 60 km/sec if the space velocity had not previously been estimated. The published radial velocities of Moore's catalogue,[4] Redman,[5] Shajn and Albitzky,[6] Joy and Wilson,[7] and Moore and Paddock[8] were drawn upon. The stars chosen were mostly brighter than the eighth visual magnitude and north of $-20°$ declination. Stars earlier than F0, variable stars, and *CH* stars, for all of which the spectroscopic criteria of luminosity are of doubtful validity, were excluded. Although no claim of completeness even within these limits is made, the group chosen appears to be representative of the brighter nonvariable stars with relatively large space motions.

Of this group, the spectra of 108 stars proved suitable for classification, and spectral types and luminosity classes were assigned. The quality of the plates permitted interpolation to about a third of a subdivision in both co-ordinates. The luminosity classes were then converted to visual absolute magnitudes by means of the reduction table given by Keenan and Morgan.[9] This table was constructed chiefly from data for stars having normally low velocities, and its application to the luminosity classes defined by the slightly different criteria of the high-velocity stars might be expected to lead to some systematic errors in the derived absolute magnitudes. For this reason it is important to take into account every bit of evidence which might give clues to the detection of such systematic effects.

The first check on the luminosities of the giant branch was furnished by the 21 high velocity giants and subgiants with apparent magnitudes between 3.5 and 5.5 and types later than G0. The trigonometric parallaxes of these stars are not large enough to define their individual distances precisely, but the group mean should be significant. The mean trigonometric parallax of the group, reduced to the fourth magnitude, is $0''.031$. The mean spectroscopic reduced parallax is $0''.027$, giving a difference $\bar{P}_s - \bar{P}_t = -0''.004$ with a mean error of $\pm 0''.0031$. The difference implies that our spectroscopic estimates make the luminosity too bright by 0.3 mag. Since, however, the difference is comparable to its error and nearly all the negative excess comes from the two stars η Sct and 31 Aql, we do not feel justified in applying any systematic correction. Rather, the comparison suggests that the spectroscopic absolute magnitudes of the high-velocity stars are comparable in accuracy to those of normal low-velocity stars. We shall, therefore, assume a probable error of 0.8 mag. in discussing the observations.

This comparison with the trigonometric data serves to confirm the luminosity scale for absolute magnitudes up to $M_v \approx 0$, but says very little about any stars which may lie above the middle of the usual giant branch. The possible existence of such objects among the high-velocity stars bears upon the question of their relationship to the members of globular clusters. Both groups have been generally considered as belonging to population type II, as defined by Baade,[10] particularly since Popper[11] noted some similarities in their spectral peculiarities on his low-dispersion plates.

[3] *A.N.*, **270**, 249, 1940.
[4] *Pub. Lick Obs.*, Vol. **18**, 1932.
[5] *Pub. Dom. Ap. Obs. Victoria*, **6**, 27, 1931.
[6] *M.N.*, **92**, 771, 1932.
[7] *Ap. J.*, **111**, 221, 1950.
[8] *Ap. J.*, **112**, 48, 1950.
[9] *Astrophysics: A Topical Symposium* (New York: McGraw-Hill Book Co., 1950), chap. ii.
[10] *Ap. J.*, **100**, 137, 1944; *Mt. W. Contr.*, No. 696.
[11] *Ap. J.*, **105**, 204, 1947.

Spectrograms of several of the brightest stars in M3 and M92, taken on a scale of 38 A/mm, have been discussed by Baum,[12] and these plates were made available to us for comparison with the material on the high-velocity stars.[13] The cluster spectra showed peculiarities, such as the weakening of *CN* and metallic lines, developed to a much greater degree than in the spectra of high-velocity stars. Judged by the distance moduli given by Baum, the values of M_v for these most luminous cluster members must be close to -3.

The comparison of the plates established the fact that no stars very similar to these are included among the high-velocity objects studied here. The two stars from the Perkins list which were assigned the highest luminosity are HR 965 ($M_v = -1.5$:) and HR 1908 ($M_v = -2.5$); and each of these has much closer spectroscopic resemblance to ordinary supergiants of low velocity than to the bright cluster stars. Thus the classification of even the brightest high-velocity stars should not be greatly in error, though additional comparisons with somewhat fainter cluster stars should be made whenever spectrograms of the latter can be obtained.[14] One modification in the criteria of luminosity has already been indicated by the cluster spectra, which show that in such objects the intensity of *Sr* II 4077 does not continue to increase with luminosity as rapidly as in standard supergiants. At least an incipient effect of this sort might be looked for in those high-velocity stars which show the characteristic peculiarities most strongly. Accordingly, we have taken into account other criteria, such as the intensity of the G band and the ratio 4376/4383, which begin to become sensitive at the higher luminosities, in classifying any high-velocity stars which are suspected of being brighter than an average giant. The resulting changes in assigned luminosities never amounted to more than a few tenths of a magnitude.

The spectroscopic absolute magnitudes of the high-velocity stars, given in column 6 of Tables 2 and 3, are the spectroscopic values except for the near-by stars. Trigonometric parallaxes (designated by "t") are given when they exceed 0".060 and for a few F- and G-type dwarfs in which the weakening of the metallic lines is so pronounced that no reliable spectroscopic estimates of luminosity could be made. If the mean of the spectroscopic and trigonometric parallaxes lay in the range between 0".020 and 0".059, this mean is given in the tables, followed by the symbol "s, t." Thus the adopted parallaxes and absolute magnitudes in Tables 2 and 3 differ in a few cases from the trigonometric values of the calibration stars in Table 1.

There is also the possibility of errors in the assignment of types. For the stars later than G5 there is no reason to expect appreciable errors, for the relative intensities of lines of the several metals give consistent results. For the earlier stars there is a more serious possibility of systematic effects, since there is evidence that the hydrogen lines are enhanced relative to the metallic lines.[14a] When the Balmer lines are used for classification, the resulting type is too early as compared to the type obtained from relative intensities of metallic lines or from color temperatures. The effect is greatest in the small group of high-velocity dwarfs which have sometimes been assigned to type A, but for which later types are indicated by their colors and by analyses of their atmospheres.[15] Of these stars only HD 140283 is included in Table 2, since the luminosities of the others are uncertain. For HD 140283 the trigonometric parallax of 0".03 has been used, together with the type A8.[16]

[12] *A.J.*, **57**, 222, 1952.

[13] We are greatly indebted to Dr. Baum and to Dr. O. C. Wilson for sending these plates for examination.

[14] The importance of such comparisons has been particularly emphasized by Dr. Baade in discussions with the authors.

[14a] M. and B. Schwarzschild, *Ap. J.*, **112**, 248, 1950; cf. also the notes to Table 2 following.

[15] Chamberlain and Aller, *Ap. J.*, **114**, 52, 1951.

[16] Dr. J. L. Greenstein has kindly made available his unpublished estimate that the relative intensities of lines on coudé spectrograms of this star indicate a type within the range A6–F0.

TABLE 2

NON-VARIABLE HIGH-VELOCITY STARS

Star	α(1950)	δ(1950)	m_v	Type	M_v	p	V	W_o	$W_o - r_w$
HD 26	0^h02^m8	+ 8°30'	8.2	G4p ?			-213		
HD 2901	0 30.0	+53 51	7.10	K2 III	+0.3	.0044 s	-107	131	129
€ And	0 35.9	+29 02	4.52	G5 III+	+1.6	.026 s,t	- 84	103	88
HD 5780	0 56.8	+ 0 31	7.78	K5 II-III	-1.4	.0015 s	-103	348	290
HR 316	1 04.0	+56 40	6.58	K2 III+	+0.8	.0069 s	- 94	133	106
μ Cas	1 04.9	+54 41	5.26	G5 V+	+5.5	.136 t	- 97	145	141
HD 6755	1 06.5	+61 17	7.8	F8 V	+4.1:	.018 s	-325	352	325
HD 6833	1 07.2	+54 28	7.10	G8 III	+0.3	.0043 s	-257	259	257
HR 375	1 16.1	+77 18	6.38	G5 III+	+1.1	.0087 s	- 73	90	74
HR 452	1 32.9	+40 49	6.39	K1 III	+0.6	.0069 s	+ 66	105	82
56 And	1 53.2	+37 00	5.82	G8 III+	+0.9	.0105 s	+ 59	91	72
HR 645	2 10.3	+50 50	5.40	G8 III:	+0.3	.0095 s	+ 28	176	113
27 Ari	2 28.1	+17 29	6.41	G5 III-IV	+1.8	.012 s	-117	126	123
HD 16397	2 35.5	+30 36	7.21	G0 V	+4.6	.030 s,t	-100	145	119
HR 965	3 20.1	+84 44	5.78	G3p:II	-1.5:	.0035 s	+ 33	188:	122
HD 21910	3 32.7	+74 36	7.60	G8 III+	+1.0	.0048 s	-104		
14 Tau	3 40.9	+19 31	6.34	G8 III	+0.3	.0063 s	+ 78	110	85
HD 23841	3 45.8	+ 9 30	6.95	K1 III	+0.1	.0043 s	- 80	119	101
HD 28424	4 26.7	+13 47	7.76	K1 III+	+0.4:	.0033 s	+ 94	236	
40 φ^2 Ori	5 34.2	+ 9 16	4.39	G6 III-IV	+1.6	.027 s,t	+ 99	94	87
HR 1908	5 34.3	+11 00	6.10	K4 II	-2.5	.0019 s	-119	173	141
δ Lep	5 49.2	-20 53	3.90	G8+ III	+0.3	.019 s	+ 99	185	128
HR 2065	5 52.4	-11 47	5.81	K3+ III-	-1.0:	.0043 s	+ 87	110	102
HR 2153	6 04.9	+41 04	6.42	G9 III+	+0.9	.0080 s	- 86	94	80
⊖ CMa	6 51.9	-11 58	4.25	K3+ III	+0.6	.018 s,t	+ 97	85	81
32 ν^3 Cnc	8 30.0	+24 15	6.41	K0 III	0.0	.0052 s	+ 75	90	74
HR 3578	8 56.4	-15 56	5.92	F6 V	+3.2	.029 s,t	+122	126	118
HD 77236	8 58.7	- 2 22	7.87	K0 III	+0.2	.0029 s	+142	130	129
HD 77408	9 00.2	+33 05	7.08	F6 IV	+2.9	.0144 s	+ 70	139	99
HD 81192	9 21.9	+20 00	6.67	G7 III+	+0.6	.0061 s	+136	161	140
ɣ Leo A	10 17.2	+20 06	2.61	K0 III-	-1.2	.017 t,d	- 37	113	77
ɣ Leo B	10 17.2	+20 06	3.80	G7 III+	0.0	.017 t,d	- 37	113	77
HD 94028	10 48.8	+20 33	8.1	F4 V+:	+3.8:	.014: s	+ 62	180	175
HD 94190	10 51.3	+77 21	7.04	M3 III-	-1.0	.0025 s	- 90	87	80
75 Leo	11 14.7	+ 2 17	5.44	M0 III+	+0.4	.0098 s	- 59	96	76
HD 100041	11 28.3	+28 44	7.00	M3 III+	0.0	.0040 s	+ 85	121	99
HR 4550	11 50.1	+38 05	6.46	G7 V+	+6.8	.116 t	- 98	290	286
HR 4609	12 02.7	+77 11	5.96	G9 III	+0.2	.0070 s	- 19	131	83
HR 4657	12 12.6	-10 01	6.12	F5 V	+3.4	.029 s,t	+ 6	165	104
16 Vir	12 17.8	+ 3 35	5.10	K1 III+	+0.5	.012 s	+ 36	106	72
HD 107760	12 20.1	+73 31	8.2	G7 V	+5.7	.032 s,t	- 98	92	89
HD 108910	12 28.1	- 3 47	7.06	K3+ III	0.0	.0039 s	+ 84	111	95
33 Vir	12 43.3	+ 9 53	5.86	K1 III-IV	+1.9	.0159 s	+ 51	169	114
HR 5102	13 30.4	+24 36	6.18	G8 III	+0.5	.0073 s	+ 7	141	90
87 Vir	13 44.2	-17 34	5.79	M2+ III-	-0.9	.0048 s	+ 63	105	82
α Boo	14 13.4	+19 27	0.24	K1 III	0.0	.090 t	- 5	103	97
HR 5455	14 34.3	-12 06	6.24	F5 V	+3.5	.032 s,t	- 70	146	101
HR 5464	14 36.3	+43 51	5.92	K2 III	0.0	.0065 s	- 48	118	78
11 Lib	14 48.2	- 2 05	5.05	G8+ III-	-0.5	.0077 s	+ 83	149	116
HD 134063	15 05.1	+22 45	7.7	G5 III+	+1.2	.0050 s	-108		
HD 134088	15 05.5	- 7 43	8.1	G0 V:	+4.4	.018 s	- 59	123	119
HD 135204	15 11.4	- 1 09	6.7:	G8 V	+5.5	.058 s,t	- 70	114	108
5 Ser	15 16.7	+ 1 57	5.18	F8 III-IV	+2.6	.030 s,t	+ 54	122	91
HD 140283	15 40.4	-10 46	7.26	A8 V	+4.7	.031 t	-170	231	203
HR 6014	16 06.7	+ 6 31	6.02	K1+ III-IV	+2.6	.021 s,t	- 3	163	103
HR 6128	16 25.0	- 7 29	5.45	M2+ III:	-1.0	.0051 s	+100	180	152
HD 148816	16 28.0	+ 4 18	7.45	F8 V+	+4.5	.026 s,t	- 52	256	161
48 Her	16 47.3	+30 02	6.68	K1 II-III	-1.5	.0023 s	- 43	205	131
HR 6286	16 51.9	+47 30	6.30	K2 III	0.0	.0055 s	- 62	96	70
HR 6364	17 04.2	+22 09	5.72	K3+ III	-0.2	.0066 s	- 96	107	88

TABLE 2 - Continued

NON-VARIABLE HIGH-VELOCITY STARS

Star	α(1950)	δ(1950)	m_v	Type	M_v	p	V	W_o	W_o-r_w
HD 157089	$17^h18.^m6$	+ 1°29'	6.96	F9 V	+4.5	.032 s,t	-162	152	146
HD 162756	17 50.3	- 7 54	7.60	G0 IV-V	+3.8	.018 s	-125	140	121
HD 165401	18 03.2	+ 4 39	6.83	G0 V	+4.8	.040 s,t	-124	109	106
HR 6840	18 14.2	- 3 01	6.11	G3 III-	-0.3:	.0053 s	+ 1	240	152
HR 6853	18 15.5	+40 54	6.10	G8 III	+0.5	.0076 s	- 74	125	88
35 ν^1Sgr	18 52.0	-22 44	5.04	K3+p		.037 t	-110		
31 Aql	19 22.5	+11 50	5.23	G8 IV	+3.8	.052 s,t	-100	120	96
α Vul	19 26.7	+24 34	4.63	M0+ III	-0.4	.010 s	- 86	106	82
HD 184499	19 31.6	+33 05	6.61	G0 V	+4.3	.035 s,t	-162	161	155
HR 7523	19 43.1	+40 36	6.44	M3 III	-0.5	.0041 s	- 96	101	85
HR 7680	20 03.0	+15 21	6.56	M2+ III-	-0.9	.0032 s	-110:	103	94
HD 191046	20 03.6	+36 05	7.17	G9 III+	+0.6	.0048 s	-100		
HD 195019	20 26.0	+18 36	6.85	G3 IV-V	+4.2	.0295 s	- 93	89	81
HR 7841	20 28.3	+45 45	6.59	K2+ III:	0.0:	.0048:s	- 31	158	100
η Cep	20 44.3	+61 39	3.59	K0 IV	+2.8	.071 t	- 87	87	85
HD 199191	20 51.9	+54 20	7.16	G8 III+	+0.9	.0055 s	-195	233	195
61 Cyg A	21 04.7	+38 30	5.57	K5 V	+7.9	.292 t	- 65	89	88
61 Cyg B	21 04.7	+38 30	6.28	K6 V	+8.6	.292 t	- 63	88	87
HR 8165	21 18.8	+23 38	5.82	K1 III	+0.1	.0071 s	- 89	180	125
HR 8325	21 44.1	+25 19	6.48	K3- III-III+	+0.4	.0061 s	- 45	123	81
HD 213893	22 32.0	+ 0 20	7.02	K5+ III	-0.3	.0034 s	- 89	136	104
γ Psc	23 14.6	+ 3 01	3.85	G5 III	+0.7	.023 s,t	- 13	140	89
HR 8875	23 17.3	+48 05	6.35	K1 III+	+0.5	.0068 s	+ 23	133	86
14 And	23 28.8	+38 58	5.34	K0 III+	+0.7	.012 s	- 59	111	79
HD 221830	23 33.0	+30 44	6.72	F9 V	+4.4	.035 s	-103	119	103

Remarks on the Spectra

HD 26 Very peculiar; similar to CH stars.
HD 2901 CN weak; H_δ, H_γ, 4172 slightly strong.
ϵ And Most lines weak; CN weak; 4172 and CH strong.
HD 5780 CN slightly weak; 4143 strong.
HR 316 Normal except 4172 slightly strong; 4352 strong.

HD 6755 Atomic lines very weak; CH strong. Classified from Mt. Wilson spectrograms.
HD 6833 CN quite weak; 4172 strong.
HR 375 CN slightly weak; 4172 and CH strong.
HR 452 H_δ slightly strong.
56 And CN slightly weak? 4172 slightly strong.

HR 645 CN strong.
27 Ari 4172 slightly strong.
HR 965 CH strong; CN and 4077 consistent in indicating luminosity class II.
HD 21910 4172 slightly strong. No proper motion published.
14 Tau 4172 strong.

40 ϕ^1 Ori Atomic lines and CN weak.
HR 1908 CN slightly weak: 4172 strong.
δ Lep CN weak; 4172 slightly strong.
HR 2065 CN slightly weak.
ρ CMa CN weak; 4172 slightly strong?

32 ν^2 Cnc CN strong.
HR 3578 Weak lines.
HD 77236 CN weak; H_δ, 4172, 4143 strong.
HD 81192 PGC 2527. CN and metallic lines weak; 4172 slightly strong.
γ Leo A CN slightly weak; 4143 strong.

γ Leo B CN slightly weak; 4172 slightly strong.
HR 4550 Groombridge 1830. Normal dwarf spectrum except that CH may be slightly weak.
HR 4609 CN slightly weak; 4172, H_δ slightly strong; 4143 strong.
16 Vir CN slightly weak; 4172 strong.
HD 108910 CN weak.

TABLE 2 - Continued

Remarks on the Spectra

33 Vir	CN weak.
HR 5102	CN slightly weak.
87 Vir	Ca 4226 weak; 4172 slightly strong? H_δ strong.
α Boo	CN slightly weak; 4172 strong.
HR 5464	CN weak; H_δ,H_γ, 4172, 4143, 4025 strong.
11 Lib	CN slightly weak; 4172 strong; H_β slightly strong.
HD 134063	Metallic lines weak; CH and 4016 strong.
5 Ser	4172 slightly strong?
HD 140283	Metallic lines very weak.
HR 6014	CN weak; 4172 strong.
HR 6128	CN weak; H_γ slightly strong.
HD 148816	Lines slightly weak.
48 Her	CN weak! 4172, 4025 strong.
HR 6286	H_β slightly strong; 4172 slightly strong?
HD 157089	CH slightly strong?
HD 162756	CH slightly strong?
HD 165401	All lines except 4172, 4187 slightly weak.
HR 6840	Lines slightly weak; CH strong.
HR 6853	CN weak! Atomic lines slightly weak? CH slightly strong.
35 ν^2 Sgr	Very peculiar. CH and CN very strong. CH star? 4143 strong. Luminosity uncertain; H_δ, H_γ too weak for a supergiant spectrum.
31 Aql	H_δ, H_γ, Mg4167 strong. 4172 slightly strong?
HD 184499	All lines weak; 4077 narrow.
HD 191046	CN weak; 4172, 4143 strong; H_β slightly strong. No proper motion in G.C.
HR 7841	H_δ, 4172 slightly strong.
λ Cep	4172 slightly strong.
HD 199191	CN weak! Other lines slightly weak? 4172 strong; 4143 slightly strong. Color may be abnormally red for type.
HR 8165	H_δ, H_γ slightly strong?
γ Psc	CN slightly weak.
14 And	CN slightly weak; 4172 strong.
HD 221830	CH slightly strong.

TABLE 3

DOUBTFUL HIGH-VELOCITY STARS (W_o-r_w 70 km/sec)

Star	α1950	δ1950	m_v	Type	M_v	p		V	W_o	W_o-r_w
μ Psc	1^h27^m6	+ 5°53'	5.12	K3+ III+	+1.4	.018	s,t	+ 35	67	47
25 Eri	3 42.4	- 0 27	5.84	K4 III+	+0.6	.0091	s	+ 70	60	56
λ Aur	5 15.8	+40 03	4.85	G0 IV-V	+4.0	.067	s,t	+ 66	74	72
51 Ori	5 39.0	+ 1 27	5.24	K1- III+	+0.9	.014	s	+ 88	74	72
55 ψ^7 Aur	6 39.4	+44 34	5.17	K5 III+	+0.5	.0115	s	- 75	83	81
20 Mon	7 07.7	- 4 09	5.02	K0- III-IV	+1.7	.022	s,t	+ 79	83	75
81 Gem	7 43.2	+18 38	5.02	K3+ III+	+1.0	.016	s	+ 82	72	70
θ UMa	9 29.5	+51 54	3.26	F6 III-IV	+1.9	.052	t	+ 15	83	74
HR 4092	10 23.1	- 6 48	5.85	M0+ III+	+0.4:	.0081	s	+ 32	106	69
71 Leo	11 19.5	+17 42	7.04	K1 III-IV	+1.7	.0088	s	+ 6	70	44
HR 4586	11 57.7	+81 08	6.44	M3 III	-0.5	.0041	s	+ 31	83	59
9 Dra	12 58.2	+66 51	5.50	K0 III	+0.4	.010	s	- 31	53	36
HD 114960	13 11.3	+ 1 43	6.76	K4 III+	+0.3	.0058	s	+ 10	46	30
84 Vir	13 40.5	+ 3 47	5.7	K1+ III-IV	+1.9	.017	s	- 42	74	52
HR 5541	14 48.5	+37 28	5.50	K0+ III-IV	+2.3	.023	s,t	- 66	62	55
HR 5924	15 52.3	+20 27	5.75	M0 III-	-0.9	.0045	s	- 60	99	69
ϕ Ser	15 54.9	+14 33	5.66	K2 III+	+1.2	.0126	s	- 68	81	63
HR 6820	18 11.1	+21 51	6.25	K4 III	0.0	.0057	s	- 66	78	58
π Sct	18 54.4	- 5 54	5.04	K1 III+	+2.0	.025	s,t	- 93	78	76
69 Dra	20 01.0	+76 20	6.43	M3: III	-0.4	.0043	s	- 68	101	75
HR 7810	20 23.3	+09 54	6.46	K5: III+	+0.2	.0056	s	- 75	63	59
30 Vul	20 42.7	+25 05	5.13	K2- III+	+0.5	.012	s	+ 31	86	65
HD 211076	22 11.9	+16 56	6.59	K4 III+	+0.6:	.0063:	s	- 35	104	67

Remarks on the Spectra

μ Psc	CN very slightly weak?
25 Eri	CN very slightly weak?
λ Aur	Nearly normal; H_δ, H_γ slightly strong.
51 Ori	CN weak; H_δ, H_γ slightly strong?
20 Mon	CN slightly weak; 4172 slightly strong; 4143 strong.
81 Gem	CN weak; 4172 strong.
θ UMa	Lines slightly weak.
71 Leo	4172 slightly strong.
HR 4586	H_δ slightly strong.
9 Dra	CN weak; 4172, 4143 slightly strong.
84 Vir	4172 slightly strong.
HR 5924	H_δ, H_γ slightly strong.
HR 7810	CN slightly weak?
HD 211076	H_δ slightly weak?

The remaining stars in Table 2 are all of type F5 or later, and these F- and G-type stars all show the G band. Since, as will be shown below, the *CH* bands tend to be enhanced in the high-velocity stars, the strength of the G band through the range F5–G4 of their spectra corresponds to a later type than would be assigned from the ratios of hydrogen to metal lines. Thus the systematic effects in *H* and *CH* tend to cancel one another in classification, and it can be hoped that the types of these stars in Table 2 are at least reasonably consistent. Eventually it should be possible to use accurate colors and excitation temperatures to make any necessary systematic corrections.

There remains the question of which stars to accept as forming the high-velocity group. A limiting space motion (W_0) in the vicinity of 60–70 km/sec has been commonly used,[17] though the frequency curves of stellar motions do not serve to define any velocity sharply separating the stars into distinct groups. On the other hand, the spectroscopic data indicate that the peculiarities characteristic of the spectra of the most rapidly moving stars become noticeable in a majority of the stars having velocities greater than about 80–85 km/sec (see Fig. 4 and the notes to Tables 2 and 3), while, of the more slowly moving objects, only a few show any evidence of these peculiarities. On physical grounds, therefore, it is useful to make a separation near this velocity; and we shall somewhat arbitrarily set the limit at $W_0 \geqslant 85$ km/sec.

For our purpose of investigating the physical properties of the high-velocity group, it is not satisfactory to accept every star for which the estimated space motion exceeds this limit. It is important to select the sample so that it will not be contaminated by any considerable number of stars for which the true value of W_0 is less than 85 km/sec, but for which the measured motion appears to exceed this amount because of the errors of observation. The individual errors in W_0 will differ greatly from star to star. The radial velocities are usually known with probable errors not exceeding 2 km/sec; and any star with a measured radial velocity, corrected for the solar motion, of 87 km/sec or more has a high probability of actually belonging to the high-velocity group as defined here. On the other hand, if almost all the motion of a star is tangential to its direction from the sun, the measured value is affected not only by the error in the proper motion but even more seriously by the uncertainty in the parallax. Thus an error of 1 mag. in M_v, which is not unlikely, changes the computed tangential motion by 60 per cent. It is chiefly for this reason that many of the space velocities in Table 2 differ greatly from those found by other investigators. For example, the space motion of μ Psc was given by Miczaika as 114 km/sec, on the basis of a parallax of 0".011. We estimate the luminosity of this K3 star as slightly, but definitely, below that of an average giant, and therefore assign it an absolute magnitude of +0.8. The corresponding spectroscopic parallax is 0".014. The trigonometric parallax is 0".021 ± 0.006, large enough to deserve consideration. We therefore take a mean parallax of 0".018 and find a corresponding space velocity of 67 km/sec, which necessarily removes the star from the high-velocity group.

Since many stars could similarly be shifted in or out of the group by quite reasonable adjustments in their measured distances, the aim of finding the properties of the real high-velocity stars can be attained best by rejecting those stars for which the probability of chance inclusion is greatest. Consequently, we shall require not only that $W_0 \geqslant 85$ km/sec but also that $W_0 - r_w \geqslant 70$ km/sec, where r_w is the probable error of the space velocity of that star. From the expression for the probable error of a function of observables, we have

$$r_w = \frac{1}{W_0}\left[V^2 r_v^2 + T^2\left(\frac{4.74}{p}\right)^2 r_\mu^2 + \frac{T^4}{p^2} r_p^2\right]^{1/2},$$

where T is the tangential velocity; r_v is the probable error of radial velocity; r_μ is the probable error of proper motion; and r_p is the probable error of parallax.

[17] J. H. Oort, *Groningen Pub.*, No. 40, 1926; Miczaika, *op. cit.*

If the parallax is derived from a spectroscopic absolute magnitude, the last term under the root sign becomes

$$\frac{T^4 r_M^2}{25\ (\text{Mod.})^2} = \frac{T^4 r_M^2}{4.70},$$

where r_M is the probable error of absolute magnitude.

In computing the probable errors in the final columns of Tables 2 and 3, a value of 0.8 mag. was assumed for r_M if the parallax of column 7 was obtained from our spectroscopic absolute magnitude, as indicated by the symbol "s." The same error was accepted for the means of trigonometric and spectroscopic parallaxes, except for a few cases where both values were rather large and agreed closely enough to justify adoption of the trigonometric error. All trigonometric parallaxes were taken from the Yale *General Catalogue of Trigonometric Stellar Parallaxes*.

In Table 3 are listed the stars which were observed but which failed to satisfy the velocity criteria for inclusion in the high-velocity group. These stars are excluded from the discussion of the following section.

III. THE LUMINOSITY-SPECTRUM DIAGRAM

Table 2 contains both luminosities and types for all the adopted high-velocity stars with the exception of HD 26 and 35 ν^2 Sgr. These two stars are notably peculiar for the strengths of the bands of the carbon compounds in their spectra and show similarities to the *Ba* II and *CH* stars.[18] The peculiarities preclude any significant spectroscopic estimate of their luminosities.

The luminosity-spectrum diagram for the remaining 83 stars of Table 2 is shown in Figure 1. Since the observing list contained relatively few stars with apparent magnitudes fainter than 7.5, the cooler and fainter part of the main sequence is only sparsely represented. For the purpose of giving a better picture of the location of the main sequence, four dwarf stars, for which radial velocities exceeding 100 km/sec were measured at Mount Wilson,[19] have been added. The trigonometric absolute magnitudes and the Mount Wilson types of these four stars are plotted as crosses.

The first question to be asked about the diagram is the extent to which it is distorted by "spurious" high-velocity stars—either those which have slipped in because of errors of observation or stars which have the physical properties of "low-velocity stars" (population type I?) but happen to lie on the upper tail of whatever velocity-frequency-curve these objects may have. The observations of the spectral peculiarities again furnish the most direct evidence; for giants in the range G5–K2, about one-third of those with $85 \leqslant W_0 < 100$ show no clear peculiarities and are, therefore, suspicious cases. In Table 2 there are 13 stars of all types in this velocity range, and accordingly we might expect four or five points in Figure 1 which do not correspond to real "high-velocity stars." Actually two such objects, HR 645 and 32 ν^2 Cnc, can be singled out as probably spurious just because they are G8–K0 giants, which should show the peculiarities but definitely do not. Among the giants later than K2 and the dwarfs of types G and K, which make up about one-quarter of the stars in Figure 1, there could easily be a couple of spurious cases, though we have found no spectroscopic means of detecting them.

Further evidence that few of the large space velocities of Table 2 are the result of chance errors is furnished by Figure 2, which shows the distribution in longitude of the projections of the velocity vectors on the galactic plane. The components from low-velocity stars are known to lie in all longitudes and would continue to do so if magnified by errors of observation. In Figure 2, however, no components exceeding 60 km/sec

[18] The peculiarities in the spectrum of 35 ν^2 Sgr were noticed by Morgan and Bidelman on Yerkes plates.

[19] A. H. Joy, *Ap. J.*, **105**, 96, 1947.

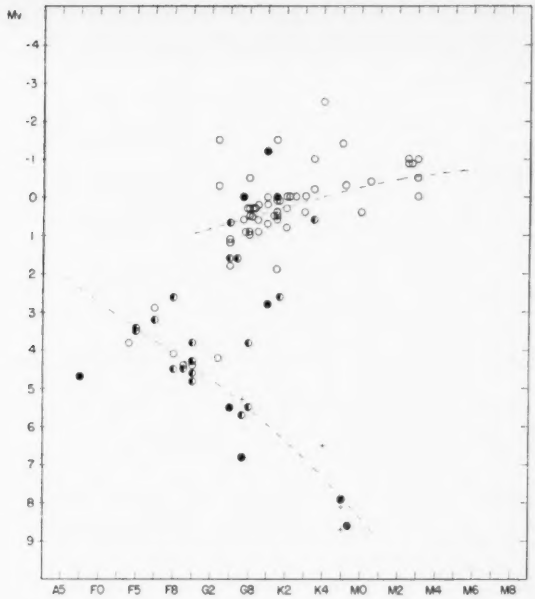

FIG. 1.—Luminosity-spectrum diagram for the high-velocity stars. Spectroscopic absolute magnitudes are plotted as open circles, trigonometric (and dynamical) as filled circles, and means of both as half-filled circles. The four dwarf stars classified at Mount Wilson are shown as crosses.

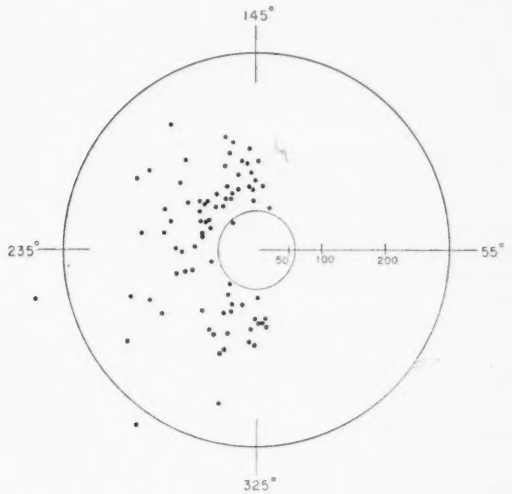

FIG. 2.—Distribution in galactic longitude of the projected space motions of the high-velocity stars. The small circle is drawn at a radius of 60 km/sec. Two points lie outside the 300-km/sec circle.

occur in the range from 340° to 120°. This zone of avoidance agrees well with that found originally for the high-velocity stars by Oort.[20]

On the whole, then, Figure 1 should give a reasonably good picture of at least the upper part of the spectrum-luminosity distribution of the high-velocity stars.

Inspection of the figure shows at once several already well-known features of the high-velocity group: the relative scarcity of both early-type stars and very bright supergiants, and the apparent tendency of large velocities to occur often among stars at the lower edge of the main sequence. This last point is not certain, for observations of many more faint dwarfs are needed properly to define the main sequence for the group.

The dashed lines in Figure 1 mark the approximate centers of the giant and main-sequence branches for normal stars of low velocity. The positions of these lines were estimated from the calibration of MKK luminosity classes against absolute magnitude for standard stars,[9] with some correction for the apparent centroid of the giant branch determined from the distribution of Mount Wilson[21] and Victoria[22] absolute magnitudes. The giant branch for high-velocity stars is also fairly well represented by the upper dashed line, though the real dispersion is large, as usual. When comparison is made with the steeply slanted giant branches for the stars in globular clusters,[11, 12] the *distribution of the high-velocity stars* could be described as *intermediate* between those of *cluster stars* and those of *low-velocity stars* in the vicinity of the sun. The major difference is the red giant branch extending well into type M for the high-velocity stars. It is worth noting that if the diagram is replotted to include only stars with space motions exceeding some larger amount, say 120 km/sec, the distribution of the remaining stars is not much different from that of Figure 1.

IV. SPECTRAL CHARACTERISTICS

The notes at the end of Table 2 summarize the spectroscopic differences remarked between the individual high-velocity stars and standard stars of the same type and luminosity. For *main-sequence stars later than G5* and for *M-type giants no consistent peculiarities are observed* on the low-dispersion spectrograms. Among the remaining stars the following characteristics tend to accompany large space velocities:

1. *General weakening of atomic lines.*—This characteristic of both giants and dwarfs in the range F5–G5 has been studied by Miss Roman,[1] who found a correlation with space motion in the sense that, while stars with low velocities might have either normal or weak absorption lines, "the conventional 'high-velocity' stars occur only in the weak-line group."

Among the giants (F5–G6) in Table 2, the general weakening of lines is noted in more than half (five out of nine). The effect is less striking among the main-sequence stars, where it is noted in only four out of fourteen dwarfs. These results do not mean that line weakening is definitely absent for the negative cases but merely that in such stars any such effect was not conspicuous enough to be noticed in the process of classification.

Among the giants of later type, general weakening of lines was observed in only three stars, all near type G8.

2. *Strengthening of the G band of CH.*—In Table 2, six out of the nine giants (F5–G6) are noted as having the G band unusually strong. In two of the stars (HD 6755 and 35 ν^2 Sgr) the enhancement is so pronounced that it is possible that these stars should be grouped with HD 26[23] as marginal members of the *CH* group of the carbon stars.

[20] J. H. Oort, *B.A.N.*, **4**, 273, 1928.

[21] W. S. Adams *et al.*, *Ap. J.*, **81**, 187, 1935; *Mt. W. Contr.*, No. 511.

[22] Young and Harper, *Pub. Dom. Ap. Obs. Victoria*, Vol. **3**, No. 1, 1924.

[23] Keenan and Keller, *Ap. J.*, **113**, 700, 1951.

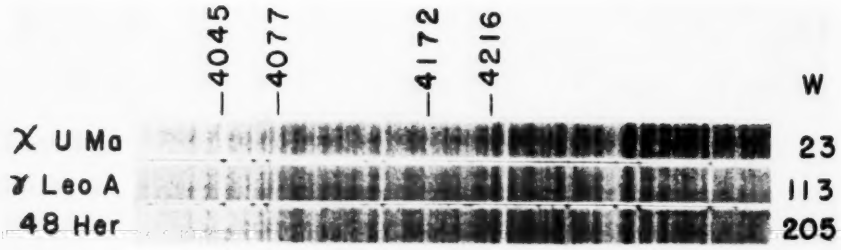

FIG. 3.—Spectra of three giants (K0–K1) of differing space motions. The two lower spectra represent stars in the high-velocity group.

Among the dwarfs, however, marked strengthening of *CH* is noted for only four out of the fourteen stars.

It appears that an abnormally strong G band or abnormally weak metallic lines are about equally good spectroscopic indicators of the high-velocity character among late F-type or early G-type stars.

3. *Weakening of the CN bands.*—On spectrograms with a scale ≈ 100 A/mm, none of the individual *CN* bands is resolved; but, since the strong head at 4216 A degrades to the violet, the ratio of intensities of the continuum just to the red and to the violet of λ 4216 is a fairly good measure of the strength of *CN* (see Fig. 3).[24]

It is helpful also to use the strength of the λ 4216 line itself, for the apparent line observed on low-dispersion spectrograms is a blend of the *Sr* II atomic line at 4215.5 A and the *CN* head at 4216.0 A. Since the λ 4216 blend is not used in classifying the high-velocity stars, the difference between its intensity in one of their spectra and in that of a standard star of the same luminosity and spectral type is another measure of abnormality of the *CN* absorption in the high-velocity star.

These two differential estimates define what can conveniently be termed the "cyanogen discrepancy" of any star. Photometric measurements to set up a scale for expressing the magnitude of this discrepancy are under way, but for the purposes of this paper it is sufficient to use the qualitative estimates given in the notes to Table 2. The peculiarities noted range from slightly greater than normal strength in the two stars, HR 645 and 32 ν^2 Cnc, already mentioned, through slightly weak *CN* (γ Leo A), weak *CN* (δ Lep), to very weak *CN* (48 Her and HD 199191; see Fig. 3). Table 4 summarizes the

TABLE 4

RELATIVE INTENSITY OF *CN* IN HIGH-VELOCITY STARS

CN Intensity	No. of Stars	*CN* Intensity	No. of Stars
Strong	2	Weak	13
Normal	15	Very weak	3
Slightly weak	12		

estimates for giants in the range G5–K3$^+$ and shows that, on the average, there is a *deficiency of CN* in the high-velocity group. Not included in this tabulation is the peculiar star 35 ν^2 Sgr, in which the absolute strength of *CN* is great, but its intensity relative to *CH* is low.

In this same group of giants the blended line at approximately 4172 A is noted as strengthened relative to near-by metallic lines in twenty-six out of the forty-five stars. This may be partly an absolute effect[25] and partly a relative enhancement due to the weakening of the partially overlying *CN* bands. It seems improbable that the latter effect can fully explain the behavior of λ 4172, for in passing from standard giants to subgiants we find that the reduced *CN* absorption is accompanied by weakening rather than strengthening of λ 4172.

From these observations we should expect that the *ratio* 4172/4216 would be a useful *spectroscopic criterion for the recognition of stars of high velocity*, and it has proved the most sensitive criterion on the spectrograms used in this investigation. A plot of the

[24] The relative intensities in the continuum on either side of λ 4216 were first used as a measure of *CN* strength by B. Lindblad, *Ap. J.*, **55**, 85, 1922.

[25] M. Schwarzschild and B. Schwarzschild have kindly informed us that their examination of λ 4172 on Mount Wilson coudé spectrograms permitted the identification of a number of metallic contributors, including several lines of iron, but that no one component was definitely enhanced in the high-velocity stars. Tracings of Perkins spectrograms of various dispersions indicate that in these stars the blending on the red side of the line causes an apparent widening which makes the line appear stronger on small-scale plates.

difference in the visual estimates of the two lines, against space velocity, is shown in Figure 4. The points for velocities below 60 km/sec were taken chiefly from standard stars. This selection may contribute to the absence of any ordinates above -2 among the low-velocity group, for the stars chosen as spectroscopic standards tend to be more homogeneous than stars selected at random. Nevertheless, the correlation of the 4172–4216 intensity difference with velocity appears definite. An intensity difference of -2 is ambiguous, but any star with a difference in the range -1.5 to $+1.5$ has a high probability of being a physical member of the high-velocity group.

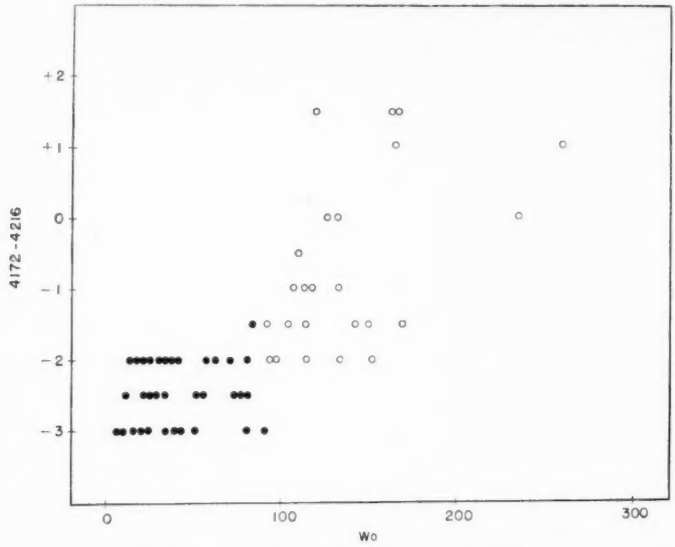

FIG. 4.—Plot of estimated differences in intensity of the lines 4172–4216 against space velocity (km/sec). Stars in the high-velocity group are shown as open circles.

This question may be raised: Does the diagram represent two slightly overlapping groups of stars which are homogeneous in the physical property measured by this line difference, or does it evidence a considerable range of values of a variable? The fact that the dispersion in the values of 4172–4216 is real, at least among the high-velocity stars, shows that the second alternative is true. The line difference clearly changes sign between such stars as γ Leo A and 48 Her (see Fig. 3), and it is unlikely that the points in the diagram are uncertain by more than half a step. For the three stars in the reproduction the values of the difference are: χ UMa, -2.5; γ Leo A, -1.5; and 48 Her, $+1.5$. These three stars are all bright giants, though 48 Her is probably somewhat more luminous than the other two and would, therefore, be expected to have *stronger CN* bands if the peculiarity were not present.

The general conclusions from the spectroscopic evidence are:

1. The spectra of the high-velocity giants and subgiants (G6–K4) show a *cyanogen deficiency* which can be measured either by the *break in the continuum at λ 4216*, or by the *difference between the estimates of intensity of the lines* 4172 and 4216.

2. For stars in the range F5–G5, the corresponding characteristics are the general *weakening of atomic lines* (as discussed by N. G. Roman) and the *strengthening of the G band of CH*.

3. In stars of the same type and luminosity, a considerable range in the *cyanogen discrepancy* is observed. This quantity appears to represent another dimension in spectral classification, in addition to *temperature* and *luminosity*. Schwarzschild, Spitzer, and Wildt[26] have suggested that *chemical composition* is the variable involved.

It is a pleasure to thank Mrs. Mary Fenwick for her help in the computations and the preparation of the drawings.

[26] *Ap. J.*, **114**, 398, 1951.

EXPANDING MOTIONS IN THE LACERTA AGGREGATE

A. Blaauw and W. W. Morgan
Leiden and Yerkes Observatories
Received November 26, 1952

ABSTRACT

The aggregate of O–B5 stars in Lacerta, centered at $l = 67°$, $b = -14°$ and containing, among others, the stars 6, 8, 10, 12, 14, and 16 Lacertae, is found to show an expansion similar to that of the ζ Persei aggregate. Figure 3 shows the proper motions. The coefficient of expansion is 0".00086 per year per degree and hence the age of the aggregate probably is 4.2×10^6 years. Its distance is about 460 parsecs, and the projected dimensions are 120×70 parsecs. Table 1 lists the stars in the aggregate. Table 2 summarizes its principal properties.

INTRODUCTION

The two-dimensional spectral classifications of O–B5 stars in the system of the Yerkes *Atlas of Stellar Spectra*, accumulated during recent years at the Yerkes Observatory, provide a new basis for the study of the motions and the distribution in space of these stars. The present paper deals with a group of stars in Lacerta and is part of a general study of the nature of the peculiar motions of the early-type stars. The recent discovery of the expanding motions in the ζ Persei aggregate[1] suggested that this phenomenon might be detectable also in other near-by aggregates. It is indeed found to be present in the one in Lacerta.

The luminosity classifications in the Yerkes system are in terms of the luminosity classes I–V. The final calibration of these luminosity classes will have to be based, at least partly, on proper motions as a criterion of distance. Their interpretation requires knowledge of the kinematical properties of the stars concerned. Therefore, the study of the peculiar motions precedes the final calibrations.

THE DISTRIBUTION IN THE SKY

The aggregate in Lacerta can be recognized rather easily on a plot of the O–B5 stars in the *Henry Draper Catalogue*. Figure 1 shows the distribution in the region $l = 45°$–$90°$, $b = 0°$ to $-30°$. Those stars which, according to the new spectral classifications and provisionally adopted absolute magnitudes,[2] have distance moduli between 7.0 and 9.5 (250–800 parsecs) are represented by dots. Newly classified stars outside these limits of distance modulus are not represented. All stars for which no reliable determination of the distance modulus was available are represented by plus signs. These include stars not yet observed for new classification, as well as the newly classified stars to which no luminosity class could be assigned and those not occurring in Stebbins, Huffer, and Whitford's list of colors.[3] There is a conspicuous clustering in the central region of the chart. It includes, among others, the stars 8 and 10 Lacertae and the β Canis Majoris type stars, 12 and 16 Lacertae.

Table 1 lists the 29 stars, represented on the chart in the area between the limits $l = 60°$ and $75°$, $b = -5°$ and $-20°$. The visual magnitude m is taken from the *Henry Draper Catalogue*. The color excess E_1 is from the catalogue of Stebbins, Huffer, and Whitford,[3] with a slightly corrected zero point. The visual magnitudes corrected for interstellar absorption $m_0 = m - 7E_1$ are in the next column. The visual absolute magnitudes M_v are derived from these corrected apparent magnitudes and the mean distance modulus of the

[1] A. Blaauw, *B.A.N.*, No. 433, 1952.

[2] P. C. Keenan and W. W. Morgan, *Astrophysics*, ed. J. A. Hynek (1952), chap. i, Table 1.5.

[3] *Ap. J.*, **91**, 20, 1940; *Mt. W. Contr.*, No. 621, 1940.

group $m_0 - M = 8.3$ (distance 460 parsecs). The latter is based mainly on the B2 V and B3 V stars for which the provisional calibration of the mean absolute magnitudes has the largest weight. The H-R diagram, based on the absolute magnitudes of Table 1 and on the Yerkes spectra, is shown in Figure 2. It should be borne in mind that the stars studied were selected from the *Henry Draper Catalogue*, which is incomplete beyond $m = 8.3$. It is quite possible that there are other, undetected, members of the aggregate not listed in Table 1, with m_0 between 7 and 8 or even brighter, but more heavily obscured by interstellar absorption than the stars listed. Very little can yet be said about the membership of stars of later types than B3. A survey of the spectral classes of faint stars in the region

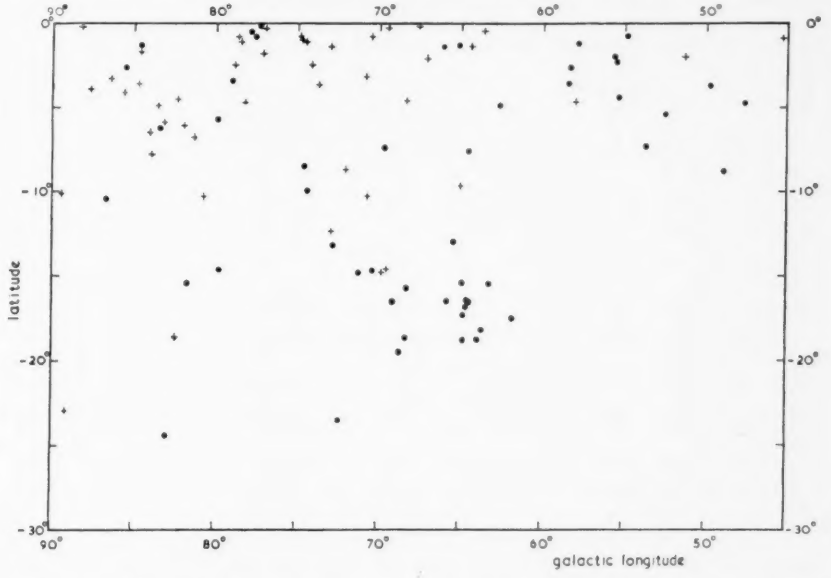

FIG. 1.—Distribution of the O–B5 stars in the *Henry Draper Catalogue*. Dots represent stars with well-determined distance modulus between 7.0 and 9.5; plus signs, stars with uncertain distance modulus. Stars with reliable distance modulus outside the interval 7.0–9.5 are not represented.

of the aggregate and adjacent ones, supplemented with luminosity classifications and color measures, would be necessary to settle this question. The average color excess of the stars in Table 1 is +0.083 mag. and, hence, the average amount of absorption in visual light is 0.6 mag.

THE PROPER MOTIONS

Annual proper motions for most of the stars are given in the tenth and eleventh columns of Table 1. They are in the average of the systems of FK3 and N30 with precessional corrections applied. Twenty-one stars are in B. Boss's *General Catalogue*. Many of the faint ones are in the *Second Greenwich Catalogue* ($Gr_2 25$). For four stars no proper motions are available. In many cases the GC proper motion was improved by combining it with the $Gr_2 25$ value and with an independent value derived from modern meridian observations, computed by Dr. H. R. Morgan at the Naval Observatory and kindly put at our disposal.

TABLE 1

STARS IN THE LACERTA AGGREGATE

	HD	1900 R.A.	1900 Decl.	l	b	m	E_{1}	m_0	Sp.	M_v	Unit 0".001 $\mu_\alpha \cos\delta$ p.e.	Unit 0".001 μ_δ p.e.	Radial Vel. p.e. (Km/Sec)	Remarks
	209961	22h 2m0	47° 45′	64°.5	− 7°.6	6.16	+0.08	5.6	B2 V	−2.7	− 1± 3.5	+ 4± 3.3	−17.8 Orb.	1
	211835	14.9	45 18	65.0	− 9.7	8.47			B3:Ve					
	212883	22.4	36 57	61.8	−17.5	6.39	+ .08	5.8	B2 V	−2.5	+ 6± 4.2	− 4± 2.6	− 6.5±0.7	Field star?
	212978	23.1	39 19	63.2	−15.5	6.07	+ .06	5.7	B2 V	−2.6	+14± 3.7	− 2± 3.6	−16.8±0.8	Field star?
6 Lac	213420	26.1	42 36	65.4	−13.0	4.54	+ .09	3.9	B2 IV	−4.4	− 7± 2.0	− 2± 1.4	− 9.8±0.9	
	213976	30.1	40 16	64.9	−15.4	7.00	+ .10	6.3	B1.5 V	−2.0	−17± 4.0	− 3± 3.0	−17.2±1.9	
8 Lac ft	214167	31.4	39 7	64.5	−16.5	6.55	+ .00	6.5	B2 V	−1.8	− 7± 4.2	− 6± 3.3	−13.4±1.5	
8 Lac br	214168	31.4	39 7	64.5	−16.5	5.83	+ .11	5.1	B1 Vne	−3.2	− 2± 2.0	−10± 1.5	−12.5±4	
	214240	31.8	49 33	69.7	− 7.4	6.20	+ .12	5.4	B3 V	−2.9	0± 2.0	+ 7± 1.8	−15.3 Orb.	2
	214263	31.9	37 19	63.7	−18.1	6.75	+ .04	6.5	B2 V	−1.8	− 4± 8.3	0± 5.9	−19.5±0.4	
	214432	33.0	38 55	64.7	−16.8	7.4	+ .08	6.8	B3 V	−1.5	−10± 7.0	−11± 7.0		
	214652	34.6	36 51	63.9	−18.8	6.67	+ .09	6.0	B2:V	−2.3	0± 4.4	− 6± 3.4	−12.6 Orb.	3
10 Lac	214680	34.8	38 52	64.8	−17.3	4.91	+ .06	4.5	O9 V	−3.8	+ 4± 1.1	− 4± 0.8	− 9.5±0.4	
12 Lac	214993	37.0	39 43	65.8	−16.5	5.18	+ .04	4.9	B2 III	−3.4	− 2± 2.6	− 3± 1.8	−15	4
	215191	38.4	37 17	64.8	−18.8	6.22	+ .11	5.5	B1 V	−2.8	+11± 7.0	−11± 5.0	−17.8±1.5	
	216092	44.9	47 24	70.7	−10.3	8.1			B1:V					
14 Lac	216200	45.8	41 26	68.2	−15.7	5.84	+ .16	4.7	B3 IV:	−3.6	+ 9± 1.8	0± 1.7	−20.2±0.7	
	216534	48.6	49 20	72.0	− 8.7	8.0			B3 V					
	216684	49.8	43 0	69.5	−14.6	7.8			B3 V		+ 1±10.0	+10±10.0		
	216851	51.3	43 2	69.8	−14.7	7.68			B3 V:n		+ 1± 9.0	− 6± 9.0		
	216916	51.9	41 4	69.1	−16.5	5.54	+ .07	5.1	B2 IV	−3.2	+ 1± 2.1	− 4± 1.5	−13.6	5
16 Lac	217101	53.1	38 48	68.3	−18.7	6.07	+ .07	5.6	B2 IV–V	−2.7	0± 2.5	− 9± 1.9	−15.5±0.7	
	217227	54.2	43 18	70.4	−14.7	7.02	+ .07	6.5	B2: V	−1.8	+14± 8.0	+13± 7.0	−14.4±0.7	
	217543	56.3	38 10	68.6	−19.5	6.39	+ .07	5.9	B3	−2.4	+ 8± 6.0	− 5± 6.5	−13.7±3.4	
	217811	58.2	43 31	71.2	−14.8	6.32	+ .12	5.5	B2 V	−2.8	− 1± 3.5	− 1± 2.4	− 8.3±0.4	
	218325	23 2.0	46 23	72.9	−12.4	8.0			B3 V					
	218344	2.1	50 33	74.6	− 8.5	7.17	+ .06	6.8	B2 V	−1.5	− 6±11.0	+12±11.0	−12.7±1.2	
	218407	2.7	45 33	72.8	−13.2	6.56	+ .09	5.9	B2 V	−2.4	− 1± 3.0	0± 2.5	−15.1 Orb.	6
	218674	4.8	49 7	74.4	−10.0	6.53	+0.13	5.6	B3 IV	−2.7	+ 6± 4.0	0± 3.0	− 3.9±3.9	

NOTES TO TABLE 1

1. Orbit by R. K. Young, *Pub. Dom. Ap. Obs. Victoria*, **1**, 193, 1920, based on 32 observations in 1918 and 1919.
2. Orbit by S. N. Hill, *Pub. Dom. Ap. Obs. Victoria*, **3**, 358, 1926, based on 32 observations in 1925 and 1926.
3. Orbit by A. McKellar, *Pub. Dom. Ap. Obs. Victoria*, **6**, 369, 1937, based on 55 observations in the years 1925–1937.
4. 12 Lacerta, β Canis Majoris type, see O. Struve, *Ap. J.*, **113**, 589, 1951, and papers referred to by this author.
5. 16 Lacerta, β Canis Majoris type, see O. Struve *et al.*, *Ap. J.* **116**, 81, 1952, and papers referred to by this author.
6. Orbit by R. K. Young, *Pub. Dom. Ap. Obs. Victoria*, **1**, 239, 1920, based on 27 observations in the years 1918–1920.

In comparing the GC and the Greenwich catalogues it was found that a systematic difference exists between the proper motions in right ascension for stars fainter than $m = 6$. It amounts to 0^s.0012 per year and does not seem to vary much with the apparent brightness for magnitudes fainter than 6, but does not occur for the brighter stars. We have assumed that it represents a magnitude error in the $Gr_2 25$ motions and accordingly have applied a correction of $-0^s.0012$ to the μ_α's for $m > 6$ in that catalogue. However, it is not certain that the error is wholly in the Greenwich catalogue and therefore there is considerable uncertainty in the proper motions in right ascension as used in the present investigation. The amount of 0^s.0012 is large compared to the observed internal motions. The components μ_α are not used in the evaluation of the coefficient of expansion.

Total proper motions are represented as arrows in Figure 3. The scale and the directions of α and δ are indicated in the lower left-hand corner. Dotted arrows represent proper motions with probable errors larger than $\pm 0''.005$. The size of the dots indicates the apparent brightness of the stars. Faint stars for which no proper motions are available are represented by circles.

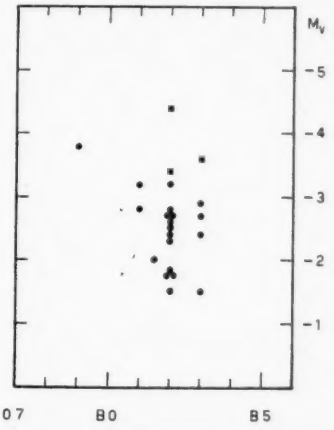

FIG. 2.—H-R diagram of the Lacerta aggregate

The heavy arrows at the lower left-hand corner represent the directions and amounts of the proper motions which correspond to the reflex of the standard solar motion for stars at the center of the aggregate (the v component), the effect of differential galactic rotation, and the combined proper motion. As will be seen from Figure 3, the stars generally do not show this latter proper motion, but rather have the tendency to move outward from the center of the aggregate. There is considerable uncertainty in some of the proper motions, and there are a few cases, as, for instance, the star HD 212978 at $l = 63°.2$, $b = -15°.5$, which definitely move in the opposite direction. However, such exceptions are to be expected in the case of an expanding aggregate mixed with some field stars. On the whole, there appears to be fairly strong evidence that the Lacerta aggregate does show an expansion, similar to the ζ Persei aggregate.

EVALUATION OF THE EXPANSION

The expansion has been derived quantitatively only from the proper motions in declination, the components in right ascension being excluded for the reasons mentioned above. All stars with known proper motion in Table 1 were used, including some doubtful members. Apart from the uncertainty with regard to the magnitude error in the μ_α's, the

proper motions in right ascension are a less reliable basis than those in declination, because the reflected solar motion of possible field stars affects the motions in right ascension much more than those in declination. The influence of a possible field star like HD 212978 mentioned before is thus reduced. Another favorable circumstance is that the aggregate is elongated in the direction of declination, indicating faster expansion in this direction.

Figure 4 shows the μ_δ's plotted against the declinations. The size of the dots indicates the weight of the μ_δ's. The expansion of the aggregate is revealed by the increase of μ_δ

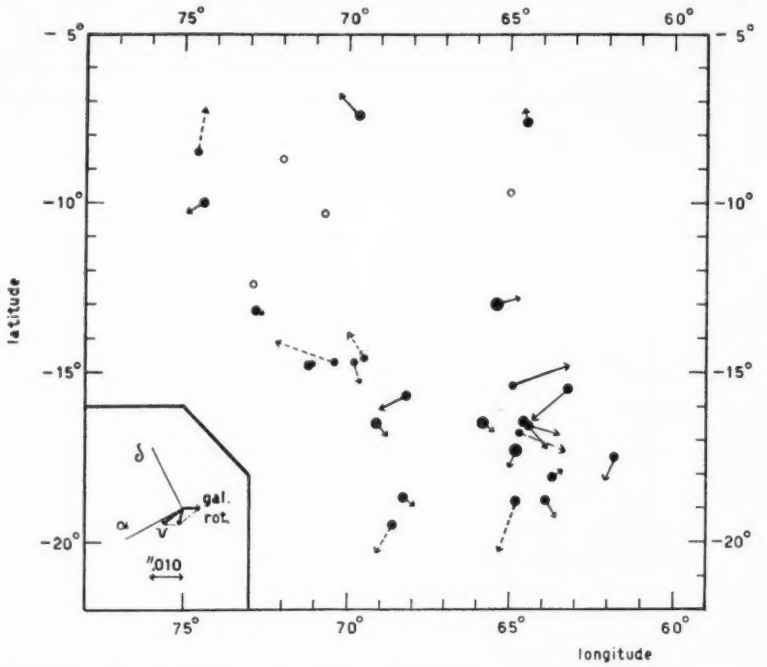

FIG. 3.—Proper motions of stars in the region of the Lacerta aggregate. Dashed arrows represent proper motions with probable errors exceeding ±0″.005. Circles represent stars with unknown proper motion. The scale of the proper motions and the directions of increasing α and δ are indicated in the lower left-hand corner.

with increasing declination. A linear relation has been adopted, and the coefficient of expansion as found from a least-squares solution is

$$\frac{d\mu_\delta}{d\delta} = +0''.00096 \text{ per year per degree} \pm 0''.00013 \text{ (p.e.)}.$$

The correction for spurious expansion due to the motion of the aggregate with respect to the sun along the line of sight is $-0''.00010$ per year per degree, based on the mean radial velocity -13.6 km/sec. Hence the real expansion is

$$\frac{d\mu_\delta}{d\delta} = +0''.00086 \text{ per year per degree} \pm 0''.00013 \text{ (p.e.)}.$$

Interpreting this result on the assumption that the stars originated in a volume of space much smaller than the present size of the aggregate and that they started their motions simultaneously, we find the age of the aggregate to be

$$T_x = 4.2 \times 10^6 \text{ years}.$$

The assumptions made here—the same as those on which the determination of the age of the ζ Persei aggregate were based—are, of course, rather simplifying. Especially with regard to the second assumption, it may be noticed that the time elapsed between the

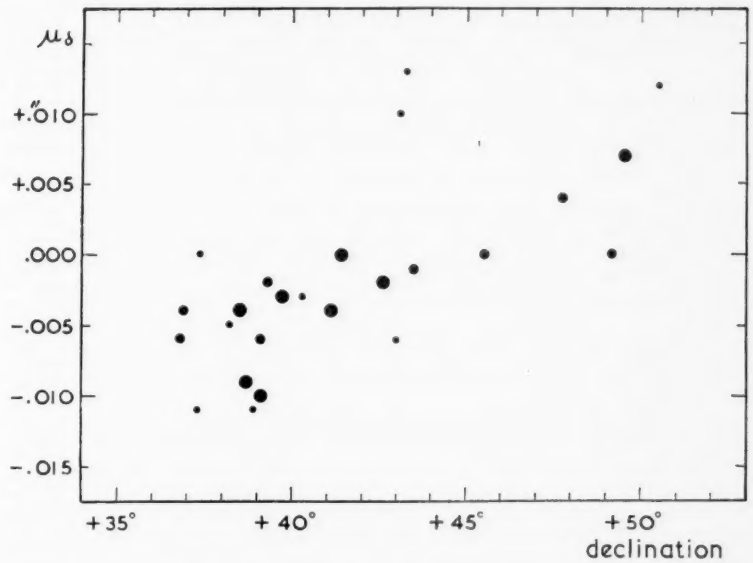

FIG. 4.—Components of proper motion in declination, μ_δ plotted against the declination. The sizes of the dots indicate the relative weights of the proper motions.

formation of different stars in the aggregate may well be an appreciable fraction of the ages found (1.3×10^6 years for the ζ Persei aggregate). The derived ages refer mainly to the stars which have moved farthest from the center of formation, as these contribute most of the weight in the solution for the coefficient of expansion. These may be the oldest stars.

THE MEAN VELOCITY OF EXPANSION

The radial velocities of the stars in the aggregate are in the next to the last column of Table 1. Most of them are taken from the Victoria lists[4] or from Moore's catalogue;[5] a few are from a recent Mount Wilson list.[6] Systemic velocities of spectroscopic binaries and mean velocities of 12 and 16 Lacertae are taken from the sources referred to in the notes to the table.

After elimination of the standard solar motion from the individual velocities by means

[4] J. S. Plaskett and J. A. Pearce, *Pub. Dom. Ap. Obs. Victoria*, Vol. **5**, 1931; J. A. Pearce and R. M. Petrie, *Pub. Dom. Ap. Obs. Victoria*, Vol. **8**, 1951.

[5] *Pub. Lick Obs.*, Vol. **18**, 1932.

[6] R. E. Wilson and A. H. Joy, *Ap. J.*, **111**, 221, 1950.

of the Prague tables,[7] we find the mean of the velocities left to be -2.4 km/sec. The average residual without regard to sign with respect to this mean, derived from 16 stars with the most reliable velocities and corrected for the influence of accidental errors, is

$$\eta_{\text{rad}} = \pm 3.1 \text{ km/sec}.$$

The relatively large accidental errors of the proper motions exclude a reliable determination of the mean velocity of expansion directly from the proper motions as given in Table 1. We can, however, derive it from the coefficient of expansion already determined and from the positions of the stars with respect to the center of the aggregate. In this way we find from the components in δ and α, respectively,

$$\eta_\delta = \pm 6 \text{ km/sec} \quad \text{and} \quad \eta_\alpha = \pm 4 \text{ km/sec},$$

and for the average velocity of the stars with respect to the center,

$$\eta = 8 \text{ km/sec}.$$

POSSIBLE MEMBERS OUTSIDE THE REGION OF FIGURE 3

The region of the aggregate to which the data in Table 1 and Figure 3 refer may seem to be chosen somewhat arbitrarily; the concentration of stars noticed in the center of Figure 1 merges gradually into the star field in the upper and left-hand parts of the diagram. Whether there are members of the aggregate outside the region of Figure 3 can be decided only on the basis of the directions and amounts of the proper motions. These must be expected to point radially outward from the center of the aggregate (if the center is at rest and corrections for solar motion have been applied) and to be proportional to the angular distance from this center (assuming the expanding motions to have started simultaneously).

There are some stars in the left-hand part of Figure 1 for which the proper motions seem to meet these requirements, but the evidence is not conclusive. The uncertainty arises mainly from the fact that the directions of expanding motions for these stars do not deviate much from the direction of the reflected solar motion. Accidental errors in the elimination of the latter, due to errors in the estimated distances of the stars, can easily have caused spurious residual proper motions resembling the expected expanding proper motions.

The situation is somewhat different in the region west of the aggregate. Near the upper right corner of Figure 1 the proper motions of possible members of the aggregate must be directed approximately opposite to the solar reflex. Three stars for which this is the case are:

HD 197419: GC 28861, at $l = 44\overset{\circ}{.}4$, $b = -5\overset{\circ}{.}0$, B2 V, $m_0 - M = 8.7$;
HD 199356: $\text{Gr}_2$25 8841, at $l = 49\overset{\circ}{.}8$, $b = -3\overset{\circ}{.}8$, B2e, $m_0 - M = 8.8$;
HD 201910: GC 29627, at $l = 52\overset{\circ}{.}5$, $b = -5\overset{\circ}{.}4$, B5 V, $m_0 - M = 8.3$.

Their total proper motions with respect to the center of the aggregate are: $0''.018 \pm 0''.004$; $0''.014 \pm 0''.012$ and $0''.012 \pm 0''.005$ (p.e.), respectively. At the average angular distance of these stars from the center of the aggregate (about 20°) the predicted proper motion is $0''.018$. These stars may thus have originated in the aggregate. However, the observational data are still very weak and certainly are no proof of an association of these stars with the aggregate. There is a fair chance that they are field stars with peculiar motions which happen to fit the picture of the expansion. The only way to obtain conclusive evidence is the determination of new positions from meridian observations in order to improve the accuracy of the proper motions.

At the present stage of the investigations of expanding aggregates we prefer to take a conservative attitude when considering the possible membership of stars at large angu-

[7] *Tables d'apex solaire*, ed. F. Link. ("Mem. and Obs. Czechoslovak Astr. Soc.," No. 9 [1948]).

lar distances from the centers. The somewhat arbitrary way in which investigators in the past have sometimes selected lists of (spurious) members of moving clusters indicates the need for care in this matter.

THE β CANIS MAJORIS TYPE MEMBERS

An interesting feature of the aggregate is the presence of the two β Canis Majoris type stars, 12 and 16 Lacertae. Both are B2 stars of intermediate luminosity; the values found here, $M_v = -3.4$ and -3.2, respectively, are very close. It is of some interest to compare these stars with others of the same category. σ Scorpii[8] is classified as B1 III, and its visual absolute magnitude, taken from *Groningen Publications*, No. 52, Table 33*a*, and corrected for interstellar absorption, is $M_v = -4.5$. For β Cephei, type B2 III, and β Canis Majoris, type B1 II–III, we derive, from the v component of the proper motions, $M_v = -2.8$ and -4.9, respectively.

These results suggest that the β Canis Majoris type of variation is closely related to the small region of the Hertzsprung-Russell diagram defined by the intermediate luminosities at spectral types B1 and B2. Other examples are ν Eridani,[9] type B2 III, and HD 199140,[10] type B2 III.

TABLE 2

	Lacerta Aggregate	ζ Persei Aggregate
Mean co-ordinates	$l = 67°$; $b = -14°$	$l = 128°$; $b = -15°$
Number of stars	29	17
Dimensions	120×70 psc	40×25 psc
Distance	460 psc	300 psc
Space velocity	< 6 km/sec	15 km/sec
Mean velocity of expansion	8 km/sec	12 km/sec
Coefficient of expansion	0".00086 per year per degree	0".00268 per year per degree
Age derived from expansion	4.2×10^6 years	1.3×10^6 years

PROPERTIES OF THE AGGREGATE AS A WHOLE

The mean co-ordinates for 1900 are $\alpha = 22^h40^m$, $\delta = +42°$, $l = 67°$, $b = -14°$; and the projected dimensions are about $15° \times 9°$, corresponding to linear dimensions of 120×70 parsecs.

The mean components of proper motion in galactic longitude and latitude corrected for solar motion and differential galactic rotation are $-0".0014$ and $+0".0020$, respectively, corresponding to linear velocities of -3 and $+4$ km/sec. The mean radial velocity corrected for solar motion, for differential galactic rotation, and for an estimated gravitational red shift of $+1.5$ km/sec, is -1.0 km/sec. The motion of the aggregate as a whole with respect to the field stars thus appears to be less than 6 km/sec.

It would be interesting to know whether there exists a close association between the aggregate and the interstellar matter within which it was formed, as in the case of the ζ Persei aggregate. Only a few photographs covering the region of the aggregate or parts of it have been published. On the whole, the distribution of the faint stars seems to be rather smooth, but a dark cloud in the densest part of the aggregate is weakly indicated. Further observations are required to investigate this matter.

Table 2 summarizes the principal data concerning the Lacerta aggregate. Those for the ζ Persei aggregate are added for comparison.

[8] See R. D. Levée, *Ap. J.*, **115**, 402, 1952, and references given there.

[9] See D. H. McNamara, *Pub. A.S.P.*, No. 377, p. 76, 1952, and references given by this author.

[10] R. M. Petrie, *J.R.A.S. Canada*, **40**, 149, 1946.

SOME REMARKS ON THE SPATIAL AND KINEMATIC STRUCTURE OF THE PLANETARY NEBULA IC 418

O. C. WILSON
MOUNT WILSON AND PALOMAR OBSERVATORIES
CARNEGIE INSTITUTION OF WASHINGTON
CALIFORNIA INSTITUTE OF TECHNOLOGY
Received November 3, 1952

ABSTRACT

Recent high-dispersion spectrograms have resolved the [*N* II] and [*O* II] lines in this nebula which had appeared single with the lower dispersion previously used. On collecting and discussing the kinematic data for this low-excitation nebula and correlating them with the results from slitless spectrograms, it becomes highly probable that IC 418 is built upon the same spatiokinematic model as are the high-excitation ring nebulae. A brief consideration of ring nebulae in general leads to two alternative explanations for them: (1) If the density inside the shell is higher than the density in the shell, then the flow of matter is from the inner mass into the shell. In this case the electron temperature in the inner mass must be much higher than that in the shell. (2) If, on the other hand, the inner mass consists of matter expelled inward from the shell, a relatively higher density in the shell, as compared to the interior, is adequate to account for the appearance of the ring nebulae.

Many years ago, W. H. Wright[1] noted that in the planetary nebula IC 418 the slitless images of hydrogen and of [*O* II] were rings, while the images of [*O* III] were uniform disks of slightly smaller diameter. Recently, slitless spectrograms of 10 A/mm dispersion (20 A/mm in the red) have been obtained with the coudé spectrograph of the 100-inch telescope with the aid of an image-rotating prism. The scale of these photographs is about four times greater than Wright's scale and, while confirming his results in general, shows considerably more detail. Careful examination of the images reveals the following facts: all the monochromatic images are rings without central intensity maxima, with the exception of those of [*O* III] and [*Ne* III]; the [*O* III] images show a barely discernible trace of ring structure[2] and a strengthening toward the center; the [*Ne* III] image (λ 3868) is merely a small blob, most intense at the center, and with no ring structure visible.

The appearance of several of the images is well shown in Figure 1 of a recent paper on the structure of IC 418.[3] Figure 3 of the same paper gives the radial density distributions derived from the slitless spectrograms by as straightforward a process as possible on the assumption of spherical symmetry. Unfortunately, as was pointed out at the time, it is very difficult to insure high accuracy in solving a problem of this type, and the details appearing in the final curves must be treated with considerable reserve. Careful inspection of the original spectrograms and of others obtained subsequently leads me to doubt especially the rise in density toward the center shown for hydrogen and for *N* II. The curves given for *He* I, *S* II, and *O* II are in much better accord with the appearance of the images themselves, though even here the details are not to be trusted. For instance, the rather large overlap shown for *O* III and *O* II is, as will be shown later, rendered somewhat doubtful on purely kinematic grounds. Further work on these questions is planned. At present, however, I believe that the most accurate statement which can be made concerning the structure of IC 418 is the following: All the monochromatic emissions, including those of hydrogen and excepting only those of [*O* III] and [*Ne* III], come

[1] *Pub. Lick Obs.*, **13**, 199, 1918.

[2] Better seen on direct photographs through appropriate filters taken with the 200-inch telescope by R. Minkowski.

[3] O. C. Wilson and L. H. Aller, *Ap. J.*, **114**, 421, 1951.

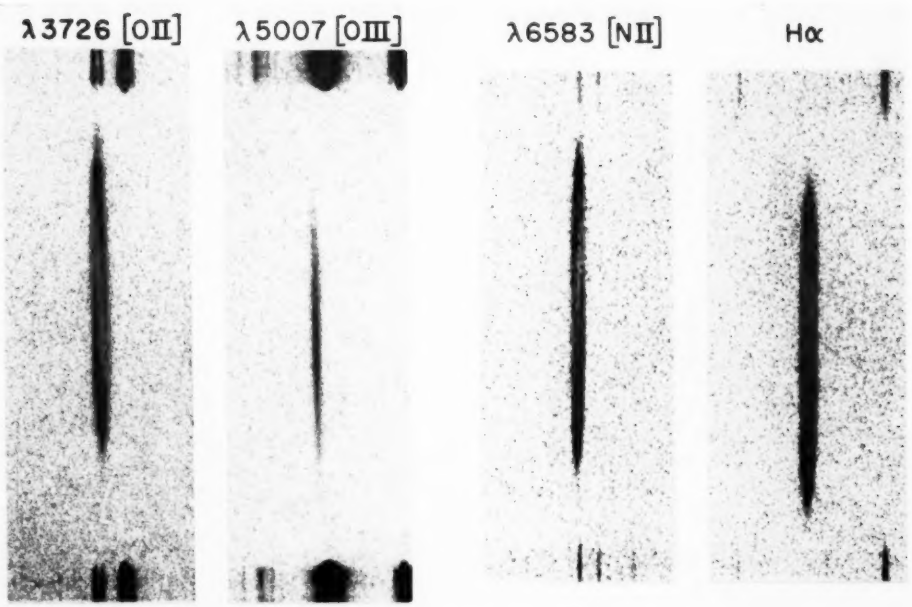

FIG. 1.—Lines in IC 418 with high dispersion. The mirror-image effect of λ3726 as compared to λ6583 appears to be real. Only a somewhat unlikely error in orienting the nebula on the slit could otherwise be held responsible.

mostly from hollow shells of nearly the same size. The [*O* III] and [*Ne* III] emissions, on the other hand, originate mostly in zones within the hollow-shell emission regions of the other ions.

The kinematic results obtained at 10 A/mm were somewhat unsatisfactory.[4] With this dispersion the lines of all the ions appeared single, with the exception of [*O* I], [*S* II], and *Mg* I, λ 4571, which gave double emissions with separations of 49.9, 34.7, and 37.5 km/sec, respectively. Slitless images of the emissions of these ions are rings; and, while one would not be surprised at a great difference between the kinematic behavior of emissions originating in an external hollow shell and of emissions arising in an interior zone, it was somewhat disconcerting to find that other ring images, notably those of [*O* II] and [*N* II], gave lines which appeared to be sharp and single.

In an effort to remove this difficulty, one spectrogram of the *Hα* region was obtained with the 73-inch camera at Mount Wilson. This plate (first order, dispersion 8.9 *A*/mm) resolved the [*N* II] lines into two components. Another spectrogram was taken with the 144-inch camera at Palomar, covering the λ 5000 region in the third order (2.2 A/mm) and the λ 3700 region in the fourth order (1.7 A/mm). On this plate the [*O* II] lines λ 3726 and λ 3728 are resolved into components, while the [*O* III] lines remain not only

TABLE 1

COMPONENT SEPARATIONS
(KM/SEC)

Element	Excitation (Volts)	ΔV (Km/Sec)
O I	0.0	47
Mg I	0.0	39
S II	10.3	34
O II	13.6	21
N II	14.5	23
H	13.5	0:
O III	35.0	0:
Ne III	40.9	0:

TABLE 2

LINE WIDTHS
(KM/SEC)

Element	Excitation (Volts)	Width (Km/Sec)
H	13.5	31
O III	35.0	15

single but fairly sharp. The hydrogen lines on these high-dispersion spectrograms remain single but are much broader than the other single lines. It is probable that they, too, would be seen as double, were it not for the widening of the components, a phenomenon common to all planetaries,[4] which masks the duplicity.[5] The foregoing statements are illustrated in Figure 1, and measures of component separation and line width are collected in Tables 1 and 2. Where the data of Table 1 differ from those previously published, it is due to the inclusion of more recent observations. The line widths given in Table 2 were measured on images of moderate intensity and are thus to be regarded as minimum values only.

The first point to be noted is that the kinematic data indicate a rather complete separation of the three stages of oxygen in the nebula. It would seem that there cannot be much overlapping of *O* III with *O* II, or of *O* II with *O* I. In particular, the results mentioned previously, which show a considerable physical overlap of *O* III and *O* II, are rendered doubtful. Under favorable circumstances the kinematic method is a powerful

[4] O. C. Wilson, *Ap. J.*, **111**, 279, 1950.

[5] Graphs of line shape indicate the following: kinetic temperatures of 10,000° or of 5000°, together with component separations of 20 and 15 km/sec, respectively, yield hydrogen lines in which the duplicity is completely masked by the overlapping of the components; for oxygen at 10,000°, a component separation of 6 km/sec should be noticeable. It seems probable, therefore, that in IC 418 the expansion velocity in the *H* shell is at least three times as large as that in the central mass.

tool for deciding whether various lines arise in the same or in different portions of a nebula.

The next point to notice is the analogy which now emerges between the spatiokinematic structure of IC 418 and those of the high-excitation ring nebulae.[4] In the latter it is *Ne* V which occurs in the innermost zone and which gives the smallest expansion velocity, whereas in IC 418 this role is played by *Ne* III and *O* III. In the high-excitation nebulae both the expansion velocities and the dimensions of the slitless images agree in placing the emission shells of *H* and of *O* III and *Ne* III very close together, if not in actual coincidence. In IC 418, on the other hand, we have seen that the [*O* III] and [*Ne* III] emissions definitely do not originate in the same part of the nebula which is responsible for most of the *H* emission. The slitless images do, however, make very probable a near coincidence of the *O* II and *N* II shells with that of hydrogen. Furthermore, comparison of the measured width of the hydrogen lines with the component separations of [*O* II] and [*N* II] is consistent with the idea that the hydrogen expansion velocity is of the same order as that for these ions.

Lastly, the general run of increasing velocity with decreasing excitation, which is a universal feature of the high-excitation ring nebulae,[4] is now seen to hold also for IC 418. Thus, to sum up, it appears that IC 418 is built upon the same spatiokinematic model as the high-excitation ring nebulae; the only significant difference is that at corresponding points the level of ionization is lower in IC 418.

In view of the fact that the low-excitation ring nebulae appear to be analogous in structure and kinematic behavior to those of high excitation, I should like to discuss briefly the subject of ring nebulae in general and to point out some of the difficulties they present. In so doing, attention will be focused on IC 418; but, where necessary or desirable, reference will be made to results from other nebulae.

One of the most important questions is this: Why is most of the hydrogen emission concentrated in a relatively thin shell instead of being distributed more generally throughout the whole nebula? If the ring nebulae were simple Strömgren spheres in gas masses of uniform density and electron temperature, or masses in which the density decreases monotonically outward, no bright shell would be expected. In fact, an inspection of Strömgren's original calculations[6] shows that under these circumstances the nebula should appear brightest at the center and should decrease in brightness outward, finally terminating at a sharp boundary. Because of this fundamental difference between theoretical prediction and observation, I do not believe it legitimate, at least without justification, to apply the results of Strömgren's theory to the ring nebulae.

Returning, now, to the above question, there is no reason to doubt that the hydrogen emission is the result of photoionization of hydrogen and subsequent recapture of electrons by protons. Complete formulae describing these processes are available,[7] but for our present requirements a simpler, less accurate, expression[8] is entirely adequate. This equation states that the number of captures on the nth hydrogen level is proportional to

$$C(n, T) = \frac{n_i n_e}{n^3 T^{3/2}} e^{X_n/kT} Ei\left(\frac{X_n}{kT}\right)$$

where n_i and n_e are the ionic and electronic densities (equal for hydrogen), T is electron temperature, X_n the nth ionization potential, and

$$Ei(X_0) = \int_{x_0}^{\infty} \frac{e^{-x} dx}{x}.$$

[6] *Ap. J.*, **89**, 526, 1939.

[7] D. H. Menzel and J. G. Baker, *Ap. J.*, **86**, 70, 1937.

[8] G. Cillié, *M.N.*, **92**, 820, 1932.

Hence, as long as the ionization remains fairly high, the hydrogen emission per unit volume depends only upon the square of the density multiplied by a function of T_e which decreases with increasing T_e. Thus, in comparing the bright hydrogen shell with near-by interior regions, we may make the following statement: The existence of a bright hydrogen shell must mean either that the density is higher or the electron temperature lower in the shell than in the interior. There are no other possibilities.

The kinematic results show that the expansion velocity in the hydrogen shell ordinarily exceeds that in the inner zone by 10 km/sec or more. It is true that in IC 418 we cannot measure the hydrogen velocity directly because it is too small with respect to the line width; but the preceding statement is known to be true for a number of other nebulae,[4] and we have seen that it is consistent with the observed features of IC 418.[5]

Now if the present measured velocities of the inner zone and of the hydrogen shell represent real motions of independent masses of matter, the inescapable conclusion is that the shell and the inner mass must be separating. In fact, since 10 km/sec $= 3 \times 10^{13}$ cm/year, the shell should separate from the inner zone by an appreciable fraction of the nebular radius in times as short as 10^3 years. One might expect to find, at least occasionally, a nebula in which there is a gap between the outer edge of the inner mass and the inner surface of the hydrogen shell; but no gaps of this kind have been found in any of the nebulae observed. Moreover, if the inner mass and the shell have moved out from the nucleus with their present apparent velocities, it is impossible to account for their present relative dimensions. For these reasons it is unrealistic to adopt the view that the central mass and the shell are separate entities, and one is forced to conclude instead that we are dealing here with a continuous flow of some kind.

In fact, the simplest way of accounting for the observations is to suppose that a continuous flow of gas is taking place, either from the central mass into the shell, or from the shell into the central mass. Flow in either direction could account for the observed spatiokinematic relationships; but the two alternatives imply certain other distinct consequences, which we shall now briefly examine.

Consider, first, that the matter from the central mass is flowing into and through the shell. As long as the interior supply is large, one can assume that the density at any point is not a function of time, and thus the equation of continuity takes the simple form $\rho v r^2 = \text{Const}$. Hence, if the velocity in the shell is three times greater than that in the interior, the density in the shell must be one-third that in the adjacent portions of the central mass. Accordingly, the density factor alone favors hydrogen emission in the central mass, as compared to the shell, by a ratio of 9:1. In order to overcome and reverse the density effect by means of a change in electron temperature, the following approximate figures may be taken from Cillié's tabulated results:[8] If the electron temperature in the shell is as low as 1000°, it must exceed 20,000° in the interior; while if it is 5000° in the shell, it must exceed 50,000° in the interior. Therefore, if the flow is from the central mass into the shell, the observations require that some mechanism be found which can maintain a very much higher electron temperature in the interior than in the shell. This result is not altogether satisfactory.

Alternatively, the continuous flow could take place from the shell into the interior. In this case the shell must be regarded as a real concentration of matter expanding with the measured velocity. As it expands, material is expelled from it, presumably both outward and inward (Lyman-α pressure?).[9] Matter expelled inward forms what we have called the central mass, and its density can be much less than that of the shell itself. Hence the relative hydrogen emissivities of the shell and the adjacent interior can be accounted for merely on the basis of relative densities without the need for invoking a large difference of electron temperature. Depending upon the relative velocities of expansion and expulsion, the inner surface of the central mass, if it has one, could either approach

[9] S. Chandrasekhar, *Ap. J.*, **102**, 402, 1945.

or recede from the nucleus. In any event, the volume of the central mass would increase continuously at the expense of the shell.

In the foregoing brief discussion we have asked a simple question concerning the distribution of hydrogen emission in IC 418. In attempting to answer it, we have employed, in qualitative fashion, some equally simple spatiokinematic observations. These have led to the apparent necessity of postulating continuous flow of matter, either from the central mass into the shell, or vice versa. These two possibilities imply, in turn, distinct differences in the physical conditions prevailing in the two parts of the nebula, and it may happen that some observational test capable of distinguishing between them can be devised. In any event, application of modern equipment to the planetaries is beginning to clarify the nature of the problems which must be solved in order to understand their kinematic and spatial structures and is, at the same time, limiting the field of speculation.

I am indebted to L. H. Aller and R. Minkowski for reading this paper prior to publication and for several valuable suggestions.

A PECULIARITY OF THE SPECTRUM OF PI PEGASI

JESSE L. GREENSTEIN
MOUNT WILSON AND PALOMAR OBSERVATORIES
CARNEGIE INSTITUTION OF WASHINGTON
CALIFORNIA INSTITUTE OF TECHNOLOGY
Received October 27, 1952

ABSTRACT

The F5 giant star π Peg has large rotational broadening. Strongly exposed coudé spectra show relatively sharp, deep, absorption cores in H, K, and *Hα*. They are displaced longward from the stellar velocity by about +7 km/sec. Some effects of the cores may exist in the infrared *Ca* II triplet. It is possible that π Peg is a very close double, in which case the companion is a late A giant. More probably, the star has a shell of very low ionization. Rotation in an F5 giant results in a tendency for ejection to occur at much lower velocity than in the Be stars.

The fourth-magnitude star π Pegasi (HD 210459) is a possible member of the Ursa Major stream.[1] Its spectrum has been described as F5 II–III, strong lines,[2] with a luminosity near −2 mag. if it is a real member of the stream. See, below, a further remark on its luminosity. It has not been reported as a visual or spectroscopic binary. The trigonometric parallax is small. The spectrum shows wide shallow lines, presumably broadened by rotation. Heavily overexposed Mount Wilson coudé spectra showed that a very unusual structure, which has not changed substantially in the last year, exists in the cores of the H and K lines.

TABLE 1

VELOCITIES OF LINE CORES

Date	Line	Velocity (Km/Sec)	Width (Km/Sec)
8/12/51.....	K	+13.6	30*
9/12/51.....	K	+ 9.3	34*
8/13/52.....	K	+ 9.4	38*
8/12/51.....	H	+12.1	.....
9/12/51.....	H	+ 5.5	.....
8/13/52.....	H	+15.0	.....
9/11/51.....	*Hα*	+ 6.5	52
10/17/51.....	*Hα*	+ 7.5	.....
10/17/51.....	λ 8498	+14	170
10/17/51.....	λ 8542	+19	120
10/17/51.....	λ 8662	+23	170

* Mean width of H and K.

Spectra available cover the region from λ 3900 to λ 8800, at dispersions of 4.5A/mm in the blue and 9 A/mm in the red. Table 1 contains the measured velocities of the cores of H and K of *Ca* II, of the infrared triplet of *Ca* II, and of *Hα*. In addition, a very weak

[1] N. G. Roman, *Ap. J.*, **110**, 205, 1949.
[2] *Ibid.*, **112**, 554, 1950.

sharp line is seen at λ 5890; it is probably the interstellar D line. It has a velocity of −11.6 km/sec. Since the solar motion in this direction is about −14 km/sec, it is probable that the line is actually interstellar. More distant stars in the same direction have interstellar-line velocities of about −14 km/sec. The stellar velocity has been suspected of variability; it is given as +2 km/sec in R. E. Wilson's unpublished catalogue of radial velocities. Measures on one plate (8/11/51) give a stellar velocity of -6 ± 4 km/sec. (The lines are so poor that velocity measurements on these high-dispersion spectra are very unsatisfactory.)

Figure 1 shows the H and K absorption cores on plate Ce 7247 (8/12/51), together with a section of a normally exposed plate near λ 4100. It can be seen that the stellar lines are very greatly widened and that their width exceeds that of the cores of H and K. The width of the normal stellar lines at half-intensity was found to be about 185 km/sec (which corresponds to a rotational $v \sin i$ of about 100 km/sec) from measurements on a microphotometer tracing. The width of the H and K cores is only 34 km/sec, from measurements both on the plate and on tracings. The H and K cores show a positive displacement of +9 km/sec from R. E. Wilson's stellar velocity and an even larger positive displacement from my stellar velocity of −6 km/sec. There is little doubt that *Hα* has a relatively sharp core, which is apparently also displaced longward by about +5 km/sec. The reality of the core at *Hα* is demonstrated mainly by the sharpness of the longward wing of the line. *Hγ* and *Hδ* do not show any cores. There seems to be no emission at *Hα*.

The infrared spectrum shows very peculiar behavior on the part of the *Ca* II triplet. The lines are extremely wide, i.e., mainly stellar, but the measured velocities show a positive displacement (Table 1). Blending with Paschen lines P13, P15, and P16, which occur longward of each *Ca* II line, might be responsible. But P14 is not visible, and the *Ca* II line at λ 8542 is reasonably sharp. The lower states of the *Ca* II triplet are metastable and might be overpopulated in an extended stellar envelope. The [*Ca* II] emission lines are absent. The existence of cores in the infrared *Ca* II triplet should not be viewed as definitely proved.

Four old one-prism spectra are available. They do not reach the K line. They show that the stellar spectrum has not changed substantially in 36 years. On two plates (July 7, 1917, and July 6, 1920) there is an indication of sharp, longward-displaced cores in *Hγ* and *Hδ*.

Figure 2 shows the profile of the K line on Ce 7247 (8/12/51). Since the plate is very greatly overexposed for the continuum, the photometric accuracy is poor. Nevertheless, the sharp core is visible and reaches down to only 0.02 residual intensity. Such a deep line occurs nowhere else in the spectrum and strongly suggests the presence of a shell of *Ca* II with predominantly starward motion. However, if π Peg has a shell, it is an extraordinarily poor one, with only *Ca* II and *H* present.

We should first explore the possibility that π Peg is, in fact, a very close double. If a purely optical double, little can be said about the companion except that it has sharp and nearly equal H and K (i.e., it is of late A type) and is about 1 or 2 mag. fainter than the primary. If physically connected, the period could be too long to have permitted detection spectroscopically, in view of the poor lines of the primary. It could ultimately be found from the variation in velocity of the sharp cores belonging to the presumably less massive secondary. The maximum brightness of the secondary is about 1 mag. fainter than the primary, since Miss Roman classified π Peg as a "strong-line" star.[2] In her later work, Miss Roman[2] gives a spectroscopic parallax of 0".012, twice her cluster parallax of 0".006. Consequently, we shall adopt the revised luminosity of the primary as −0.2 mag. The secondary probably is not more than 2.5 mag. fainter, if it is to have any effect on the line profiles of H and K. It would then have an absolute magnitude somewhere between 0 and +2. It cannot be a late B star, because of the strength of K, and therefore would have to be a sharp-lined A or early F giant (a rather rare species). The other sharp

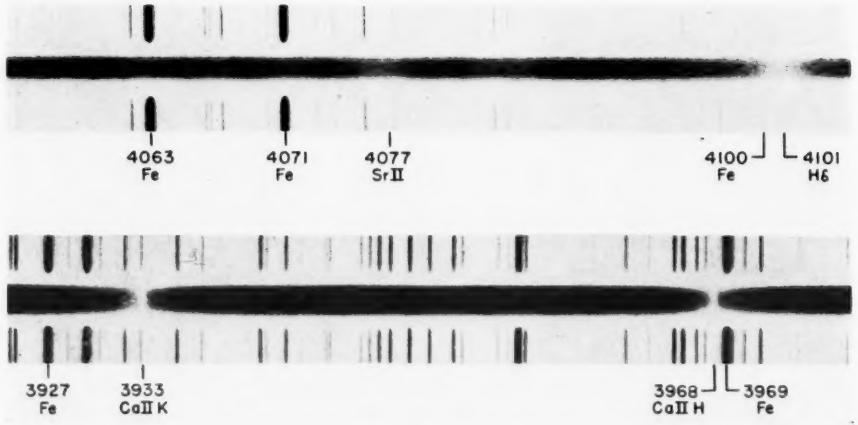

FIG. 1.—*Top*, normal exposure in λλ 4030–4100 region. *Bottom*, heavily overexposed spectrum of π Pegasi in H and K region. Dispersion in these reproductions, 0.4 A/mm, for both.

lines that one expects in a late A or F giant star are not found, so that I incline to believe that π Peg actually is a shell star.

The latest known star with a shell is 14 Comae,[3] of type A5. Its shell shows *Fe* I and some ionized elements, is relatively stable, and has small velocity. The shell of π Peg, an F5 star, could therefore consist mainly of *Ca* II, as far as level of ionization goes, although one might expect some of the resonance lines of *Fe* I. The large rotation of π Peg (about 100 km/sec) is unusual for an F5 star; it should be pointed out, however, that an unusually large number of stars called late A and early F giants on the Yerkes system show appreciable rotation on my coudé spectra. Of about twenty so far examined (types A5 III to F5 III) only two have sharp lines. The radius of π Peg is large, 27 $R\odot$ if we adopt a luminosity of -0.2 mag., and 55 $R\odot$ if -2 mag. The rotational velocity at which ejection occurs varies as $(M/R)^{1/2}$. If the masses are similar, the ejection phenomena occurring in a Be star at 300 km/sec would appear in π Peg at 130 km/sec, or 100 km/sec, depending on which luminosity is correct. The low level of ionization would prevent the appear-

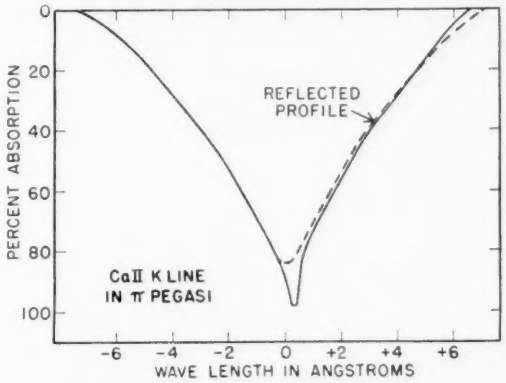

FIG. 2.—The profile of the K line in π Pegasi, on August 12, 1951. The dashed line is the shortward wing reflected about the center of the broad line. Note the longward-displaced deep core.

ance of hydrogen emission lines. The dominantly positive velocities of the cores observed are unexpected but remind one of phenomena in the solar chromosphere, and in G and K stars with emission *Ca* II lines.[4] Many of these show emission with $V > R$, indicating a positive displacement of the *Ca* II absorption cores.

Since so many of the A and F giants show rotation, it is possible that others will show incipient, weak shell phenomena. These stars play an important part in speculations on stellar evolution. They are rare (since they occur in the Hertzsprung gap) and deserve further study.

[3] O. Struve, *Stellar Evolution* (Princeton: Princeton University Press, 1950), p. 150; *Ap. J.*, **94**, 305, 1941.

[4] J. L. Greenstein, *Pub. A.S.P.*, **64**, 71, 1952.

A NEW DETERMINATION OF THE SPECTROGRAPHIC ORBIT OF CAPELLA*

OTTO STRUVE AND RUTH F. KILBY
Berkeley Astronomical Department, University of California
Received August 29, 1952

ABSTRACT

The velocity-curve of the G-type component of Capella was derived from forty-two spectrograms, thirty-seven of which were obtained with the Mount Wilson coudé spectrograph and five with the Mills spectrograph of the Lick Observatory. The elements resemble those by W. Struve, except that our velocities are systematically lower by 2.3 km/sec. The final elements are: $P = 104.023$ days (W. Struve); $\omega = 343°.04$; $T = \text{JD } 2433481.10$ (phase 21.246 days); $e = 0.0147$; $K = 26.38$ km/sec; $\gamma = 29.14$ km/sec; $a \sin i = 37{,}723{,}300$ km; $f(m) = 0.198\odot$.

TABLE 1

LIST OF STAR LINES

Adopted λ	Identification	No. of Plates	Adopted λ	Identification	No. of Plates
4006.635	*Fe*	17	4374.474	*Sc*⁺, *Fe*	2
4009.719	*Fe*	17	4379.240	*V*	2
4014.532	*Sc*⁺, *Fe*	17	4389.256	*Fe*	2
4017.129	*Fe* 7.097, *Fe* 7.161	17	4407.654	*V*	2
4017.473	⊙	17	4417.725	*Ti*⁺	35
4023.386	*V*⁺, *Co*	17	4433.232	*Fe*	36
4023.688	*Sc*	17	4442.351	*Fe*	35
4024.100	*Fe*	17	4447.730	*Fe*	35
4033.077	*Mn*	17	4455.867	*Mn* 5.817, *Ca* 5.901	35
4034.494	*Mn*	17	4457.494	*Ti* 7.439, *Mn* 7.549	35
4041.379	*Mn*	17	4461.662	*Fe*	1
4048.763	*Mn*, *Cr*	17	4468.502	*Ti*⁺	34
4055.553	*Mn*	17	4476.052	*Fe* 6.023, *Fe* 6.091	34
4066.986	*Fe*	17	4482.214	*Fe* 2.176, *Fe* 2.276	34
			4482.742	*Ti*, *Fe*	34
4121.327	*Co*	23	4490.780	*Fe*	2
4121.812	*Fe*, *Cr*	23			
4130.046	*Fe*	22	4515.345	*Fe*⁺	5
4136.530	*Fe*	23	4528.629	*Fe*	5
4139.929	*Fe*	22	4529.688	*Fe*	5
4147.677	*Fe*	21	4533.251	*Ti*	5
4153.391	*Fe*	21	4533.973	*Ti*⁺, *Co*	5
4158.800	*Fe*	23	4534.789	*Ti*	5
4159.188	⊙	23	4563.768	*Ti*	5
4175.645	*Fe*	18	4564.705	*V*⁺, *Fe*	5
			4565.520	*Cr*	5

The orbit of Capella has been determined previously by H. M. Reese,[1] at the Lick Observatory in 1901; by F. Goos,[2] at Bonn in 1908; by P. W. Merrill[3] with the inter-

* The spectrograms used in this investigation were obtained by Mr. Struve as a guest investigator at the Mount Wilson and Lick Observatories.

[1] *Lick Obs. Bull.*, 1, No. 6, 34, 1901.

[2] Dissertation, Bonn, 1908.

[3] *Ap. J.*, 56, 44, 1922.

TABLE 2

RADIAL VELOCITIES

Plate No.	Date	U.T.	Phase (Days)	Velocity (Km/Sec)	O−C (Km/Sec)
1	1929 Dec. 30	5:47	6.541	+38.3	−0.6
2	30	8:01	6.634	+37.9	−1.1
3	1930 Jan. 3	5:26	10.526	+43.1	−1.5
4	Sept. 2	12:29	43.774	+40.6	−1.1
5	1932 Aug. 15	11:35	29.576	+55.8	+0.6
6	15	12:30	29.614	+55.5	+0.3
7	16	12:04	30.596	+55.5	+0.6
8	1933 Aug. 10	11:55	77.520	+ 3.2	0.0
9	14	12:00	81.524	+ 3.5	−0.1
10	Sept. 5	11:30	103.503	+28.0	+0.3
11	Nov. 3	7:45	58.324	+19.6	+0.3
12	1938 Nov. 15	8:55	23.959	+57.1	+1.4
13	Oct. 16	10:55	98.065	+19.8	+0.5
14	1950 Sept. 23	12:25	88.161	+ 8.2	+0.7
15	23	12:46	88.176	+ 7.9	+0.4
16	Dec. 31	4:10	82.795	+ 3.4	−0.7
17	31	5:25	82.847	+ 2.7	−1.4
18	1951 Jan. 2	2:35	84.729	+ 3.4	−1.6
19	2	3:07	84.751	+ 3.1	−1.9
20	27	2:15	5.692	+37.0	−0.6
21	28	8:06	6.936	+39.6	+0.2
22	Feb. 19	3:47	28.756	+56.1	+0.6
23	19	4:49	28.799	+55.6	+0.1
24	20	6:35	29.872	+54.2	−0.9
25	21	4:11	30.772	+53.7	−1.1
26	Mar. 20	2:59	57.723	+19.8	−0.4
27	20	3:35	57.747	+21.0	+0.9
28	22	6:19	59.861	+17.5	+0.4
29	23	2:53	60.718	+16.8	+0.8
30	27	3:38	64.749	+11.5	+0.3
31	27	4:22	64.780	+11.8	+0.8
32	Aug. 15	12:15	102.085	+25.9	+0.5
33	16	12:14	103.085	+28.2	+1.1
34	18	12:16	1.063	+30.7	+0.4
35	Oct. 22	9:55	65.965	+ 9.3	−0.4
36	22	10:28	65.988	+ 9.6	−0.2
37	1952 Feb. 10	8:28	72.882	+ 4.7	+0.6
38	1950 Oct. 8	13:10	103.193	+29.0	+1.8
39	Nov. 5	8:32	26.977	+56.5	+0.7
40	5	8:34	26.978	+56.2	+0.3
41	12	8:40	33.982	+52.1	−0.6
42	Dec. 10	12:40	62.149	+14.7	+0.6
1c	1952 Apr. 15	4:30	33.694	+52.6	−0.3
2c	15	5:02	33.716	+52.4	−0.5
3c	16	3:16	34.642	+51.8	−0.4

ferometer in 1921; and by W. Struve[4] at Berlin-Babelsberg in 1937. In 1922 R. F. Sanford[5] concluded from the measurements of seven 60-inch spectrograms at Mount Wilson that Reese's period was not in error by more than 0.01 day, but that a decrease in the velocity of the center of mass by 0.9 km/sec was indicated.

In the present determination forty-two spectrograms were used, thirty-seven of which were obtained with the Mount Wilson coudé spectrograph and five with the Mills spectrograph of the Lick Observatory. Of the Mount Wilson plates, thirteen were prism and grating spectrograms taken by W. S. Adams and Theodore Dunham, Jr., between 1929 and 1938. The dispersion ranged between 3 and 5 A/mm. The remaining twenty-four were coudé grating spectrograms obtained from 1950 to 1952, with a dispersion of 2.8 A/mm. The Lick spectrograms were taken between August and December, 1950, with the Mills three-prism spectrograph, which has a dispersion of 10 A/mm (Nos. 38–42 in Table 2).

The Lick plates were measured in the region between λ 4501 and λ 4572. On all the twenty-four Mount Wilson grating spectrograms, and on seven of the thirteen prism

TABLE 3

NORMAL VELOCITIES

No.	Wt.	Plates	Mean Phase (Days)	Velocity (Km/Sec)	O−C (Km/Sec)
1	2	20, 1, 2, 21	6.314	+38.1	−0.5
2	1	3	10.526	+43.1	−1.5
3	1	12	23.959	+57.1	+1.4
4	2	39, 40, 22, 23, 5	28.276	+56.0	+0.4
5	2	6, 24, 7, 25, 41	30.772	+54.4	−0.3
6	1	4	43.774	+40.5	−1.1
7	2	26, 27, 11, 28, 29	59.221	+18.4	+0.4
8	2	42, 30, 31, 35, 36	65.000	+10.9	+0.1
9	1	37	72.882	+ 4.7	+0.3
10	1	8	77.520	+ 3.2	0.0
11	2	9, 16, 17, 18, 19	83.138	+ 3.2	−1.0
12	1.4	14, 15	88.169	+ 8.0	+0.6
13	1	13	98.065	+19.8	+0.5
14	2	32, 33, 38, 10, 34	103.586	+28.6	+0.8

spectrograms, two or three regions were measured. A list of the lines in each region is given in Table 1. Because of the peculiar suppression of the strong lines of *Fe* I, *Mg* I, *Ti* II, etc., in the G-type component,[6] the lines selected were chosen from the large number of faint absorption features belonging to the G star which are in no way complicated by the presence of the F-component.

Table 2 shows the final radial velocities and the values of O−C resulting from least-squares solutions. The plates were grouped into 14 normal places, as shown in Table 3, together with the residuals resulting from the final least-squares solution. The weight assigned to each normal place was roughly the square root of the number of observations included.

The orbit of this star is so nearly circular that ω and e are not well determined. Preliminary values of γ and K were found by the Lehmann-Filhés graphical method, and various preliminary elements were tried. The period had been determined accurately by

[4] *Zs. f. Ap.*, **17**, 61, 1939.

[5] *Pub. A.S.P.*, **34**, 178, 1922.

[6] *Ap. J.*, in press.

TABLE 4

ORBITAL ELEMENTS OF G-TYPE COMPONENT OF CAPELLA

Element	Reese (1896–1900)	Probable Error	Goos (1905–1907)	W. Struve (1935–1937)	Mean Error	Merrill (1920–1921)	O.S. and R.K. (1929–1952)	Mean Error
P	104.022 days	± 0.024 day	104.035 days	104.023 days	.....	104.022 days	104.023 days	.....
ω	117°.3	±18°.3	(Reese)	358°.14	±29°.83	114°.30	343°.04	±16°.22
T (JD)	2414899.5	± 5.3 days	(Reese)	2428076.000	± 8.599 days	2422596.79	2433481.10 ($21^d.246$)	± 5.01 days
e	0.0164	± 0.0055	(Reese)	0.0155	± 0.0094	0.0086	0.0147	± 0.0048
K	25.76 km/sec	± 0.12 km/sec	26.5 km/sec	26.05 km/sec	± 0.24 km/sec	.....	26.38 km/sec	± 0.10 km/sec
γ	+30.17 km/sec	± 0.104 km/sec	+30.79 km/sec	+31.43 km/sec	.....	.....	+29.14 km/sec	± 0.12 km/sec
$a \sin i$	36,847,900 km	.....	37,906,400 km	37,258,000 km	.....	.....	37,723,300 km	.....
i	.....	.....	.....	.....	.....	−41°.08	.....	.....
$f(m)$	.....	.....	.....	.....	.....	.....	0.198 ⊙	.....

Reese and W. Struve; Struve's value, 104.023 days, was adopted and not corrected in our solution.

A least-squares solution was made, using the method of T. Sterne[7] (in which the preliminary orbit is circular) with the initial values:

$P = 104.023$ days, $\gamma = 29.25$ km/sec,
$T_0 = $ JD 2433486.200 (phase 26.344 days), $K = 27.15$ km/sec.

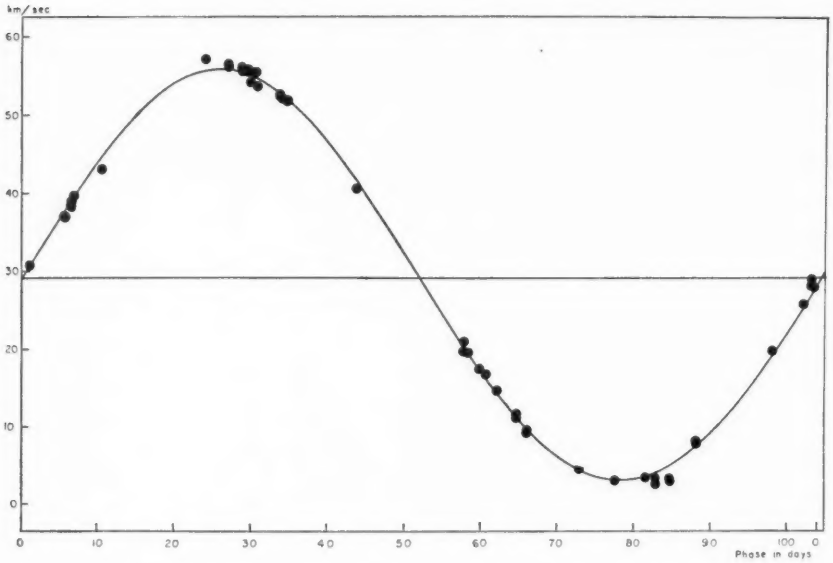

FIG. 1.—New velocity-curve of Capella with Mount Wilson and Lick observations

The value of T_0, the time of nodal passage, was, of course, read from the observed curve. The resulting preliminary elements were

$\omega = 339°.56$ $T = 20.248$ days
$e = 0.0138$ $\gamma = 29.14$ km/sec
$K = 26.37$ km/sec
Zero epoch = JD 2433549.856.

The values of e and ω are similar to those of W. Struve.

From these elements a second least-squares solution was made, using Schlesinger's method as modified by Paddock[8] for small eccentricity. The final elements and their mean square errors are given in Table 4. The value of $\Sigma\Delta v^2$, which is 29.2 for the single observations, was not altered appreciably by the second least-squares solution. The mean square error of a single normal point is ± 0.77 km/sec, and that of a single plate is ± 0.89 km/sec. Figure 1 shows the new velocity-curve. Three check observations obtained after the computations had been concluded are also shown in Figure 1; they are listed at the end of Table 2, with the letter "c."

[7] Harvard Reprint No. 222 (*Proc. Nat. Acad. Sci.*, **27**, 175, 1941).

[8] *Lick Obs. Bull.*, No. 274, 1915.

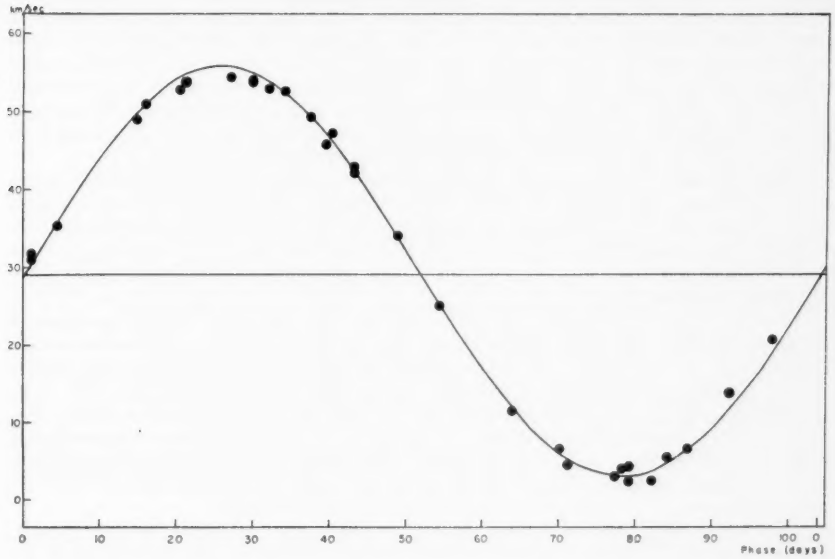

FIG. 2.—New velocity-curve of Capella with Reese's old Lick observations

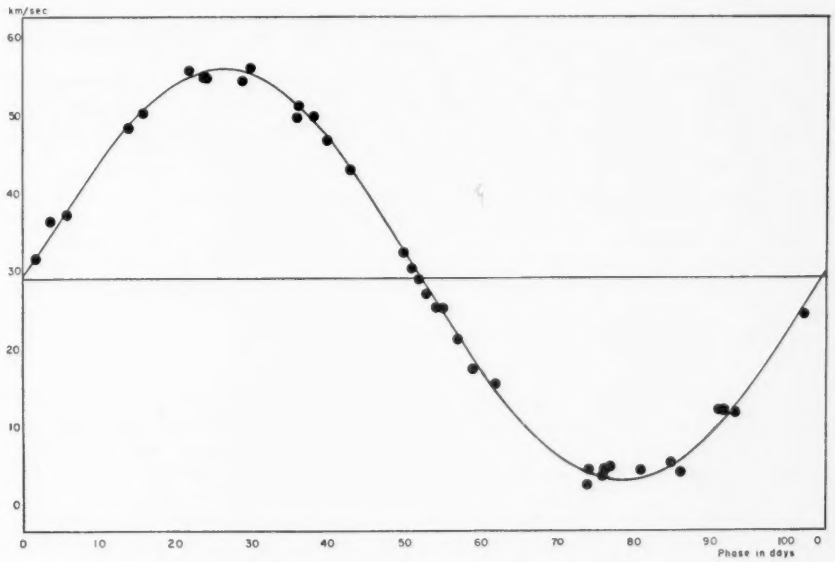

FIG. 3.—New velocity-curve of Capella with W. Struve's Berlin-Babelsberg observations

The departures of the observations from the curve just before maximum and just after minimum may represent deviations from elliptical motion. Every effort was made to fit them by trying various preliminary elements and by means of the least-squares solution, but no improvement was possible. The deviation near maximum is represented by only one plate. The four conspicuous deviations near minimum represent observations which were all made within a few days at Mount Wilson; without further check we cannot be certain that there is a real departure from elliptical motion.

Figures 2 and 3 are comparisons of our velocity-curve with the observations by Reese and W. Struve, respectively. In both comparisons the observations have been shifted vertically to allow for the rather large differences in γ; and the phases given in W. Struve's paper have been corrected for the fact that they were based on a period and zero epoch slightly different from his final ones. The new curve fits both Reese's and W. Struve's observations.

In Table 4 the final elements are compared with the elements derived by others. It is interesting that our elements resemble so closely those of W. Struve. It is especially striking that our value of ω is so near to that of W. Struve and so different from that of Reese. The latter is, however, supported by Merrill's determination with the interferometer. It should, however, be noted that Merrill[8] has stated that, "by taking $T = 2{,}422{,}563.76$, $\omega = 0.0°$, $e = 0.01$, the residuals in distance are considerably reduced, while those in angle are somewhat increased. With a circular orbit the representation is also very good." It would be of interest to secure a new set of measurements with the interferometer.

The differences in center-of-mass velocity are not definitely explained; our γ is 2.3 km/sec lower than that of W. Struve, and 1.0 km/sec below Reese's. To detect a possible systematic error in our observations, two spectrograms of the standard-velocity star Arcturus were taken on February 10, 1952, at almost the same time as plate No. 37 of Capella. Measurement of the same lines that were used for Capella yielded the mean velocity -5.74 km/sec, which agrees well with the accurate value, -5.62 km/sec, determined with the same instrument by Adams[9] in 1941. (The I.A.U. standard value, -5.1 km/sec, has not been revised since 1928.[10])

The systematic error of the prewar radial velocities obtained by W. Struve with Professor P. Guthnick's spectrograph attached to the 50-inch reflector, has never been determined. It is therefore not now possible to conclude that the γ-velocity is variable.

[9] *Ap. J.*, **93**, 11, 1941.

[10] *Trans. I.A.U.*, **3**, 171, 1928; *ibid.*, **7**, 311, 1950.

THE SPECTRA OF NOVAE NEAR MINIMUM

DEAN B. MCLAUGHLIN
Observatory of the University of Michigan
Received October 6, 1952

ABSTRACT

The bright-line spectra of the stellar components of novae near the end of decline to minimum show indications of change toward lower excitation during an interval of several years. The record is most complete for Nova Aquilae 1918. The recurrent novae, RS Ophiuchi and T Coronae Borealis, appear consistent with this picture.

Nova Sagittae 1913, in the late decline from its outburst in 1946, had hydrogen emission-absorption features similar to those of a Be shell star, but about 50 A wide.

Faint absorption lines on shortward edges of emission were found in Nova Aquilae 1918, and on one occasion Nova Persei 1901 had apparent absorption superimposed on its bright lines. Widths and structures of emission indicate velocities far below that of escape. Alternatively, Doppler broadening by turbulent motion or by the rotation of a gaseous ring (as in Be stars) is considered.

Possible structural variations, absorption, and occultation are believed to make measures of bright lines unreliable as indications of true radial velocities of old novae.

INTRODUCTION

The spectra of a number of old novae at minimum light were observed and described by Humason.[1] He found that all the objects he observed had continuous spectra of great violet extent and that several had, in addition, bright lines of hydrogen, *He* II, and occasionally *He* I. In addition, Wyse[2] identified a line at λ 4649 in the spectrum of Nova Aquilae 1918 as a blend due to C III. The present paper is a discussion of spectroscopic data on novae during the last 2 or 3 mag. of the decline and, so far as is possible, a comparison of the late declining stage with the stable minimum.

The available material consists chiefly of plates taken at Mount Wilson, some of which were used by Humason in his investigation. Several plates taken at Lick Observatory have been used, and the material is supplemented by several taken at Michigan. The data are chiefly qualitative, but detailed measures were made of spectrograms of Nova Aquilae 1918, Nova Sagittae 1913 (recurrent in 1946), and a few of Nova Persei 1901. Most of the measures and other studies of Mount Wilson plates were made during a visit in 1940. A few additional plates were measured there in 1951. The measures of Lick spectrograms were made in 1951.

The typical novae will be discussed first, followed by the recurrent objects. In each group the order of discussion will be that of the abundance of data, with the richest collections first.

TYPICAL NOVAE

NOVA AQUILAE 1918

Many spectrograms of Nova Aquilae 1918 were taken at both Mount Wilson and Lick Observatories in 1919 and following years. I selected, for study and measurement, 14 Mount Wilson plates, covering the interval 1919–1947, and two Lick spectrograms taken in 1937 and 1947. These are supplemented by four Michigan spectrograms, taken in 1941, 1942, 1949, and 1950.

Throughout the interval 1919–1950, bright lines have been visible in the spectrum of this nova. Though the composition of the emission spectrum has changed, the average intensity of lines relative to the continuum has not altered greatly. The apparent con-

[1] *Ap. J.*, **88**, 228, 1938.

[2] *Pub. Lick Obs.*, **14**, 140, 1939.

trast of bright lines with the continuum is a function of the width of the spectrum. The two Michigan plates taken in 1949 and 1950 are widened, and the lines appear more conspicuous than on unwidened spectrograms taken with the same instrument in 1941 and 1942. Actually, it is believed that no appreciable change occurred.

Changes in relative intensities of the lines have proceeded slowly, but are very conspicuous. Table 1 contains eye estimates made on a number of spectrograms. Only the year is given in the date column; more accurate dates are given in Table 2. In summary the changes were as follows. During 1919 and 1920 only 4686 *He* II could be seen. In 1921 $H\beta$ and $H\gamma$ were noted as traces; $H\delta$ was first seen in 1923. In 1922, *C* III 4650 emerged and was stronger than the hydrogen lines in 1923. By 1925, hydrogen had increased to equality with 4650, but 4686 was still the strongest line. From that time on, there has been a gain of hydrogen relative to *He* II. Lines of *He* I were occasionally noted

TABLE 1

EMISSION-LINE INTENSITIES IN NOVA AQUILAE 1918

Year	Mag.	$H\epsilon$	4026	$H\delta$	$H\gamma$	4472	4650	4686	$H\beta$
1919–1920	7.2–9.0	.....	.....	.....	.....	.....	.....	4	.....
1921	9.5	.....	.....	.....	Tr	.....	.....	4	Tr
1922	10.0	.....	.....	.....	0+	.....	1−	3	0+
1923	10.1	.....	.....	0+	1	.....	1+	3	0.5
1925	10.5	.....	.....	1.5	2+	.....	2	4	2
1934	10.7	0+	0+	1.5	2+	.....	2	3	1
1937	11.0	.....	p*	p	p	.....	p	p	p
1938	11.3	.....	.....	p	p	p	.....	p	p
1941	.....	.....	.....	0+	1.5	.....	0.5	1	0.5
1942	.....	.....	0+	1+	2+	.....	1+	1.5	1.5
1947	.....	p	p	p	p	p	p	p	p
1949	11.4	1	1	3	4	0.5	1.5	1.5	2
1950	.....	.....	.....	3	4	1	1	2+	2+

* "p" indicates line present and measured, but no estimate made.

from 1934 on, and have gained appreciably with the passage of time. There is no doubt that the excitation decreased considerably from 1920 to 1925, while the star faded approximately 2 mag. A further marked drop of excitation is indicated for the interval 1925–1950, while the star declined from magnitude 10.6 to 11.4, according to Steavenson's estimates.[3]

Results of measures of the spectrograms are presented in Tables 2–5. Table 2 contains data for the four strongest emission lines, as measured on individual plates. For each spectrum line a double column gives, first, the radial velocity for the center of the line and, second, the total width of the line, expressed in km/sec. A footnote to the table contains velocities and widths of additional lines and other features that were measured. The dispersion of each plate is indicated in the third column by a letter: a, b, or c, where a = approximately 35 A/mm at $H\gamma$; b = ≈80 A/mm; and c = ≈120–140 A/mm.

Table 3 gives the means of the radial velocities of the four strongest lines, taken separately for each of the three dispersions. The differences are not larger than we might expect for accidental errors of measures on features of such mediocre definition. Means are formed at the right of the table for each line, and at the bottom for each dispersion. The final weighted mean of all measures is −36 km/sec.

All three dispersions agree in showing a systematically negative velocity of 4686 *He* II relative to $H\beta$ and $H\gamma$. This may be attributed tentatively to absorption depressing the

[3] Numerous annual papers, e.g., *M.N.*, **82**, 51, 1922; *ibid.*, **110**, 621, 1950.

TABLE 2*

RADIAL VELOCITIES OF EMISSION LINES, NOVA AQUILAE 1918 (KM/SEC)

DATE	OBS.	DISP.	$H\delta$		$H\gamma$		4686		$H\beta$	
			V	W	V	W	V	W	V	W
1919 Sept. 1	Mt. W.	a	.....	.....	.....	.....	− 79	435	.....	.....
1920 Apr. 29	Mt. W.	a	.....	.....	.....	.....	− 26	362	.....	.....
July 3	Mt. W.	a	.....	.....	.....	.....	+ 5	413	.....	.....
23	Mt. W.	a	.....	.....	.....	.....	− 97	419	.....	.....
Aug. 27	Mt. W.	a	.....	.....	.....	.....	− 22	447	.....	.....
Oct. 2	Mt. W.	a	.....	.....	.....	.....	− 79	289	.....	.....
1921 July 13	Mt. W.	a	.....	.....	−21	.....	+ 23	524	− 19	398
1922 June 22	Mt. W.	a	.....	.....	+18	.....	− 43	514	− 20	.....
1923 Aug. 19	Mt. W.	b	− 56	462	− 7	405	− 47	623	− 47	.....
1925 July 30	Mt. W.	b	−114	316	−48	450	− 53	622	− 33	494
1934 May 21	Mt. W.	c	−132	545	−34	500	− 47	702	− 42	681
22	Mt. W.	b	− 77	443	−17	532	−129	600	+ 11	.....
1937 July 4	Lick	b	+ 34		−24	520	− 50	478	− 14	.....
1938 June 6	Mt. W.	b	+ 54	416	+14	399	− 44	.....	(−133)	.....
1941 Aug. 3	Mich.	c	+ 5	661	−26	678	− 72	563	+ 86	.....
1942 July 19	Mich.	c	− 85	572	−15	587	+ 5	829	+107	494
1947 Apr. 29	Mt. W.	b	− 55	572	.....	.....	+ 7	585	−106	448
Oct. 19	Lick	c	− 73	.....	− 5	701	−135	.....	− 12	721
1949 July 24	Mich.	c	− 61	610	−88	725	+ 52	786	+151	.....
1950 July 19	Mich.	c	− 94	787	+14	637	−125	667	+ 26	758

* The following additional lines and features were measured:

Additional lines:

1922 June 22: λ 4650, $V = +22$.
1925 July 30: λ 4650, $V = +43$.
1934 May 21: He, $V = +44$, $W = 340$; λ 4026, $V = +61$.
1934 May 22: λ 4650, $V = -58$.
1942 July 19: λ 4026, $V = -8$, $W = 537$.
1947 Oct. 19: λ 4472, $V = -90$.
1949 July 24: λ 4026, $V = -42$, $W = 402$; λ 4472, $V = +26$, $W = 742$.
1950 July 19: λ 4472, $V = +138$, $W = 590$.

Additional features:

1942 July 19: Outer longward emission edges; $H\delta$, +689; $H\gamma$, +739; $H\beta$, +786.
1949 July 24: $H\beta$ emission maximum, −289.

TABLE 3

MEANS OF RADIAL VELOCITIES OF NOVA AQUILAE 1918

LINE	VELOCITIES (KM/SEC)			WEIGHTED MEANS
	Disp. a	Disp. b	Disp. c	
$H\delta$	.....	−36 (6)*	−73 (6)	−48
$H\gamma$	− 2 (2)	−16 (5)	−26 (6)	−14
4686	−40 (8)	−53 (6)	−54 (6)	−45
$H\beta$	−20 (2)	−38 (5)	[+53 (6)]†	−30
Means	−30 (12)	−36 (22)	−51 (18)	−36

* Figures in parentheses indicate number of measures.
† Excluded from weighted mean.

shortward edge of hydrogen emission. The negative tendency of $H\delta$ may be due to blending with emission of *N* III 4097 and 4103.

Means of widths of the lines are given in Table 4. These correlate strongly with the dispersion. Since the earliest plates were obtained with the highest dispersion and the latest with the lowest, an apparent increase of width with time is seen in Table 2. The difference between widths measured on plates of dispersions b and c is believed to be due entirely to instrumental broadening, since the same difference appears during the time

TABLE 4

MEANS OF EMISSION WIDTHS, NOVA AQUILAE 1918
(KM/SEC)

Line	Disp. a	Disp. b	Disp. c
$H\delta$	.....	442 (5)	635 (5)
$H\gamma$	.....	461 (5)	638 (6)
4686	425 (8)	582 (5)	709 (5)
$H\beta$	398 (1)	471 (2)	664 (4)
Means	422	492	662

TABLE 5

VELOCITIES OF ABSORPTION LINES, NOVA AQUILAE 1918 (KM/SEC)

Date	$H\epsilon$	4026	$H\delta$	$H\gamma$	4472	4686	$H\beta$
1920 July 23	.....	.....	.....	−514	.....	.....	.....
1921 July 13	.....	.....	.....	−452	.....	.....	.....
1922 June 26	.....	.....	.....	− 68	.....	.....	+231
1923 Aug. 19	.....	.....	.....	+301	.....	.....	.....
1925 July 30	.....	.....	−333	.....	.....	.....	−300:
1934 May 21	−203	−154	−577	−370	.....	.....	−663
22	.....	.....	−417	−400	.....	.....	.....
1937 July 4	.....	.....	−214	.....	.....	.....	.....
1938 June 6	.....	.....	−242	−274	−425	.....	.....
1941 Aug. 3	.....	.....	−403	.....	.....	.....	.....
1942 July 19	.....	−374	.....	−353	.....	.....	+436
1947 Apr. 29	.....	.....	−394	−670	.....	−432	−488
Oct. 19	.....	.....	−590	.....	.....	.....	.....
1949 July 24	.....	−311	−504	.....	.....	.....	+159*
1950 July 19	.....	−374	−568	−373	.....	.....	.....

* Superimposed on emission line.

of overlap in the use of the two dispersions. The same statement cannot be made with equal confidence in regard to the difference between widths measured on plates of dispersions a and b, since the plates of highest dispersion themselves show a suggestion of increase in widths from 1919 to 1921.

Table 5 contains the collected measures of all absorption lines, real or suspected, that could be referred to elements that might be expected to show absorption. It is noteworthy that no absorption was found at 4686 *He* II, with the exception of one plate taken in 1947. Furthermore, absorption was measurable at $H\beta$ on only a few plates, probably in part an effect of the low dispersion there. On the other hand, it was often measured at $H\gamma$ and $H\delta$, and more commonly on plates of dispersion b than on those of lower dispersion. These absorption lines of hydrogen are believed to be mainly real, though they were always faint and somewhat difficult. Attention is called especially to a few measures of positively displaced absorption, which suggest the fall of erupted gases back to the star.

These features, however, must be classed as doubtful. A clearer example of probable absorption with positive displacement will be noted in the discussion of Nova Persei 1901.

The composition of the spectrum of Nova Aquilae in 1950 suggests a level of excitation roughly equal to that of a Wolf-Rayet star of class WC8. For purposes of calculation, we shall assume temperatures of 40,000° and 50,000° K. Although the assumption of black-body distribution may be considerably in error, some indication of the dimensions of the star may be obtained by the use of the formula

$$\log R = 8.52 - 2 \log T - 0.2\, M_{\text{bol}} .$$

The rate of expansion of the nebula gives a rather accurate distance of 430 parsecs.[4] With visual apparent magnitude 11.4, this gives visual absolute magnitude +3.2. We then obtain the results given in Table 6. The high velocities of escape are not readily

TABLE 6

DIMENSIONS AND ESCAPE VELOCITY FOR NOVA AQUILAE 1918

T ° K	Bolometric Correction (Mag.)	M_{bol}	R $\odot = 1$	Assumed Mass	Velocity of Escape (Km/Sec)
40,000	−3.8	−0.6	0.27	1.0	1190
				5.0	2600
50,000	−4.3	−1.1	0.22	1.0	1320
				5.0	2960

TABLE 7

MEASURES OF NOVA PERSEI 1901: NOVEMBER 4, 1937

Line	Width (Km/Sec)	Velocity of Center (Km/Sec)	Line	Width (Km/Sec)	Velocity of Center (Km/Sec)
$H\zeta$	1080	+299	4472	1253	+381
$H\epsilon$	1190	+195	4686	1152	+369
$H\delta$	1086	+234	$H\beta$	1532	+ 28
$H\gamma$	1394	+ 32			

compatible with the interpretation of emission widths in terms of continuing ejection of gases from the star. Consideration of alternative interpretations of emission widths is reserved for the discussion at the end of this paper.

NOVA PERSEI 1901

This is the only typical nova discussed here that continues to show large fluctuations long after the outburst. Humason has given estimates of the stellar emissions on a number of plates, and I have obtained estimates in substantial agreement with his. The details will not be reproduced here. Large changes of excitation evidently occur, as 4686 *He* II varies from weaker than, to much stronger than, the hydrogen lines. In general, *He* II is strongest when the star is brightest, but a few observations are discordant.

I have measured one Mount Wilson plate taken in 1937 and two taken on December 9, 1939. The latter are noteworthy as the only ones on which the emissions showed clear indications of internal structure.

Table 7 contains results of measures on the plate taken in 1937. Curvature of the lines

[4] Baade (*Mt. Wilson Report*), *Pub. A.S.P.*, **53**, 319, 1941.

introduces an uncertainty, but the systematic error due to this cause probably does not exceed 15 km/sec. The velocities of most of the emission lines on that date were very strongly positive.

On the two plates taken on December 9, 1939, the hydrogen lines have a remarkable appearance. In each there is a slight depression in a nearly central position, dividing the emission into two parts of unequal strength, the shortward half being much the stronger. The appearance closely resembles that of the lines in a Be star that shows V/R variation. This structure was entirely lacking at 4686 *He* II, which appeared of fairly uniform strength over its whole width. The structure is tentatively regarded as due to absorption overlying the center and longward halves of the hydrogen emission lines. If a particularly large eruption of gas had recently occurred at a velocity below that of escape, its return to the star could produce the observed profile. In this connection we may recall the occasional measurement of positively displaced absorption at $H\gamma$ and $H\beta$ in the spectrum of Nova Aquilae 1918.

The results of the measures of the two plates of December 9, 1939, are given in Table 8. Data for each feature are given in adjoining columns (*a* and *b*) for the two plates separately, in order to indicate the degree of accordance or discordance. The correction for curvature of lines is again somewhat uncertain, but it is very small for the second plate and probably not in error by more than 20 km/sec for the first. The velocities of most of the line centers are conspicuously negative, as contrasted with the decidedly positive velocities on November 4, 1937. The conclusion seems justified that very large variations occur in the apparent velocities of emission bands of Nova Persei. While it appears likely that these changes, as well as those of the structure of the lines, are related to the continuing variations of brightness of the star, it would probably require a very extended series of observations to establish the character of the correlation. Obviously, no conclusion can be drawn now concerning the actual radial velocity of the star.

TABLE 8

NOVA PERSEI: MEASURES OF TWO PLATES, DECEMBER 9, 1939

Line	Width (Km/Sec)		Velocity of Center (Km/Sec)		Velocity of Shortward Maximum (Km/Sec)	
	a	*b*	*a*	*b*	*a*	*b*
$H\zeta$	722	936	−131	− 15	−275	−283
$H\epsilon$	(568)	947	.....	+ 15	−272	.....
4026	.....	.....	.....	.....	−276	.....
$H\delta$	941	968	−128	− 67	−323	.....
4144	.....	.....	.....	.....	−286	.....
$H\gamma$	1149	1142	+108	− 5	−201	−210
4472	.....	.....	.....	.....	−363	.....
4640	.....	.....	.....	.....	−371	.....
4686	1042	879	−122	−105	.....	.....
$H\beta$	879	981	− 66	−117	.....	−176

The parallax of Nova Persei is known with considerable accuracy from the rate of expansion of the nebula. Baade and Humason[5] found a distance of 470 parsecs. With a visual apparent magnitude of 13.0 at minimum, this leads to a visual absolute magnitude of +4.6. Assuming $T = 50{,}000°$ K, we obtain:

Bolometric absolute magnitude = +0.3,
Radius = 0.115 ⊙,
Velocity of escape (mass = sun) = 1840 km/sec.

[5] *Pub. A.S.P.*, **55**, 260, 1943.

NOVA GEMINORUM 1912

Estimates of intensities of emission lines on a number of Mount Wilson plates are tabulated in Table 9. The nebular [*O* III] emissions faded rapidly in 1914 and were not recorded in 1915 or any following year. Hydrogen emission was present on all plates. From 1914 to 1917 the line 4686 *He* II was much stronger than the hydrogen lines. In 1933, when the star was next observed, 4686 and the hydrogen lines were all very nearly equal in strength. There is thus a clear indication of a decrease in excitation over an interval of sixteen years.

TABLE 9

EMISSION INTENSITIES IN SPECTRUM OF NOVA GEMINORUM 1912

Date	Mag.	*He*	*Hδ*	4200	*Hγ*	4363	4515	4542	4607	4640	4686	*Hβ*	4959	5007	Continuum
1914 Feb. 22	11.3	1	3	1	3	4	2.5		8	1.5	10	3	5	8	Strong
May 20	11:				0.5		1		2		3	1+	1	1	V. weak
1915 Feb. 12	11.7				1		1				2.5	0+			V. weak
Apr. 11	11.6		1−	1−	1.5		1		1−		4	1			Medium
1916 Feb. 12	12.0		1	0.5	1.5			0.5	0.5		5	1			Medium
1917 Mar. 24	11.8		1−	0+	1		0+	0+			4	1.5			Medium
1933 Nov. 19	14.5		1−		1−						1−	1−			Medium

TABLE 10

EMISSION INTENSITIES IN SPECTRUM OF NOVA CYGNI 1920
(Estimates by Milton Humason)

Date	Mag.	*He*	*Hδ*	*Hγ*	4363	4686	*Hβ*	4959	5007	Continuum
1923 May 7	11.5			2	0	2	5	60	100	Moderate
1927 June 18	14.1			2	0	5	5	25	60	Moderate
1934 Sept. 6	15.4	5	8	10	2	15	15	2	5	Strong
1936 June 17	15.5	2	12	15	2	12	8	0	2	Strong
1938 May 26	15.4		2	2		2	2			Strong

No expanding nebula has been observed about this star. From the strength of interstellar *Ca* II absorption, the distance is estimated as 790 parsecs. The visual apparent magnitude is about 14.8. The visual absolute magnitude (with an allowance of 0.4 mag. for interstellar absorption) is then +4.9. Dimensions are obviously similar to those of Nova Persei.

NOVA CYGNI 1920

Humason gave estimates of emission intensities on all the Mount Wilson plates from 1923 on. For completeness, and in order to facilitate comparison with other novae, his data are reproduced in Table 10. I did not make independent estimates of all the lines, but noted particularly the ratios 4686 : *Hβ* and 4959 : *Hβ*. These estimates are given in Table 11.

Interpretation of the tabulated data requires some assumption as to the relative amounts of line radiation from the expanding nebula or principal shell and from the close-in atmosphere of the star itself. Certainly, in 1923 and 1927, most of the radiation in all lines came from the nebula. On the plate taken in 1934, probably 4686 and the hydrogen lines were due chiefly to the atmosphere close to the star. The change in the ratio 4686 : *Hβ* from 1923 to 1927 tells us only how the excitation of the nebula changed.

From 1934 to 1938 there was little change in excitation of the star's atmosphere, but a slight decrease is suspected.

In 1944 Baade[6] observed a small nebula about Nova Cygni. Its diameter, 4".3, and the velocity of expansion of the principal shell, about 650 km/sec, give a distance of 1470 parsecs. The visual apparent magnitude, according to Steavenson,[3] has been about 15.5 for a number of years. With an allowance of 0.6 mag. for interstellar absorption, we obtain a visual absolute magnitude of +4.1.

In 1948 and 1949, Steavenson[7] found the star about 0.5 mag. fainter than in previous years. Further observations of the spectrum would be of interest.

NOVA LACERTAE 1910

I have estimated the emission lines of this star on several Mount Wilson plates. These data are given in Table 12. The evidence is noncommittal as regards change of excitation.

TABLE 11

EMISSION RATIOS IN SPECTRUM OF NOVA CYGNI 1920

Year	4686:$H\beta$	4959:$H\beta$	Year	4686:$H\beta$	4959:$H\beta$
1923	0.3	10	1936	1.3	.....
1927	1.2	6	1938	1.0	.....
1934	1.2	0.2			

TABLE 12

EMISSION INTENSITIES IN SPECTRUM OF NOVA LACERTAE 1910

Date	Mag.	$H\delta$	$H\gamma$	4472	4542	4650	4686	$H\beta$	4959	5007	Continuum
1913 Aug. 2	13:	.....	...	.....	.....	...	.....	.....	1	2	None
Sept. 29	13:	.....	Tr	.....	.....	0.5	0.5	Tr	1	3−	Weak
Oct. 30	13:	1.5	2	.....	.....	2	2	2.5	4	8	Strong
1915 Sept. 4	14:	1+	1.5	Tr	Tr	1	1.5	1.5	1+	3−	Strong
1936 July 22	14.4	.....	...	.....	.....	.....	.....	.....	.....	.....	Strong
1941 July 28	14.4	.....	Tr?	.....	.....	.....	Tr?	.....	.....	.....	Strong

When the nebular lines had become weak (1915), the composition of the spectrum resembled that of Nova Aquilae 1918 in 1950. By 1936 the emissions had subsided until they were no longer seen above the continuum. The plate taken in 1941 appears similar; the traces of $H\gamma$ and 4686 are extremely doubtful.

RECURRENT NOVAE

T CORONAE BOREALIS

The spectrographic record of this recurrent nova is voluminous, and it is beyond the scope of this paper to discuss it in any detail. Table 13 contains eye estimates of selected lines on several typical Michigan spectrograms taken during the interval August, 1946, to May, 1952. This includes the decline from the low secondary maximum that occurred in July, 1946, five months after the principal maximum. I have also had access to the extensive collections of spectrograms at Mount Wilson and Palomar Observatories and at Lick Observatory.

[6] *Pub. A.S.P.*, **56**, 218, 1944.

[7] *M.N.*, **110**, 622, 1950.

In August, 1946, there was a very rich emission spectrum with strong hydrogen, *He* II, and *N* III, and conspicuous *Fe* II, [*Fe* II], [*O* III], and [*Ne* III]. From that date until 1949 only slight changes of relative intensities occurred. Most noticeable was a fading of *N* III relative to hydrogen. Mount Wilson coudé spectrograms show that the red coronal line, 6374 [*Fe* X], was present in September, 1946, and January, 1947, but it had definitely disappeared by May, 1948. The coudé plates also show the presence of "shell" absorption lines of hydrogen and *He* I superimposed on the emissions during late 1946 and early 1947. By August, 1947, all these had disappeared, with the exception of 3889 *He* I.

From 1949 to 1952 the changes were more conspicuous. The nebular lines faded until, in May, 1952, only a trace of 4363 was seen. *N* III and *He* II weakened considerably relative to hydrogen, indicating a marked decline of excitation. In May, 1952, the spectrum appeared practically identical with a Mount Wilson plate taken in 1921. The only conspicuous emissions were those of hydrogen and *He* II 4686. All others had faded until they showed faintly or not at all above the continuum. Throughout the interval discussed, the bright lines were rather narrow, approximately 3 A in width.

In August and September, 1946, the class M spectrum was almost obliterated by a strong continuous spectrum of great violet extent. This had partially subsided by October, 1946. There is little or no indication of this "hot" continuum from 1949 on.

TABLE 13

INTENSITIES OF SELECTED EMISSION LINES IN SPECTRUM OF T CORONAE BOREALIS

Date	Mag.*	3869	*Hε*	4026	4097	*Hδ*	4233	4244	*Hγ*	4359	4363	4472	4584	4640	4650	4686	*Hβ*	5007	5015
1946 Aug. 23	8.6	2	3	3	7	10	3	1.5	12	1.5	2.5	5	4	10	4	20	18	2	2+
Sept. 17	9.3	2	1.5	1.5	3	5	1	1−	8	1	3	4	3	7	2	15	14	1.5	1
Oct. 2	9.5	2	2	1.5	3	5	1.5	1	8	....	2.5	3+	1+	5	0+	9	9	1.5	1−
1947 July 29	10.0	....	....	....	1.5	3	0+	0	5	....	2	1+	0+	3	1	7	7	1+	0+
1949 June 2	9.6	2.5	3	3	3+	10	1.5	1	10	0+	3	1	2	5	1−	12	12	2	1
1950 Apr. 16	10:	2	6	2	3	12	1.5	1	12	....	2.5	3	2+	5	2	12	18	2−	2−
1951 May 8	10:	2	6	1−	2	8	1.5	1+	12	....	1.5	1+	2−	4	1	10	15	1.5	2−
1952 May 4	10:	....	0	....	1	4	....	0.5	10	0?	0.5	0+	1−	2.5	....	6	12	....	....

* Magnitudes previous to 1950 are based on Pettit's light-curve, *Pub. A.S.P.*, **58,** 359, 1946; and **62,** 65, 1950.

RS OPHIUCHI

Occasional spectrograms of this recurrent nova were taken at Mount Wilson after 1933, the year of the second recorded outburst. These are supplemented by several Michigan spectrograms with dispersion of 140 A/mm at *Hγ*. Intensity classes, strong, medium, and weak, are given for several elements in Table 14. Numerical estimates have been made only for the ratio 4686 : *Hβ*.

Emission of *He* II was strong during the last part of the decline, late in 1933, but by June, 1934, it had become very weak. The nebular lines of [*O* III] likewise faded. From 1940 to 1946, *He* II was again strong, and [*O* III] reappeared. In 1947 the spectrum reverted to the appearance it had had in late 1934, with no *He* II or [*O* III] lines and weak *Fe* II, [*Fe* II], and *He* I emission. No further changes were recorded up to June, 1952, inclusive.

The star fluctuates irregularly between the 11th and 12th magnitudes between major outbursts. A categorical statement concerning the "stable" minimum condition would be somewhat hazardous. However, 4686 *He* II tends to be weak the greater part of the time between outbursts, and the excitation is appreciably lower than near the end of the decline from maximum. The appearance of the spectrum in 1952 is almost identical with that of a Mount Wilson plate taken in 1921, about 23 years after and 12 years before a major outburst.

NOVA SAGITTAE 1913; RECURRENT IN 1946

News of the second observed outburst of Nova Sagittae was distributed to the world with considerable delay. As a result, there is no information on the spectrum near maximum or during some 6 mag. of the decline. The increase of brightness was observed by Himpel on June 28, 1946. A rise from 11.9 to 9.3 mag. was recorded in about 3 hours. Light-curves have been published by Lohmann and Miczaika[8] and by Mrs. Mayall.[9]

TABLE 14

EMISSION SPECTRUM OF RS OPHIUCHI—INTENSITY CLASSES OF ELEMENTS

Date	Hydrogen	*He* II 4686	*Fe* II	[*Fe* II]	*He* I	[*O* III]	Observatory
1934 Mar. 1	Strong	$=H\beta$	Weak	Weak	Weak	Moderate	Mt. W.
Apr. 23	Strong	0.7 $H\beta$	Weak	Weak	Weak	Moderate	Mt. W.
May 3	Strong	0.5 $H\beta$	V. weak	.....	.....	Moderate	Mt. W.
June 24	Strong	V. weak	V. weak	.....	.....	Weak	Mt. W.
Sept. 26	Moderate	Absent	Weak	.....	.....	Absent	Mt. W.
1936 Aug. 16	Moderate	Absent	.....	.....	.....	Weak	Mt. W.
1937 May 19	Strong	0.3 $H\beta$	Weak	Weak	Weak	Absent	Mt. W.
1940 Sept. 25	Strong	0.8 $H\beta$	Weak	Weak	Weak	Weak	Mt. W.
1941 July 29	Strong	0.9 $H\beta$	Weak	Weak	Weak	Weak	Mt. W.
1942 July 16	Strong	0.6 $H\beta$	Moderate	Moderate	Weak	Weak	Mich.
1946 July 5	Strong	0.8 $H\beta$	V. weak	.....	.....	Weak	Mich.
1946 July 20	Moderate	0.4 $H\beta$	Weak	Weak	Weak	Weak	Mt. W.
1947 May 5	Moderate	0.2 $H\beta$	V. weak	.....	.....	.....	Mt. W.
1947 July 26	Strong	Absent	V. weak	V. weak	V. weak	Absent	Mt. W. coudé
1948 May 16	Strong	Absent	V. weak	.....	Tr	.....	Mt. W.
1949 June 24	Moderate	Absent	V. weak	Weak	.....	Absent	Mich.
1950 July 8	Moderate	Absent	Weak	V. weak	Weak	Absent	Mich.
1952 June 18	Strong	Absent	Moderate	Weak	Weak	Absent	Mich.

At the Lick Observatory, Dr. George Herbig obtained four spectrograms, on August 11, 13, 19, and 23. The first two were taken with the two-prism spectrograph and 3½-inch camera (dispersion about 140 A/mm at $H\gamma$) attached to the 36-inch refractor. The later two were obtained with the nebular spectrograph (dispersion 430 A/mm at $H\gamma$) on the Crossley reflector. During the interval of 12 days the star faded from magnitude 13.0 to 13.4. The steep decline had leveled off several days earlier. The last spectrogram is the best, and, so far as they go, the others confirm its general character and show no conclusive evidence of changes.

The results of the measurements of these plates are presented in Table 15. The appearance of the spectrum is unique among the known spectra of novae. Superficially, it resembles an extremely broadened spectrum of class Be. The hydrogen lines show conspicuous absorption about 15 A wide, with centers approximately undisplaced. These are superimposed centrally on emission with an over-all width of about 50 A, which contrasts sufficiently with the neighboring continuum to permit accordant measures of its outer edges. Dr. Herbig has called my attention to an apparently similar structure at λ 4233 *Fe* II, which shows on microphotometer tracings. He also points out an apparent continuous emission that extends from λ 3735 toward shorter wave lengths. This is probably to be explained as Balmer continuum combined with overlapping higher members of the Balmer series. Wide, weak absorptions at *He* I 4026 and 4472 have positive displacements of a few hundred km/sec. In addition, vague weak absorption with velocity −2400 km/sec appears at the shortward edges of $H\gamma$ and $H\delta$ emission. Similar absorp-

[8] *Veröff., Badisch. Landessternwarte, Heidelberg*, **14**, 77, 1946.

[9] *Harvard Bull.*, No. 918, 1946.

tion at $H\beta$ yields a velocity of -3700 km/sec. No other absorption or emission features could be established. The "4640" and nebular lines were specifically searched for, but no trace of them could be found.

On the first two plates, which are underexposed, the undisplaced hydrogen absorption lines appear somewhat narrower, 8–10 A in width, and the emissions are difficult to distinguish at all. It is not certain that these differences of appearance represent a real change in the spectrum.

The undisplaced wide absorption lines are too strong to be interpreted as due to pure rotational broadening of an intrinsically sharp line formed in a thin reversing layer. The fact that they are visible at all, with such a width, appears to imply turbulent broadening. Stark effect seems less probable, since the lines do not have diffuse wings.

TABLE 15

VELOCITIES OF FEATURES IN SPECTRUM OF NOVA SAGITTAE 1913

	$H\zeta$	$H\epsilon$	4026	$H\delta$	$H\gamma$	4472	$H\beta$
	August 11						
Short edge of absorp.	.....	.....	.....	− 356	− 193	.....	− 650
Center of absorp.	.....	.....	.....	− 36*	+ 50*	−696	− 242*
Long edge of absorp.	.....	.....	.....	+ 285	+ 292	.....	+ 167
Long edge of emission	.....	.....	.....	.....	+ 732	.....	.....
	August 13						
Center of wide absorp.?	.....	.....	.....	.....	− 975	.....	.....
Short edge of emission	.....	.....	.....	.....	− 792	.....	.....
Short edge of absorp.	.....	.....	.....	.....	− 355	.....	− 488
Center of absorp.	.....	.....	.....	− 400	− 45	.....	− 199
Long edge of absorp.	.....	.....	.....	.....	+ 207	.....	+ 251
Long edge of emission?	.....	.....	.....	.....	.....	.....	+ 715
	August 19						
Center of wide absorp.	.....	.....	.....	−2310	−2500	.....	.....
Short edge of emission	.....	.....	.....	−1590	−2070	.....	.....
Short edge of absorp.	.....	.....	.....	.....	− 750	.....	.....
Center of absorp.	.....	.....	+495	+ 135	− 111	+554	.....
Long edge of absorp.	.....	.....	.....	.....	+ 765	.....	.....
Long edge of emission	.....	.....	.....	+1502	+2160	.....	.....
	August 23†						
Center of wide absorp.	.....	.....	.....	.....	−2440	.....	−3700
Short edge of emission	−1350	−2120	.....	−1950	−1830	.....	−2560
Short edge of absorp.	− 432	− 693	.....	− 540	− 618	.....	.....
Center of absorp.	+ 122	− 53	+204	− 154	− 97	+320	.....
Long edge of absorp.	+ 731	+ 405	.....	+ 526	+ 484	.....	.....
Long edge of emission	+2100	+1610	.....	+1860	+1890	.....	+2640

* Mean of absorption edges.

† Additional measures: $H\eta$ absorption, +288; $H\theta$ absorption, +35.

The lack of displacement of these lines is, interestingly enough, a feature in common with two other recurrent novae, though the extreme width in Nova Sagittae sets it apart from the others. T Coronae Borealis had narrow "shell" absorption lines nearly central on hydrogen and *He* I emission during the latter part of 1946. RS Ophiuchi near its maximum in 1933 had narrow strong absorption, only slightly displaced in the negative sense and superimposed almost centrally on its broad and hazy emission bands. Some years after its outburst, RS Ophiuchi also had a fine "shell" absorption spectrum with small displacement, recorded on a coudé plate in 1947.[10]

Two low-dispersion Mount Wilson plates of Nova Sagittae taken in 1934 and 1943, when the star was at minimum, show a strong continuous spectrum with great violet extent. On the plate taken in 1934, $H\beta$ emission is suspected; in 1943 the spectrum appeared purely continuous. There was nothing to distinguish it from the spectra of any of several other old novae.

Nova Sagittae has a measured parallax of 0".013 and proper motion of 0".080 per year.[11] It has been regarded as a "dwarf nova." The absolute magnitude at minimum is about +11, which, with a temperature of 30,000° K or higher, indicates a radius of about 0.01 ⊙ or less. The star should probably be regarded as a true white dwarf. It may represent a class truly intermediate between U Geminorum stars and novae.

DISCUSSION

The decline of Nova Aquilae 1918 through the last 2 mag. was accompanied by a conspicuous decrease of excitation. Nova Geminorum 1912 probably behaved similarly, and a like effect is suspected in Nova Cygni 1920. Among the recurrent novae, T Coronae Borealis showed a decline of excitation after its nova component had become fainter than the M-type star. RS Ophiuchi behaved similarly but showed an increase of excitation a few years later, followed by a decline after several more years. Though the number of cases may be considered perilously small for generalization, it is tentatively concluded that the end of the decline of light (the last 1.0–1.5 mag.) is due chiefly to a lowering of temperature of the superficial layers of the star.

The change of visual magnitude implies a much greater bolometric variation. If we assume black-body distribution, a decrease of temperature from 80,000° to 40,000° K without change of radius would produce a change of 3.0 in bolometric magnitude. The bolometric corrections for these two temperatures differ by 1.8 mag., which gives a change of 1.2 visual mag. Such a change of temperature appears consistent with the observed variation in the spectrum of Nova Aquilae. A simultaneous decrease of radius would be required to explain a much larger difference of magnitude, unless we are prepared to admit improbably high temperatures.

All the novae observed in their late decline, after the ejected principal shell has faded, have shown somewhat widened bright lines that originate close to the central star. There is no indication that the widening of these lines is produced in any other way than through Doppler effect, though the exact mechanism is not known.

We consider, first, the possibility that the widening is due to symmetrical radial ejection of gas from the star: in other words, that a "gentle" nova-like activity continues long after the star has subsided. The frequent measurement of faint absorption on the shortward edges of hydrogen emissions in Nova Aquilae 1918 is favorable to interpretation as a continued P Cygni-like behavior.

The computed velocities of escape, of the order of 1000–2000 km/sec, are not readily compatible with ejection of gases at the low speeds indicated by the measures of emission-line widths. In Nova Aquilae the velocity is approximately 250 km/sec; in Nova Persei 500 km/sec, only about one-fourth the velocity of escape. If the widths indicate the terminal velocities of atoms that leave the star with velocities above that of escape, then it is difficult to see how we can have lines with measurable edges at all. At best they

[10] Sanford, *Pub. A.S.P.*, **59**, 331, 1947.

[11] Van Maanen, *Mt. W. Contr.*, No. 321, 1926.

should be extremely vague maxima on a broader and more vague band, whose outer edges would merge imperceptibly with the continuum. It seems unlikely that any of the gas that produces the bright lines in the postnova stage ever escapes from the star. The apparent absorption lines that were occasionally measured on the longward edges of emission in Nova Aquilae suggest a return of gas to the star; but the most striking indication of return is given by the apparent absorption superimposed on the emissions of Nova Persei as observed on December 9, 1939.

In view of the preceding discussion, turbulence in a chromosphere of rather limited extent appears to be a tenable hypothesis of widening. Continuous prominence activity, with eruption and return of gases at the speeds indicated by the measures, is compatible with the observations of widening, variable structure and both negatively and positively displaced absorption. We may also entertain the possibility that scattering of the bright-line radiation by free electrons in the outer layers of the atmosphere produces a "magnification" of the line widths, after the manner suggested by Münch[12] in the Wolf-Rayet stars.

Another possible mechanism is rotation of the star and its emitting atmosphere, which may be a chromosphere of rather small extent, a fraction of the stellar radius, or perhaps a ring of gas at a distance of several radii. If the emission originates in a chromosphere close to the star and if the axis is perpendicular to the line of sight, the velocities indicate a rotation period of about 1 hour for Nova Aquilae.

The structure of the emissions of Nova Persei resembles that of the lines of Be stars sufficiently to suggest a like origin, perhaps in a detached rotating ring or shell. If we assume inclination 90° and a stellar mass of 1 $\odot$, the radius of the ring about Nova Persei is 5×10^5 km and that of Nova Aquilae is 2×10^6 km. These figures are about ten times the computed radii of the respective stars. The result is not unfavorable to the gaseous-ring hypothesis, particularly when we note that a different inclination and a reasonable decrease of the assumed mass would yield smaller radii.

Nova Sagittae 1913–1946 is of special interest in this connection, because of the very great width of its emissions and their close resemblance to those of Be stars. If we take the velocity as 2000 km/sec, mass 1 $\odot$, and inclination 90°, the radius of the ring is 3.4×10^4 km, of the order of five times the radius of the star, in good agreement with the ratio of rings to stars of class Be, as suggested by Struve and Wurm.[13]

At present there appears to be no evidence that will permit a choice between these hypotheses. Observations with much higher dispersion will almost certainly be required if any significant advance is to be made.

It should be pointed out that measurements of radial velocities of the postnova emission lines cannot be relied upon to yield the radial velocities of the stars. Even if the changes of structure in the bright lines of Nova Persei are a unique exception, the probable presence of absorption superimposed upon one or the other edge of the emission could vitiate measures. If absorption were lacking, occultation of part of the atmosphere by the star could produce asymmetries of lines, since it is not to be expected that the velocities of ascending and descending currents or prominence material would precisely cancel. Determination of proper motions would appear to offer a more hopeful approach to the problem of space motions and population affiliations of novae.

I am grateful to the past and present directors of Mount Wilson and Palomar Observatories and to Dr. Milton Humason for the use of the Mount Wilson spectrograms. The director of the Lick Observatory and Dr. George Herbig very kindly placed the Lick spectrograms at my disposal.

It is also a pleasure to acknowledge a grant for travel expenses, from Faculty Research Funds of the Horace H. Rackham School of Graduate Studies, University of Michigan. The Michigan spectrograms of low dispersion were secured with a camera lens of 3 inches in focal length, purchased under an earlier grant from the same source.

[12] *Ap. J.*, **112**, 286, 1950.

[13] *Ap. J.*, **88**, 105, 1938.

ERUPTIVE PROMINENCE ASSOCIATED WITH LIMB FLARE OF MAY 8, 1951

THOMAS J. BARTLETT, BRUNO WITTE, AND WALTER ORR ROBERTS

Chamberlin Observatory, University of Denver, and High Altitude Observatory
of Harvard University and University of Colorado

Received October 31, 1952

ABSTRACT

A solar prominence of violently eruptive character accompanied the limb flare of May 8, 1951. Measures of several knots in the prominence show that forces large compared with solar gravitation were present, but no simple laws of motion emerge from the data.

INTRODUCTION

The limb flare of May 8, 1951, and the large prominence associated with it were observed at the McMath-Hulbert Observatory and at the Sacramento Peak Observatory in New Mexico. An excellent description of the behavior of the flare and solar prominence has been given by Dodson and McMath.[1] According to their report, the flare, which was associated with the great sunspot of mid-May, 1951,[2] exhibited typical flare characteristics of great broadening of $H\alpha$ and rapid rise of brightness and was accompanied by a sudden ionospheric disturbance and a sharp rise in 200 Mc/sec solar radio noise. Dodson and McMath point out that the accompanying prominence exhibited an upward motion that reached the order of 500 km/sec and line-of-sight velocities exceeding 228 km/sec.

The measures included in this paper refer only to the prominence described by Dodson and McMath, and not to the later prominence from the same region that accompanied a later and smaller limb flare. Our work is confined to measurements of position projected onto the plane perpendicular to the line of sight.

LIMB FLARES OF MAY 8, 1951

Films were taken on May 8, 1951, by the observers at the Harvard College Observatory station at Sacramento Peak both in the "flare patrol camera" and in the prominence camera. These two instruments, designed and built at the High Altitude Observatory, utilize narrow-band birefringent filters centered on $H\alpha$. The former uses a Baird filter of band half-width 1.2 A.; the latter uses a filter built by John W. Evans of band half-width 4 A. Films from these cameras were lent to the High Altitude Observatory during the summer of 1951 and were measured by one of the authors (Bartlett). The analysis of these measures has been a joint work of the three authors.

The film records show limb flares that reached maximum at 15:08 U.T. and 15:47 U.T. Measurements of the flares tabulated by Mr. George K. Schnable, observer at Sacramento Peak, are shown in Table 1.

The solar region from which the flares arose was apparently just beyond the solar limb, as already mentioned by Dodson and McMath. The large sunspots did not appear at the east limb of the sun until the following day. The rarely observed yellow coronal line, usually associated with abnormally intense solar activity,[3] was recorded in coronal

[1] *Ap. J.*, **115**, 78, 1952.

[2] See photograph in *Pub. A.S.P.*, **63**, 1951 (facing p. 161).

[3] Roberts, *Ap. J.*, **115**, 488, 1952.

spectra photographed at Sacramento Peak on May 9, and at Climax on May 10. If the sky clarity had been better on May 8 at Sacramento Peak or Climax, the yellow coronal line might have been observed. On May 9 Climax had no observations, and on May 10 Sacramento Peak had none. The data suggest, in spite of these gaps, that the center of the active region had not yet reached the limb on May 8.

Climax spectra taken at 15:37 U.T. on May 8 revealed the broadened emission line of the flare as well as the high line-of-sight prominence velocities reported by Dodson and McMath. The green and red coronal lines on all Sacramento Peak and Climax spectra for May 8, 9, and 10, gave evidence of the active region.

Solar radio noise bursts occurred in conjunction with the first flare on May 8, not only on 200 Mc/sec, at about 15:09 U.T., as reported by Dodson and McMath, but also at 2800 Mc/sec, at 15:05 U.T., as reported by A. E. Covington,[4] of the National

TABLE 1*

LIMB FLARES OF MAY 8, 1951

No.	Start (U.T.)	Max. (U.T.)	End (U.T.)	Brightness *a*	Area *b*	P.A. *c*	R.V. *d*
1.....	15:05	15:08	15:20	35	556	78°	1.04
2.....	15:40	15:47	16:00	20	268	79°	1.03

* The letters in the last four columns have the following meaning:
a = Brightness on an arbitrary scale of 0 faintest to 35 brightest.
b = Area in millionths of the area of the solar disk ($[A \times 10^6/\pi R^2]$, where A = measured area, R = radius of projected image of the sun).
c = Position angle of radius vector to center of flare, measured from the north end of the solar rotation axis toward the east.
d = Magnitude of radius vector of center of flare, expressed in units of the solar radius.

Research Council at Ottawa, Canada. Moreover, a sudden enhancement of atmospheric noise at 27 kc/sec was reported by Ellison at 15:06 U.T., and to the accompanying flare Ellison attributed the great magnetic storm of May 9 that began at 17:00 U.T.[5] The second flare, at 15:40 U.T., caused a much weaker SID reported by the Central Radio Propagation Laboratory of the National Bureau of Standards from 15:50 to 16:20 U.T.[6]

The same solar region exhibited a limb flare at the west limb of the sun on June 19, 1951, and more than 60 disk flares in its May passage of the solar disk.[7]

ASSOCIATED PROMINENCE MEASURES

The observers at Sacramento Peak took photographs through the prominence camera at the rate of four frames/min before 15:13 U.T. and at the rate of 12 frames/min thereafter. The filter, as already mentioned, has a half-width of about 4 A, so that material with the higher Doppler velocities reported by Dodson and McMath would not be visible in the filter.

Our measures encompass four knots, labeled A, B, C, and D. For each frame of the film we measured the positions, x and y, corresponding to the known times, t. (The co-ordinate system is defined in the appendix.) Figure 1 shows the trajectories of the four knots, with each of the positions shown by a small dot. The individual knots are also identified in Figure 3.

[4] Private communication.
[5] *Observatory*, **72**, 62, 1952 (transcript of verbal report to Royal Astron. Soc.).
[6] CRPL F-Series, Pub. F 82, June, 1951, p. 43.
[7] CRPL F-Series, Pub. F 83, July, 1951, p. 46.

We then fitted each of the eight data sequences, four of $x = f(t)$, and four of $y = f(t)$, with a series of orthogonal Tchebycheff polynomials in t, using the least-squares method described by Birge.[8] In the appendix we give the polynomials used in our analysis. These methods have the advantage of allowing us to estimate quickly (*a*) the lowest power of t that is needed in the polynomial to allow an adequate fit to the observed data; and (*b*) the errors of x and y and of their time derivatives.

In Figure 1 we have shown, at the origin of the vectors, positions of best fit to our observations computed from the polynomials for equal time intervals. The origin of each vector is actually a tiny rectangle that gives the computed standard errors in x and y for the positions. For all practical purposes here, these rectangles may be regarded as points.

The vectors of Figure 1 show the magnitude and direction of the projected accelera-

[8] *Rev. Mod. Phys.*, **19**, 298, 1947.

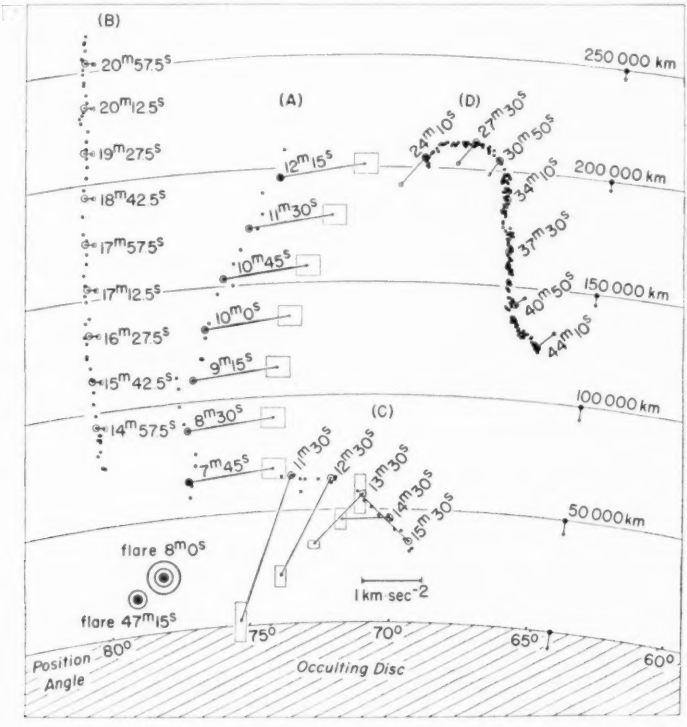

FIG. 1.—Acceleration vectors derived for selected knots *A*, *B*, *C*, and *D* in prominences associated with limb flares of May 8, 1951. The origin of each vector lies at the computed position of each knot at the indicated equally spaced times. All times are 15h U.T. plus the indicated time.

Note that in knots *A* and *B* the acceleration vectors are equal, reflecting the fact that a second-order polynomial satisfied our criteria of adequate fit to the measured points, which are shown as small black dots. For *C* and *D*, third-order fits were necessary, so that the accelerations vary with time, as shown.

The scale of the acceleration vectors is the same for all vectors. The accelerations due to solar gravitation are given for the appropriate heights at the right-hand margin.

tions derived from the eight polynomials representing the four knots. Even though it is impossible from the observations available to us to evaluate line-of-sight accelerations, one might reasonably hope to find simple relationships affecting the behavior of the accelerations in the plane perpendicular to the line of sight if the force field controlling the motion of the prominence bears any simple relationship to the flare position or to the center of the sun.

As is evident from Figure 1, no such simple relationship appears. The two-dimensional accelerations computed for the four knots do not show similar patterns from knot to knot, nor do they exhibit recognizable systematic relationships to the position of the flare or of the center of the sun. The magnitudes, as shown, generally exceed the value of solar gravitation marked at the right of the figure. The ends of the vectors terminate at the center of the "error rectangle" that indicates the standard errors of the two components of acceleration, for the order of the polynomial used. For knots B and D these errors are small, as shown by the scarcely discernible rectangles.

The projected accelerations of knots A and B are constant within the accuracy of the observations. Carrying the $x = f(t)$ and $y = f(t)$ polynomials beyond the second degree did not, in these cases, substantially reduce the standard errors of the fit of the polynomial to the original measures. But going to the higher degree would have increased the degrees of freedom utilized in the fit. The changing accelerations of knots A and C reflect the fact that it was necessary to go to the third order to obtain satisfactory fits in those cases.

In order to show the effect of going to the next-higher-order fit, where it was not required by the data, we also analyzed knot B, using a polynomial of degree 3. The barely more accurate fit showed the results given in Figure 2 (same scale as Fig. 1). However, one must recognize that the data do not call for the results shown in Figure 2 but are adequately described by the single mean projected acceleration of Figure 1. One should use caution in interpreting the reality of accelerations derived where the fit involves a higher number of degrees of freedom than is demanded by the data.

Inspection of the pattern of projected accelerations shows that no simple force law related to the position of the flare or the solar center is obeyed by the eruptive prominences associated with the limb flares of this study. The following conclusions are evident:

a) The knots were subject sometimes to accelerations very large compared with gravitation, and to larger accelerations than we are familiar with from the literature except for those cases where actual discontinuities in prominence velocities were assumed in the reduction procedure.

b) In case B, solar gravitation appears roughly balanced, that is, the net acceleration in the direction of gravity was small compared to the gravitational acceleration shown at the right. In this case a substantial acceleration perpendicular to gravitation remained. In cases A, C, and D no such "balance" existed.

c) For knot A the component of acceleration along the trajectory was away from the sun, showing that the knot increased its speed as it erupted. Both C and D in their later stages also experienced upward accelerations.

d) Neither the location of the flares nor the sun's center acted as a focus of a central force field for the motions examined.

We found it unnecessary to assume the existence of sharp discontinuities of velocity in order to obtain suitable fits to our data, even though these discontinuities have been reported by some authors.

The projected velocity of knot A reached 600 km/sec. It surpassed the velocity of escape at a height of about 160,000 km from the solar limb. Knot B kept a constant velocity of about 450 km/sec. Knot C decreased its descent velocity from about 320 to about 200 km/sec. Knot D showed a range of velocities from 20 to about 240 km/sec.

Figure 3 shows the flares and associated prominences at various stages in their development, with knots A, B, C, and D indicated.

We wish to thank the Chancellor's Education Fund of the University of Denver for support of the measurements and other work of one of the authors (Bartlett). Our gratitude is also due the Air Force Cambridge Research Center, to Donald H. Menzel, and to the observers at Sacramento Peak Station of Harvard College Observatory for use of films employed in this analysis. Parts of the research were assisted by Research Corporation and the Office of Naval Research. All analysis work was carried out at High Altitude Observatory at Boulder, Colorado.

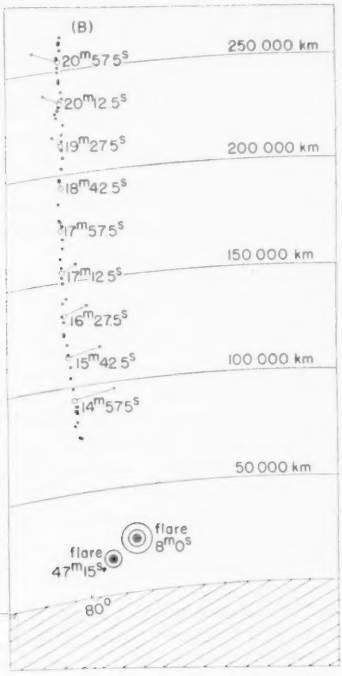

FIG. 2.—Similar to Fig. 1, for knot *B* only, showing acceleration vectors derived from use of a higher-order fit than required by the data. As described in the text, the distribution of the measured points did not, in this case, justify the use of a third-order fit, so that the varying accelerations shown cannot be regarded as necessary to explain the motion of knot *B*.

APPENDIX

We give here the expansions involving the Tchebycheff orthogonal polynomials, in terms of which we have expressed $x = f(t)$ and $y = f(t)$. We have replaced t by ϵ, according to the substitution shown, for the sake of convenience and in accord with the procedures given by Birge.

All errors shown are standard errors of the coefficients. Here x and y are the Cartesian position co-ordinates, the origin of the x and y system being on the limb of the sun at the position angle P.A. = 71°; the x-axis, tangent to the limb, is measured positively in the direction of decreasing position angles; the y-axis, the radial direction, is measured positively with increasing heights above the limb.

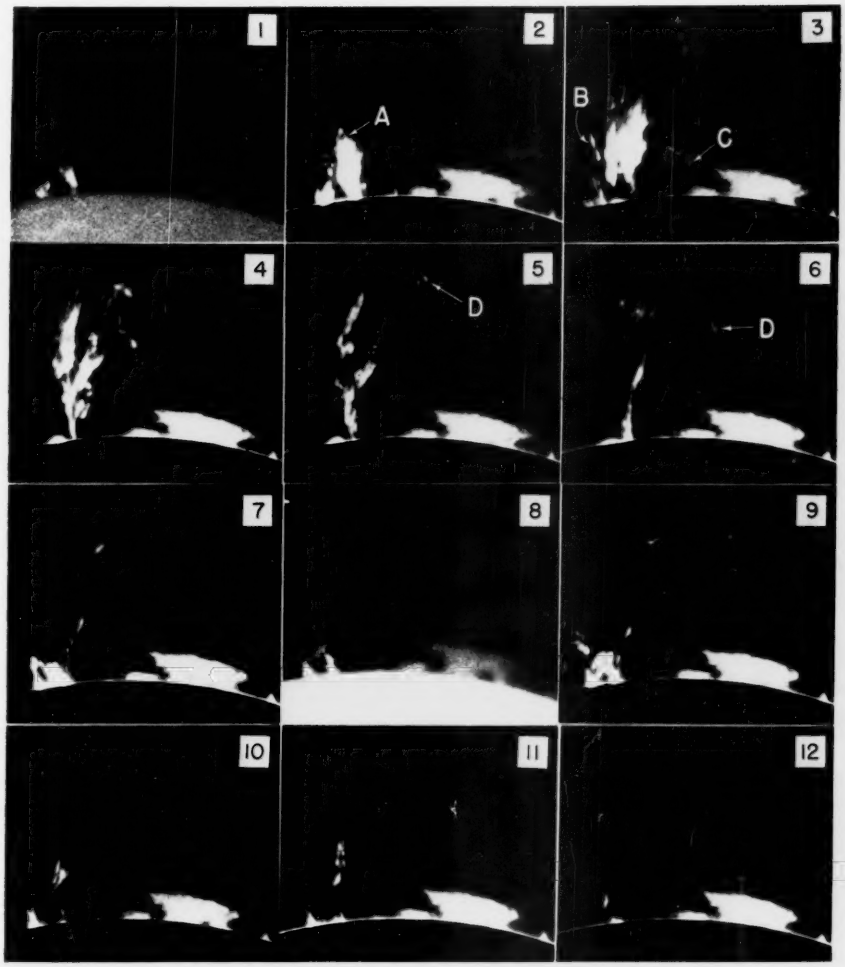

FIG. 3.—Photographs in *IIa*, showing development of limb flares and associated prominences of May 8, 1951. Times of photos as follows:

*(1) 15:08 U.T.	(2) 15:08 U.T.	(3) 15:14 U.T.
(4) 15:23 U.T.	(5) 15:28 U.T.	(6) 15:40 U.T.
(7) 15:46 U.T.	*(8) 15:47 U.T.	(9) 15:47 U.T.
(10) 15:54 U.T.	(11) 15:57 U.T.	(12) 16:03 U.T.

The photos marked * were narrow-band ($\frac{1}{2}$ A) flare patrol photographs. All others were made with a wide-band (4 A) filter. Features *A*, *B*, *C*, and *D* indicated in Fig. 1 are marked by corresponding letters here. (Courtesy Sacramento Peak Station of Harvard College Observatory.)

Feature A

$$x = -(1.2214 \pm 0.0094) \cdot \mathit{1} + (0.04116 \pm 0.0016) \cdot \boldsymbol{\varepsilon} + (0.001020 \pm 0.000096) \cdot (-\mathit{110} + 3\boldsymbol{\varepsilon}^2);^{9}$$

$$y = (2.4423 \pm 0.0081) \cdot \mathit{1} + (0.1426 \pm 0.0013) \cdot \boldsymbol{\varepsilon}.$$

Feature B

$$x = -(2.3258 \pm 0.0014) \cdot \mathit{1} - (0.00513 \pm 0.00018) \cdot \boldsymbol{\varepsilon} + (0.000108 \pm 0.000009) \cdot (-\mathit{182} + 3\boldsymbol{\varepsilon}^2);$$

$$y = (3.1563 \pm 0.0028) \cdot \mathit{1} + (0.12814 \pm 0.00036) \cdot \boldsymbol{\varepsilon}.$$

Feature C

$$x = -(0.0496 \pm 0.0037) \cdot \mathit{1} + (0.06163 \pm 0.00067) \cdot \boldsymbol{\varepsilon} - (0.00173 \pm 0.00014) \cdot (-\mathit{30} + \boldsymbol{\varepsilon}^2);$$

$$y = +(1.0062 \pm 0.0025) \cdot \mathit{1} - (0.03602 \pm 0.00046) \cdot \boldsymbol{\varepsilon} - (0.001814 \pm 0.000094) \cdot (-\mathit{30} + \boldsymbol{\varepsilon}^2) + (0.000176 \pm 0.000024) \cdot (-\mathit{44.83}^* \boldsymbol{\varepsilon} + \mathit{0.83}^* \boldsymbol{\varepsilon}^3).^{10}$$

Feature D

$$x = (1.0995 \pm 0.0069) \cdot \mathit{1} + (0.0588 \pm 0.0019) \cdot \boldsymbol{\varepsilon} - (0.00601 \pm 0.00056) \cdot (\boldsymbol{\varepsilon}^2 - \mathit{14}) + (0.0111 \pm 0.0010) \cdot (\mathit{0.16}^* \boldsymbol{\varepsilon}^3 - \mathit{4.16}^* \boldsymbol{\varepsilon});$$

$$y = (3.3692 \pm 0.0067) \cdot \mathit{1} - (0.15418 \pm 0.0018) \cdot \boldsymbol{\varepsilon} - (0.01226 \pm 0.00054) \cdot (\boldsymbol{\varepsilon}^2 - \mathit{14}) + (0.0112 \pm 0.0010) \cdot (\mathit{0.16}^* \boldsymbol{\varepsilon}^3 - \mathit{4.16}^* \boldsymbol{\varepsilon}).$$

In the above expressions all lengths, x and y, are expressed in inches of the projected image of the sun. To obtain the corresponding lengths on the sun in kilometers, multiply by 52,400.

ϵ represents the time. To convert the time, t (in seconds after 15:00 U. T.), into units of ϵ, use the following relations:

Feature A

$$\epsilon = \frac{t - 600}{15}.$$

Feature C

$$\epsilon = \frac{t - 810}{15}.$$

Feature B

$$\epsilon = \frac{t - 1077.5}{15}.$$

Feature D

$$\epsilon = \frac{t - 2050}{100}.$$

EXAMPLE: What is the x-co-ordinate of feature D at $15^h40^m50^s$?

ANSWER:

$40^m50^s = 2450^s$

with $t = 2450$, we obtain $\epsilon = 4$;

with $\epsilon = 4$ we obtain

$x = 1.2561$ inches

$= 65{,}814$ km.

Velocities and accelerations are easily derived from the above expressions.

[9] The italic numerals and boldface epsilon are the orthogonal polynomials.

[10] 0.83^* indicates $0.833333\ldots$, etc.

COMPTON SCATTERING BY ELECTRONS WITH A MAXWELLIAN DISTRIBUTION OF THERMAL VELOCITIES*

FRANK N. EDMONDS, JR.
Department of Applied Mathematics and Astronomy, University of Texas, Austin, Texas
Received October 16, 1952

ABSTRACT

The theory of the Compton effect is applied to the problem of scattering of radiation by electrons with a Maxwellian distribution of thermal velocities; and a spectral distribution function for scattered radiation is obtained in the second approximation. This function, equation (26), is asymmetric, and the frequency shift of scattered radiation corresponding to this asymmetry is given by

$$\frac{\nu - \nu'}{\nu'} = \frac{1 - \cos\theta}{m_0 c^2}(h\nu - 3kT),$$

where ν is the incident frequency, ν' the scattered frequency, θ the angle of scattering, and the other symbols have their usual meaning. The red shift in this expression is due to the Compton effect, while the blue shift is a result of the thermal motions of the electrons, as first pointed out by Dirac.

I. INTRODUCTION

The Compton effect in the scattering of radiation by electrons at rest produces an increase in wave length; and it has been shown,[1] using the methods of radiative-transfer theory, that this particular type of noncoherent scattering produces a red shift in the profile of a spectral line of the order of magnitude of the Compton wave length (0.024 A). In 1925 Dirac[2] extended the Compton theory for electron scattering to the problem of electrons with a Maxwellian distribution of thermal velocities and obtained the interesting result that, for sufficiently high temperatures and low frequencies, the red shift due to the Compton effect could be reduced or even changed to a blue shift by an additional effect resulting from the thermal motions. This effect may be explained qualitatively in terms of the intensity of incident radiation measured in a frame of reference moving with a scattering electron. Such an intensity, by its definition, will appear to be greater for electrons moving toward the incident radiation. Since the classical Thomson electron-scattering coefficient used by Dirac is frequency-independent, these electrons will perform a larger percentage of the scattering than electrons moving with the incident radiation, and so will give rise to a tendency to decrease the wave length in scattering. Dirac's result would indicate that in high-temperature stellar atmospheres, where the importance of scattering by free electrons is well recognized, blue shifts in the profiles of spectral lines may be expected.

In this paper the problem discussed by Dirac is re-examined for the purpose of determining whether the Klein-Nishina formula for electron scattering will change Dirac's results. To the second approximation no change is introduced by the Klein-Nishina formula. A somewhat different formulation of the problem is given, and the spectral distribution function obtained is defined differently, but the results obtained by Dirac are confirmed.

* A portion of the work reported was performed at the Laws Observatory, University of Missouri.

[1] S. Chandrasekhar, *Proc. R. Soc. London, A*, **192**, 508, 1948; R. C. O'Rourke, *Phys. Rev.*, **85**, 881, 1952.

[2] *M.N.*, **85**, 825, 1925.

II. COMPTON SCATTERING BY A MOVING ELECTRON

For dn electrons at rest, the Klein-Nishina coefficient for electron scattering[3] may be expressed in the following form:

$$d\mathfrak{j}_0(\nu_0', \theta)\, d\nu_0' d\omega_0' = I_0(\nu_0)\, d\nu_0 d\omega_0 dn \times \frac{e^4}{m_0 c^4} \tfrac{1}{2}(1+\cos^2\theta)\left[1+\frac{h\nu_0}{m_0 c^2}(1-\cos\theta)\right]^{-3} \times \left\{1+\frac{[(h\nu_0/m_0 c^2)(1-\cos\theta)]^2}{[1+\cos^2\theta][1+(h\nu_0/m_0 c^2)(1-\cos\theta)]}\right\} d\omega_0', \tag{1}$$

where $d\mathfrak{j}_0(\nu_0', \theta)d\nu_0' d\omega_0'$ is the energy of radiation scattered per unit time by the dn electrons into the frequency interval ν_0' to $\nu_0' + d\nu_0'$ and into the solid-angle increment $d\omega_0'$; θ is the angle of scattering; $I_0(\nu_0)d\nu_0 d\omega_0$ is the intensity of radiation incident upon the dn electrons within the frequency interval ν_0 to $\nu_0 + d\nu_0$ and within the solid-angle

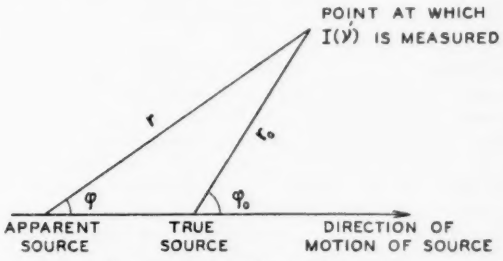

FIG. 1.—The two frames of reference

increment $d\omega_0$; m_0 is the mass of the electron; e is the charge of the electron; c is the velocity of light; and h is Planck's constant. The use of the subscript zero in equation (1) indicates that the various quantities concerned are measured in a frame of reference in which the electrons are at rest, and the prime refers to scattered radiation. The frequencies of the scattered and incident radiation differ in accordance with the Compton effect for an electron at rest,[4] the equation for which is

$$\frac{\nu_0}{\nu_0'} = 1 + \frac{h\nu_0}{m_0 c^2}(1-\cos\theta)\,. \tag{2}$$

To generalize equation (1) for electrons in motion will require the relativistic transformation of the expressions for incident and scattered radiation from a frame of reference in which the electrons are at rest to one in which they are in motion. It can be shown that $I_0(\nu_0)d\omega_0$ and ν_0 transform relativistically in the same manner;[5] and so

$$I_0(\nu_0)\, d\omega_0 = \frac{\nu_0}{\nu} I(\nu)\, d\omega\,, \tag{3}$$

[3] Cf. W. Heitler, *The Quantum Theory of Radiation* (Oxford: Clarendon Press, 1936), p. 156.

[4] Cf. G. Joos, *Theoretical Physics* (London: Blackie & Son, 1934), p. 649.

[5] This can be demonstrated by showing that the magnitude of the Poynting vector of a plane electromagnetic wave,

$$|\boldsymbol{S}| = I(\nu)\, d\nu d\omega\,,$$

transforms relativistically as ν^2 as a result of the transformations for the electric and magnetic field vectors. Since $d\nu$ transforms as ν, $I(\nu)d\omega$ transforms as ν. For discussions of relativistic transformations see Joos, *op. cit.*, chap. x, and Dirac, *Proc. R. Soc. London*, *A*, **106**, 583, 1924, and *M.N.*, **85**, 825, 1925.

where the quantities which do not bear the subscript zero are measured in the frame of reference in which the electrons are moving. The quantity $d\mathfrak{j}_0(\nu_0', \theta)$ will transform relativistically as those properties involved in its measurement. Now

$$d\mathfrak{j}_0(\nu_0', \theta)\, d\omega_0' = r_0^2 d\omega_0' I_0(\nu_0', \theta)\, d\omega_0', \tag{4}$$

where r_0 is the distance from where the intensity of the scattered radiation $I_0(\nu_0', \theta)$ is measured to the point source of $d\mathfrak{j}_0(\nu_0', \theta)$, namely, the location of the scattering electrons. In a frame of reference in which the true point source is moving, r_0 transforms to r, the distance to the apparent point source of radiation. The location of this apparent point source is the location of the true point source when it emitted the radiation.[6] Hence, for dn scattering electrons, the location of the true and apparent sources are as shown in Figure 1, and, from the law of sines,

$$\frac{r}{r_0} = \frac{\sin(\pi - \phi_0)}{\sin\phi} = \frac{\nu'}{\nu_0'}, \tag{5}$$

since $\sin\phi_0$ and $1/\nu_0'$ transforms in the same manner.

In determining the relativistic transformation of $I_0(\nu_0', \theta)d\omega_0'$, an additional effect must be considered which is due to the nature of the scattering. Consider one of the dn electrons which, in the frame of reference in which they are moving, will have the specified velocity v. This electron will have assumed this velocity as the result of a collision and will give it up as the result of the collision which follows. Hence this electron will belong to the group of electrons only for a finite time a/v, where a is the distance traveled between the two collisions. During this time the electron will emit a pulse of scattered radiation whose duration will differ slightly from the time interval a/v, because of the electron's motion. Radiation emitted at the start of the interval will have traveled a distance $a\cos\phi_0$, in addition to that traveled by radiation emitted at the end of the interval, giving rise to a pulse, of duration

$$\frac{a}{v} - \frac{a\cos\phi_0}{c}. \tag{6}$$

Hence the average intensity of scattered radiation during the time a/v will be[6]

$$1 - \frac{v}{c}\cos\phi_0 = \frac{\nu_0' m_0}{\nu' m} \tag{7}$$

times the intensity during the pulse. This means that the measured intensity of scattered radiation in a frame of reference in which the dn electrons are moving $I(\nu, \theta)d\omega'$ is equal to this factor times the pulse intensity $I_p(\nu', \theta)d\omega'$, which, in turn, transforms as ν'.[5] Therefore,

$$I(\nu', \theta)\, d\omega' = \frac{\nu_0' m_0}{\nu' m} I_p(\nu', \theta)\, d\omega' = \frac{m_0}{m} I_0(\nu_0', \theta)\, d\omega_0'. \tag{8}$$

Equations (4), (5), and (8) combine to give

$$d\mathfrak{j}_0(\nu_0', \theta) = \frac{m}{m_0}\left(\frac{\nu_0'}{\nu'}\right)^2 d\mathfrak{j}(\nu', \theta), \tag{9}$$

which is exactly equivalent to the result obtained by Dirac, using subtler but more direct arguments. Dirac shows[7] that the quantity $R(\nu')d\nu'd\omega'$ transforms relativistically

[6] Cf. Joos, *op. cit.*, p. 234.

[7] Cf. Dirac, *M.N.*, **85**, top of p. 828.

as m^{-1}, where

$$d\,\dot{\imath}\,(\nu',\ \theta) = h\nu' R\,(\nu')\,. \tag{10}$$

Since $d\nu' d\omega'$ transforms as $1/\nu'$, equation (9) follows directly. Substitution in equation (1) of equations (2), (3), (9) and the expression for $d\nu_0'/d\nu_0$ obtained from equation (2) gives, as the generalization of this equation for moving electrons,

$$d\,\dot{\imath}\,(\nu',\ \theta) = I\,(\nu)\,d\omega dn\,\frac{\nu'}{\nu}\,\frac{m_0}{m}\,\frac{\nu'}{\nu_0'}\,\frac{e^4}{m_0^2 c^4}\,\tfrac{1}{2}\,(1+\cos^2\theta) \times\left\{1+\frac{[(h\nu_0/m_0c^2)(1-\cos\theta)]^2}{[1+\cos^2\theta][1+(h\nu_0/m_0c^2)(1-\cos\theta)]}\right\}. \tag{11}$$

Let the x-axis of a Cartesian system of co-ordinates be the direction of the incident radiation, and the xy-plane be the plane of scattering. Then the frequencies of the scattered and incident radiation differ in accordance with the Compton effect and relativistic Doppler shifts resulting from the motion of the electron. Dirac[2] has obtained a relation for this difference which may be expressed in the following form:

$$\frac{\nu}{m_0 c}(m c - p_x) - \frac{\nu'}{m_0 c}(m c - p_x\cos\theta - p_y\sin\theta) = \frac{h\nu\nu'}{m_0 c^2}(1-\cos\theta)\,, \tag{12}$$

where p_x and p_y are the x- and y-components of the scattering electron's momentum. The first term of equation (12) represents the incident frequency "seen" by the scattering electron (i.e., the incident frequency corrected for the relativistic Doppler shift due to the electron's velocity along the x-axis). In a similar manner the second term represents the scattered frequency "seen" by the scattering electron; and so equation (12) effectively states that the difference between the incident and scattered frequencies in a frame of reference in which the scattering electron is at rest is that due to the Compton effect. The second term in equation (12) represents ν_0'; and so it follows that

$$\frac{\nu_0'}{\nu'} = \frac{1}{m_0 c}(m c - p_x\cos\theta - p_y\sin\theta)\,. \tag{13}$$

III. SCATTERING BY ELECTRONS WITH A MAXWELLIAN DISTRIBUTION OF THERMAL VELOCITIES

The relativistic Maxwellian distribution function normalized to N, the number of electrons per cubic centimeter, and in terms of the components of electron momentum may be expressed in the following form:[3]

$$dn = \frac{N}{(2\pi m_0 kT)^{3/2}}\left[1+\frac{15}{8}\frac{kT}{m_0c^2}+\frac{105}{128}\left(\frac{kT}{m_0c^2}\right)^2+\dots\right]^{-1} \times\exp\left\{\frac{-p^2}{2m_0kT}\left[1-\frac{p^2}{4m_0^2c^2}+\frac{p^4}{8m_0^4c^4}+\dots\right]\right\} dp_x dp_y dp_z\,, \tag{14}$$

where k is Boltzmann's constant, T is the absolute temperature, and

$$p^2 = p_x^2 + p_y^2 + p_z^2\,. \tag{15}$$

An expression for scattering by electrons with such a thermal distribution of velocities can be obtained by the substitution of equations (13) and (14) in equation (11) and

[3] Cf. S. Chandrasekhar, *An Introduction to the Study of Stellar Structure* (Chicago: University of Chicago Press, 1939), chap. x.

integrating over all values of momentum. Then, changing the variable of integration p_x to ν gives the following equation:

$$j(\nu', \theta)\, d\omega = \frac{2\pi N e^4 d\omega}{m_0^2 c^4} (1 + \cos^2 \theta) \int_0^\infty I(\nu)\, \psi(\nu', \theta, \nu)\, d\nu , \tag{16}$$

where $j(\nu', \theta)d\omega$ is the emission coefficient per cubic centimeter for radiation scattered into $d\omega$ and $\psi(\nu', \theta, \nu)$, the spectral distribution function for scattering of radiation by electrons with a Maxwellian distribution of velocities, is given by

$$\begin{aligned}\psi(\nu', \theta, \nu) = {} & \frac{1}{4\pi} (2\pi m_0 kT)^{-3/2} \left[1 + \frac{15}{8} \frac{kT}{m_0 c^2} + \frac{105}{128} \left(\frac{kT}{m_0 c^2} \right)^2 + \cdots \right]^{-1} \\ & \times \frac{\nu'}{\nu} \left\{ 1 + \frac{[(h\nu_0/m_0 c^2)(1 - \cos\theta)]^2}{[1 + \cos^2\theta][1 + (h\nu_0/m_0 c^2)(1 - \cos\theta)]} \right\} \\ & \times \int_{-\infty}^{+\infty} dp_y \int_{-\infty}^{+\infty} dp_z \frac{m_0}{m} \frac{\partial p_x}{\partial \nu} m_0 c\, (mc - p_x \cos\theta - p_y \sin\theta)^{-1} \\ & \times \exp \left\{ \frac{-p^2}{2 m_0 kT} \left[1 - \frac{p^2}{4 m_0^2 c^2} + \frac{p^4}{8 m_0^4 c^4} + \cdots \right] \right\} .\end{aligned} \tag{17}$$

In order to perform the integrations indicated in equation (17), the variables p_x, p^2, and

$$m = m_0 \left[1 + \frac{p^2}{2 m_0^2 c^2} - \frac{p^4}{8 m_0^4 c^4} + \cdots \right] \tag{18}$$

appearing in the integrand must be expressed in terms of the variables of integration, p_y and p_z and the variables ν', θ, and ν by use of equation (12).

IV. A SYSTEM OF SUCCESSIVE APPROXIMATIONS IN THE EVALUATION OF $\psi(\nu', \theta, \nu)$

In all cases of electron scattering of astrophysical interest,

$$\frac{h\nu}{m_0 c^2} < 10^{-5}, \qquad \frac{kT}{m_0 c^2} < 10^{-5} . \tag{19}$$

Hence, for $\overline{p^2}$, the mean value of p^2 for the Maxwellian distribution of velocities,

$$\frac{\overline{p^2}}{m_0^2 c^2} \simeq \frac{3\, kT}{m_0 c^2} < 3 \times 10^{-5} , \tag{20}$$

and for $\overline{(\nu - \nu')/\nu'}$, a value of $(\nu - \nu')/\nu'$ equal to the Doppler half-width produced by the Maxwellian distribution of velocities,

$$\left(\overline{\frac{\nu - \nu'}{\nu'}} \right) = \left(\frac{2\, kT}{m_0 c^2} \right)^{1/2} < 5 \times 10^{-3} . \tag{21}$$

Equations (19) can be used as criteria of order of magnitude in establishing a system of successive approximations for the evaluation of $\psi(\nu', \theta, \nu)$ as given by equation (17). Values of p^2 considerably larger than $\overline{p^2}$ are involved in integrations indicated in equation (17); but they will not contribute appreciably to the integrals, since they appear in a negative exponential, and $\overline{p^2}/2m_0 kT$ is approximately $\frac{3}{2}$. Therefore, equation (20) can also be used as a criterion of order of magnitude. Using equation (21) as a criterion will

not be valid in the wings of the spectral distribution function $\psi(\nu', \theta, \nu)$, i.e., for values of $(\nu-\nu')/\nu'$ considerably greater than $\overline{(\nu-\nu')/\nu'}$. However, as will be shown below, $\psi(\nu', \theta, \nu)$ is an exponential function of $(\nu-\nu')/\nu'$, and so inaccuracies in the wings resulting from the use of equation (21) as a criterion of order of magnitude may be neglected.

It is possible, therefore, to establish a system of successive approximations retaining terms of the order of magnitude of successive powers of

$$\left(\frac{kT}{m_0 c^2}\right)^{1/2} \simeq \left(\frac{h\nu}{m_0 c^2}\right)^{1/2} \simeq \frac{p}{m_0 c} \simeq \frac{\nu-\nu'}{\nu'} < 10^{-2}. \tag{22}$$

The exponential in equation (17) contains the coefficient $(2m_0kT)^{-1}$; and so for any given approximation it is necessary to retain terms in the exponential whose order of magnitude corresponds to a power of equation (22) equal to 2 plus the corresponding power for terms retained in other factors in equation (17). In the first approximation, therefore, terms in equation (17) of the order of magnitude of the first power of equation (22) or smaller are neglected, except in the exponential, where terms of the order of magnitude of the third power or smaller are neglected. In the second approximation the powers of equation (22) which act as criteria for neglecting terms are fourth in the exponential and second elsewhere, and criteria for higher approximations may be stated in a similar manner.

Examination of equation (17) in the first three approximations shows that frequency shifts in scattering because of thermal velocities of the electrons are accounted for in the first and higher approximations. However, frequency shifts due to the Compton effect are accounted for only in the second and higher approximations, while effects due to the relativistic change in mass of the electron, to deviation of the Klein-Nishina formula for electron scattering from the Thomson scattering coefficient, and to the relativistic correction to the Maxwellian distribution function appear only in the third and higher approximations.

Evaluation of the integrals in equation (17) in the first approximation gives an expression for $\psi(\nu', \theta, \nu)$ in agreement with the results obtained by Dirac,[2] namely, a symmetric, exponential function of $(\nu-\nu')/\nu'$.

V. EVALUATION OF $\psi(\nu', \theta, \nu)$ IN THE SECOND APPROXIMATION

Equations (12), (15), and (18) can be used to obtain the following second-approximation expressions:

$$\frac{m_0}{m}\frac{\partial p_x}{\partial \nu} m_0 c\,(m c - p_x \cos\theta - p_y \sin\theta)^{-1} = \frac{m_0 c}{\nu'(1-\cos\theta)}\left[1-\left(\frac{2-\cos\theta}{1-\cos\theta}\right)\left(\frac{\nu-\nu'}{\nu}\right)\right] \tag{23}$$

and

$$\frac{p^2}{m_0^2 c^2} = \frac{p_z^2}{m_0^2 c^2} + \frac{1}{B^2+\sin^2\theta}\left\{\frac{\nu-\nu}{\nu'} - \frac{h\nu}{m_0 c^2}(1-\cos\theta)\right\}^2 + \frac{B^2+\sin^2\theta}{B^2}\left\{\frac{p_y}{m_0 c} + \frac{\sin\theta}{B^2+\sin^2\theta}\left[\frac{\nu-\nu'}{\nu'} - \frac{h\nu}{m_0 c^2}(1-\cos\theta)\right]\right\}^2, \tag{24}$$

where

$$B = 1-\cos\theta+\frac{\nu-\nu'}{\nu'}. \tag{25}$$

Equation (24) has not been cleared of all third-approximation terms, but, when substituted along with equation (23) in equation (17), it is in a convenient form for the

integrations over p_ν and p_ε. When those integrations indicated in equation (17) are accomplished and equation (25) is substituted in the result, the following second-approximation expression for $\psi(\nu', \theta, \nu)$ is obtained:

$$\psi(\nu', \theta, \nu) = \frac{m_0 c}{4\pi} [4\pi m_0 kT(1-\cos\theta)]^{-1/2} \frac{1}{\nu} \left[1 - \frac{3}{2}\left(\frac{\nu-\nu'}{\nu'}\right)\right] \times \exp\left\{\frac{-m_0 c^2}{4kT(1-\cos\theta)} \left[\frac{\nu-\nu'}{\nu'} - \frac{h\nu}{m_0 c^2}(1-\cos\theta)\right]^2 \left[1+\frac{\nu-\nu'}{\nu'}\right]^{-1}\right\}. \quad (26)$$

For convenience in differentiating and integrating equation (26), certain third-approximation terms have been retained in the exponential. Integration of $\psi(\nu', \theta, \nu)$ over all values of ν and θ shows that, to the second approximation, it is normalized to unity.

The second-approximation expression for $\psi(\nu', \theta, \nu)$ is not symmetric in $(\nu'-\nu)/\nu'$;

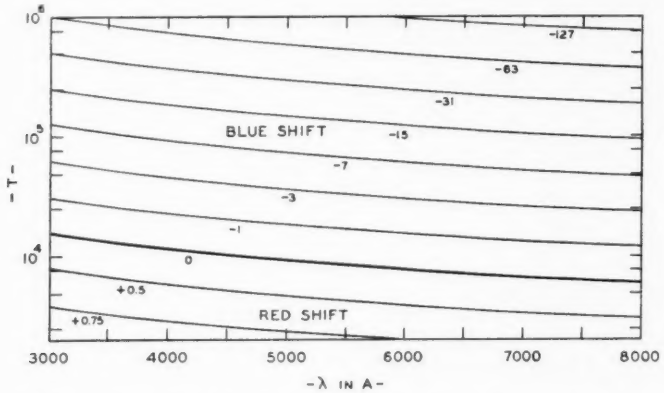

FIG. 2.—The wave-length shift $(\lambda' - \lambda)/\lambda_0(1 - \cos\theta)$ as given by equation (28) and expressed in units of λ_0, the Compton wave length (0.024 A). This shift is plotted for various values of wave length λ (in angstrom units) and absolute temperature T and is produced by the asymmetry of the special distribution function $\psi(\nu', \theta, \nu)$ as given by equation (26) in the second approximation.

and so an effective shift in frequency is given to radiation scattered by electrons in accordance with equation (26). This shift can be calculated by setting

$$\frac{\partial\psi(\nu', \theta, \nu)}{\partial\nu'} = 0, \quad (27)$$

which requires that

$$\frac{\nu-\nu'}{\nu'} = \frac{\lambda'-\lambda}{\lambda'} = \frac{1-\cos\theta}{m_0 c^2}(h\nu - 3kT), \quad (28)$$

where λ and λ' are the wave lengths corresponding to ν and ν'. The $(h\nu/m_0c^2)(1 - \cos\theta)$ term in equation (28) represents the red shift due to the Compton effect.[4] The $-(3kT/m_0c^2)(1 - \cos\theta)$ term represents the blue shift which results from thermal motions of the electrons and is discussed in Section I above. In Figure 2 the resultant shifts predicted by equation (28) are plotted for ranges of temperature and wave length of astrophysical interest.

The frequency and temperature dependence of the shift given by equation (28) should

aid in its isolation from other shifts of spectral lines in stellar atmospheres. However, except for very high temperatures, the magnitude of this shift is so small (of the order of the Compton wave length) as to present serious problems of detection. Furthermore, the spectral lines of higher-temperature stars are quite broad, while the optical thickness of free electrons in the atmospheres of cooler stars is quite small. As shown in Figure 2, for very high temperatures the shift to the blue is of the order of magnitude of 1 A, which may slightly reduce detection problems in Wolf-Rayet atmospheres or in the solar corona. A satisfactory discussion of detection, however, must await a quantitative determination of the expected shifts for various stellar atmospheres, which will be forthcoming.

With great pleasure I acknowledge my indebtedness to Dr. S. Chandrasekhar for suggesting this problem, for advice concerning it, and for making available to me correspondence from P. A. M. Dirac which clarified certain points considerably. I also wish to express my appreciation to Drs. George H. Vineyard and W. Roy Utz for helpful discussions.

CONVECTIVE CORES IN STARS*

PETER NAUR
Yerkes Observatory, Copenhagen Observatory, p.t., Watson Scientific Computing Laboratory
AND
DONALD E. OSTERBROCK
Princeton University Observatory
Received November 10, 1952

ABSTRACT

A necessary condition for the occurrence of a convective core in a star is derived. It is shown that late G dwarfs, K dwarfs, and M dwarfs, probably including the sun, cannot have convective cores but must be in radiative equilibrium at their centers. Main-sequence stars of somewhat earlier type may or may not have convective cores, while dwarfs earlier than F5 are already known to have convective cores.

It is now generally supposed that the proton-proton reaction is the mechanism by which energy is generated in the interiors of red dwarf stars.[1] The rate of energy production by this reaction varies much more slowly with temperature than does the rate of energy production by the carbon cycle, which is the energy source in early-type dwarfs.

TABLE 1

TEMPERATURE EXPONENT IN POWER LAW FOR RATE OF ENERGY PRODUCTION BY PROTON-PROTON REACTION

T	ν	T	ν
8×10^6	4.94	14×10^6	3.99
10×10^6	4.54	16×10^6	3.78
12×10^6	4.23		

These early-type dwarfs, as a result of the strong concentration of the energy sources toward their centers, do have convective cores.[2] However, in later-type dwarfs in which the energy generation is much less concentrated toward the center, the question of whether or not there are central convective cores is still an open one.[3] Cowling's paper on convective cores[2] does not cover the range of opacity laws and energy-generation laws now known to be of interest in red dwarf stars.

A convenient interpolation formula for the rate of energy production by the proton-proton reaction is

$$\epsilon = \epsilon_0 \rho T^\nu . \tag{1}$$

Values of the exponent ν for temperatures at which the proton-proton reaction may be expected to dominate the energy-production rate are listed in Table 1. For the sake of

* This work was supported in part by funds of the Eugene Higgins Trust allocated to Princeton University.

[1] B. Strömgren, *A.J.*, **57**, 65, 1952 (sec. A2) and references given there. In a paper by L. H. Aller, J. W. Chamberlain, E. M. Lewis, W. C. Liller, J. K. McDonald, W. H. Potter, and N. E. Weber, *Ap. J.*, **115**, 328, 1952, it has been shown that the computed energy production in a star like Krüger 60 A always comes out too high, irrespective of the assumed chemical composition, if the calculation is based on the usually adopted model and expression for the proton-proton energy production. However, it has been suggested that an extensive outer convection zone in these stars may reduce the central temperature and the energy content sufficiently for solutions with the proper energy production to be obtained. This question is now being investigated by one of the authors (Donald E. Osterbrock).

[2] T. G. Cowling, *M.N.*, **94**, 768, 1934.

[3] I. Epstein, *Ap. J.*, **114**, 438, 1951.

complete generality, we shall use, instead of equation (1), the energy-generation law,

$$\epsilon = \epsilon_0 \rho^{\delta} T^{\nu} , \tag{2}$$

setting $\delta = 1$ in the applications to stars.

A general interpolation formula for the opacity can be written in the form

$$\kappa = \kappa_0 \rho^{1-a} T^{-3-s} . \tag{3}$$

The case of the Kramers opacity law is, in this notation, $a = 0$, $s = 0.5$, while pure electron-scattering opacity corresponds to $a = 1, s = -3.0$. For the M dwarfs it appears that $\kappa \propto \rho^{0.5} T^{-3.5}$ is the best approximation, if the composition is such that free-free transitions in hydrogen and helium can be neglected;[4, 5] and we shall therefore also discuss the "red dwarf" case, $a = 0.5$, $s = 0.5$.

Furthermore, the assumption will be made that the chemical composition of a red dwarf star is the same throughout the star. The luminosity of these stars is so low that there has been no appreciable amount of hydrogen transformed into helium in 3×10^9 years, and the assumption of homogeneity of composition should be a good approximation. It is furthermore assumed that radiation pressure is negligible in comparison with gas pressure.

The problem of the existence or nonexistence of a central convective zone in red dwarf stars will be approached by finding the conditions under which there cannot be such a core. For deriving such a condition, it is convenient to use, besides the ordinary homology-invariant quantities,[6]

$$U = \frac{d \log M_r}{d \log r} , \qquad V = -\frac{d \log P}{d \log r} , \qquad n+1 = \frac{d \log P}{d \log T} , \tag{4}$$

the additional homology invariant

$$W = \frac{d \log L_r}{d \log r} . \tag{5}$$

Since we assume no discontinuity in chemical composition, all these homology invariants must be continuous through the star.

Now suppose an attempt is made to construct a model of a star with a convective core, integrating from the center outward. At each point in the core the condition that the radiative gradient actually is unstable and that convective equilibrium does exist is

$$\left(\frac{d \log P}{d \log T}\right)_{\text{rad}} = (n+1)_{\text{rad}} \leqslant 2.5 . \tag{6}$$

We refer here to the value which the polytropic index would have if the matter were in radiative equilibrium at the particular point considered, although in the core the true polytropic index of the structure is $(n+1)_{\text{conv}} = 2.5$. Outside the convective core $(n+1)_{\text{rad}}$ is the true polytropic index and is greater than 2.5, and just at the boundary of the core $(n+1)_{\text{rad}} = 2.5$. Therefore, we deduce that at the boundary of the convective core $(n+1)_{\text{rad}}$ is larger than at any point within the core. Hence a necessary condition that a radiative envelope can be fitted to a convective core at a particular point is that at the assumed boundary $(n+1)_{\text{rad}}$ is greater than at any other point within the core. In particular, therefore, the gradient of $(n+1)_{\text{rad}}$ must be positive at the assumed

[4] J. B. Oke, *J.R.A.S. Canada*, **44**, 135, 1950.

[5] Aller *et al.*, *op. cit.*

[6] See S. Chandrasekhar, *An Introduction to the Study of Stellar Structure* (Chicago: University of Chicago Press, 1938), chap. iv.

boundary, and so the condition that it be possible to fit a radiative envelope to a convective core with a particular radius may be expressed in the simple form

$$D \equiv \frac{d \log (n+1)_{\text{rad}}}{d \log r} \geqslant 0 \tag{7}$$

at the radius in question. In terms of the homology invariants U, V, and W, and the exponents defined by equations (2) and (3) this relation becomes

$$D = U - W - (1.2 + 0.4\,s + 0.6\,a)\,V \geqslant 0\,. \tag{8}$$

This equation does not contain ν and δ explicitly, and, in fact, its derivation does not depend on the energy generation being given by a power law such as equation (2). However, the energy-generation law enters through the values of W.

To apply condition (8), the values of U and V at any assumed boundary of the convective core can be read off from the tabulated solution[7] of the Lane-Emden equation of

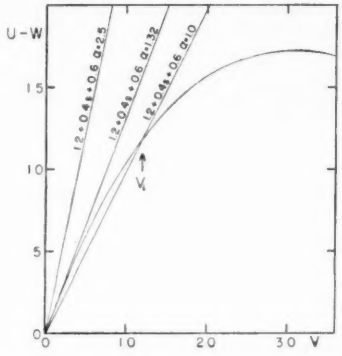

FIG. 1.—Graph of $U - W$ (for the energy-generation law $\epsilon = \epsilon_0 \rho T^4$) as a function of V, together with straight lines for various opacity laws.

index $n = 1.5$, while for a law of energy generation of the form given in equation (2) the values of W are given in terms of the Lane-Emden variables by

$$W = \frac{\xi^3 \theta^{\nu+3\delta/2+3/2}}{\int_0^{\xi} \xi^2 \theta^{\nu+3\delta/2+3/2} d\xi}\,. \tag{9}$$

This function is being computed for a number of values of $\nu + \frac{3}{2}\,\delta$ by Peter Naur at the Watson Scientific Computing Laboratory and will be published elsewhere.

With the values of U, V, and W thus obtained, we may now apply condition (8). Let us plot the quantity $U - W$ as a function of V (see Fig. 1, which corresponds to the case $\epsilon = \epsilon_0 \rho T^4$). The quantity $U - W$ is zero at the center and at the surface of the star. Going outward from the center, W drops off more rapidly than U, so that $U - W$ is an increasing function of V near the center. Let us further plot on the same diagram the straight line through the origin with slope $1.2 + 0.4\,s + 0.6\,a$ (see Fig. 1 for three particular opacity laws). The difference in height between the $U - W$ curve and this straight line is, according to equation (8), the value of D for the opacity law defined by these

[7] British Association for the Advancement of Science, *Mathematical Tables*, Vol. II (1932).

values of s and α. The value of D is positive whenever the $U - W$ curve lies above the straight line. The diagram shows that the straight lines through the origin will intersect the $U - W$ curve once, at most, apart from the intersection at the origin. For values of V smaller than the value at the intersection, V_i, D will be positive, $(n+1)_{\text{rad}}$ will increase monotonically from the center up to V, and here a radiative envelope can be fitted to the convecti.e core. For values of V larger than V_i, $(n+1)_{\text{rad}}$ will decrease, and no radiative envelope can be fitted. The point V_i thus gives an upper limit to the extent of a possible convective core. For opacity laws corresponding to lines which do not intersect the $U - W$ curve except at the origin, $(n+1)_{\text{rad}}$ will decrease monotonically from the center, and no model with a convective core and a radiative envelope can be constructed. The discriminatory case is the one in which the line is tangent to the $U - W$ curve at the origin, corresponding to zero as the upper limit of the extent of the core.

The slope of the $U - W$ curve at the origin can easily be found from the expansion of the Lane-Emden function to be

$$\left(\frac{d\,(U-W)}{dV}\right)_{V=0} = \frac{6}{25}\nu + \frac{9}{25}\,\delta\,. \tag{10}$$

Comparing this with the straight line with the slope $(1.2 + 0.4s + 0.6\,\alpha)$, we see that the condition that a convective core be possible at all is

$$6\nu + 9\delta > 15\alpha + 10s + 30\,, \tag{11}$$

or with $\delta = 1$, the usual physical case,

$$6\nu - 10s - 15\alpha > 21\,. \tag{12}$$

This necessary condition for the existence of a convective core supplements Cowling's criterion,[2] which is a sufficient condition. For the cases investigated by Cowling we find, in fact,

(i) κ is constant, $\epsilon \propto T^{\nu}$,
Convection impossible if $\nu < 2.5$ (condition [11]),
Convection certain if $\nu > 3$ to 4 (Cowling).

(ii) $\kappa \propto \rho T^{-3.5}$, $\epsilon \propto T^{\nu}$,
Convection impossible if $\nu < 5\frac{5}{6}$ (condition [11]),
Convection certain if $\nu > 7$ to 8 (Cowling).

In red dwarf stars the opacity is due to photoionization processes, with possibly some contribution from the free-free transitions in hydrogen and helium. These free-free transitions give an opacity of the Kramers form, and the total opacity will therefore correspond to a value of α between 0 and 0.5, while $s = 0.5$. The temperature dependence of the proton-proton reaction in these stars corresponds to an exponent $\nu = 4.5$. Now with $\nu = 4.5$ and $s = 0.5$ condition (12) shows that it is necessary that $\alpha < 0.07$ for any convective core to be possible, while the actual value of α certainly must be larger than this for any reasonable metal abundance. The conclusion may therefore be drawn that these stars do not have convective cores; they are in radiative equilibrium at their centers. The possibility that they may have large external convective zones—hydrogen convection zones extending far down into their interiors[8]—cannot be discussed by the above argument.

Even in the case of the sun, the existence of a convective core is not certain.[3] For the present discussion the values of the physical quantities given in Epstein's solar model[3]

[8] B. Strömgren, *Mat. Tidsskr.* (Copenhagen), 1950, B, p. 96.

will be used. At the inner edge of the radiative envelope one finds, directly from its definition (eq. [5]), $W = 2.16$. The opacity is a result of a combination of both electron scattering and photoionization processes, but near the boundary of the envelope it has the approximate dependence $\kappa \propto \rho^{0.25} T^{-1.46}$, corresponding to $a = 0.75$, $s = -1.54$. Now, if the above value of W and likewise the value of U and V at the inner edge of the radiative envelope are taken as the correct values for the boundary of the core, with $n + 1 = 2.5$, one finds $D = +0.06$, which would still leave the possibility of a convective core open. It should, however, be remarked that the opacity expression used by Epstein does not include the effect of free-free transitions in hydrogen and helium. A rough estimate indicates that this contribution probably will change the exponents in the effective opacity law to such an extent that condition (12) will not be satisfied, and that there consequently cannot be a convective core in the sun.

Therefore, the conclusion may be drawn that late G dwarfs, K dwarfs, and M dwarfs cannot have convective cores. Main-sequence stars earlier than F5 produce their energy by the carbon cycle[9] and therefore certainly do have convective cores. In the range of spectral types between these limits the existence or nonexistence of a core can be settled only by computation of specific models.

We wish to thank Professors Bengt Strömgren and Martin Schwarzschild for many stimulating and interesting discussions. One of us (Peter Naur) wishes to thank Ole Rømer Fondet, Copenhagen, and the International Astronomical Union for support while this work was carried out.

[9] B. Strömgren, *A.J.*, **57**, 65, 1952 (sec. A3).

ON THE SUN'S INTERIOR*

I. EPSTEIN AND L. MOTZ
Rutherfurd Observatory, Columbia University
Received October 20, 1952

ABSTRACT

A revised model interior for the sun is calculated, with an improved value for the rate of energy generation through the proton-proton reaction. It is found that the observed values of the radius, mass, and luminosity may be obtained if one squeezes the helium content to zero. The composition parameters for this equilibrium model are $X = 99.8$ per cent, $Z = 0.2$ per cent. The central temperature of this model is 12,000,000°, while its density is 110. The upper limit for a possible convective core is 8 per cent of the radius. Such a core could not include more than 3 per cent of the mass, nor could more than 24 per cent of the total energy be generated there. The proton-proton reaction provides all the energy generation in this model.

I. INTRODUCTION

A model interior for the sun had previously been calculated,[1] in which the source of energy generation was a combination of the proton-proton reaction and the carbon cycle. Since the publication of the investigation cited, several investigators have discovered the need for a revision of the coefficient of the energy-generation law for the proton-proton reaction.[2] The present investigation is a recalculation of the equilibrium state of the sun, using this new coefficient. The assumptions and methods employed in this investigation are identical with those used in the paper "A Two-Energy Source Solar Model,"[1] the only difference being that ϵ_p is now given by the following expression:

$$\log \epsilon_p = \log \left\{ \frac{3.82}{100} \left(\frac{X}{0.316} \right)^2 \left(\frac{1}{15 \times 10^6} \right)^4 \left(\frac{\mu H}{k} \right) \right\} + \sigma + 3\tau .$$

II. SOLUTION

Three series of integrations were performed at each of three fixed values of either X or Y, and an attempt was made to find the composition for which ΔM and ΔL vanished simultaneously at some convenient fitting point. It was discovered that one could get a luminosity fit and a mass fit simultaneously to within one part in a thousand if one drove the helium content to zero. Table 1 gives the results of three luminosity-fit models.

TABLE 1

LUMINOSITY-FIT MODELS

(X, Y)-Pair	ΔM
$X = 0.9700$, $Y = 0.0276$	$+0.008 \times 10^{33}$
$X = .9850$, $Y = 0.0127$	$+ .006 \times 10^{33}$
$X = 0.9980$, $Y = 0.0000$	$+0.002 \times 10^{33}$

It is obvious that one is forced to eliminate the entire helium content in order to attain a nearly satisfactory model for the sun, and, even then, a mass discrepancy of one part in a thousand remains.

Table 2 gives the adopted solutions for the equilibrium values $X_0 = 0.99795$, $Z_0 =$

* This work was supported in part by a contract with the Office of Naval Research, Nonr-266(19).

[1] I. Epstein, *Ap. J.*, **114**, 438, 1951.

[2] E. Frieman and L. Motz, in press; E. E. Salpeter, in press.

0.00205. Because of the increased rate of the proton-proton reaction, there is no contribution whatever from the carbon cycle.

Although the composition parameters are determined with a high degree of formal accuracy by this procedure, the model itself is not. Thus a slight lack of fit in either M_r or L_r may be reflected in a much larger discrepancy in the run of the physical variables U, V, and $n+1$ near the fitting point. The best compromise possible in our adopted model was to attach a convective core at the value of $n+1 = 2.75$ rather than the rigorous value of 2.50.

We are continuing these investigations by revising our opacity laws with particular emphasis on the inclusion of free-free transitions of hydrogen. Qualitative considerations indicate that inclusion of this source of opacity will allow a nonnegligible amount of helium in the model.

TABLE 2

A. ADOPTED SOLUTION FOR THE RADIATIVE ENVELOPE OF THE SUN

log r	log P	log T	log M_r	log L_r	log ρ	U	V	$(n+1)$	log κ_1/κ_e*
10.78	11.35	5.63	33.30	33.58	−2.50	0.00	31.16	4.10	+0.87
10.74	12.33	5.87	33.30	33.58	−1.75	0.02	19.75	4.14	+0.84
10.70	13.01	6.03	33.30	33.58	−1.24	0.05	14.78	4.14	+0.81
10.66	13.54	6.16	33.29	33.58	−0.84	0.09	11.98	4.13	+0.79
10.62	13.98	6.27	33.29	33.58	−0.50	0.15	10.16	4.11	+0.77
10.58	14.36	6.36	33.28	33.58	−0.22	0.22	8.86	4.09	+0.75
10.54	14.70	6.44	33.27	33.58	+0.04	0.31	7.86	4.07	+0.74
10.50	14.99	6.52	33.26	33.58	+0.26	0.40	7.04	4.04	+0.72
10.46	15.26	6.58	33.24	33.58	+0.46	0.50	6.36	4.00	+0.28
10.42	15.51	6.62	33.22	33.58	+0.68	0.66	6.09	6.09	+0.28
10.38	15.75	6.66	33.19	33.58	+0.87	0.83	5.66	5.19	+0.24
10.34	15.96	6.70	33.15	33.58	+1.04	1.03	5.15	4.70	+0.19
10.30	16.16	6.75	33.10	33.58	+1.19	1.23	4.61	4.41	+0.12
10.26	16.33	6.79	33.05	33.57	+1.33	1.43	4.08	4.18	+0.05
10.22	16.48	6.83	33.00	33.57	+1.44	1.63	3.56	3.98	−0.03
10.18	16.62	6.86	32.92	33.56	+1.54	1.81	3.08	3.78	−0.10
10.14	16.73	6.89	32.84	33.54	+1.62	1.98	2.64	3.59	−0.16
10.10	16.83	6.92	32.76	33.52	+1.69	2.14	2.25	3.48	+0.13
10.06	16.91	6.94	32.67	33.49	+1.75	2.28	1.90	3.39	+0.07
10.02	16.98	6.96	32.58	33.45	+1.80	2.40	1.60	3.27	+0.02
9.98	17.04	6.98	32.48	33.40	+1.84	2.50	1.34	3.20	−0.16
9.94	17.09	7.00	32.38	33.35	+1.88	2.60	1.13	3.42	−0.19
9.90	17.13	7.01	32.27	33.28	+1.91	2.69	0.94	3.24	−0.21
9.86	17.16	7.02	32.17	33.21	+1.93	2.77	0.78	3.08	−0.23
9.82	17.19	7.03	32.05	33.13	+1.95	2.85	0.65	2.95	−0.25
9.78	17.22	7.04	31.94	33.04	+1.96	2.92	0.54	2.89	−0.26
9.74	17.24	7.04	31.82	32.95	+1.98	2.99	0.44	2.75	−0.28

* In the column headed "log κ_1/κ_e," κ_T is not the electron scattering itself but 1.5 times this value, provided that the opacity arising from photoelectric ionizations exceeds the electron-scattering opacity. This is true for log $r \geq 10.14$. For log $r < 10.14$, the electron scattering dominates and the value κ_1 is 1.5 times the photoelectric ionization opacity.

B. VALUES AT CENTER OF CONVECTIVE CORE ATTACHED TO RADIATIVE ENVELOPE AT LOG $r_f = 9.74$

log P_c	log T_c	log ρ_c	U	V	$(n+1)$
17.34	7.08	2.04	3.00	0.00	2.50

Out of My Later Years

by

ALBERT EINSTEIN

THIS IS THE FIRST new collection of papers, since 1936, by the eminent physicist. A considerable number of these essays have never been published before in any language.

FROM THE CONTENTS

The Theory of Relativity — $E=MC^2$
Time, Space and Gravitation
Physics and Reality
The Fundaments of Theoretical Physics
The Common Language of Science
The Laws of Science and the Laws of Ethics
An Elementary Derivation of the Equivalence of Mass and Energy
Science and Civilization
A Message to Intellectuals
A Reply to Soviet Scientists
Atomic War or Peace
Military Intrusion in Science
Isaac Newton — Johannes Kepler
Marie Curie — Max Planck
Paul Langevin — Walther Nernst
Paul Ehrenfest

$4.75

PHILOSOPHICAL LIBRARY

Publishers

15 E. 40th St., Desk 558 New York 16, N.Y.

(Expedite shipment by enclosing remittance)

New Model

35-mm. EXAKTA "VX"

Single Lens Reflex Camera

One lens both for viewing and picture taking assures perfect sharpness, accurate exposure, maximum depth of field, and correct composition for color. You always see the exact image before you take the picture —whether the subject is an inch or a mile away, whether it is microscopic or gigantic, whether it is moving or stationary. Instantly interchangeable lenses permit telephoto, wide angle, close-up, copy and microscope photography. With f2.8 Zeiss Tessar "T" Coated Lens with Pre-Set Diaphragm Control.....$279.80 tax included

Write Dept. 1100 For Free Booklet "K"

NATURE PHOTOGRAPHY WITH MINIATURE CAMERAS by Alfred M. Bailey (Denver Museum of Natural History). This eminent explorer and scientist displays his finest Exakta photographs and others along with explanatory material. 35 full page photographs. 64 pages.....50c

EXAKTA CAMERA COMPANY

46 W. 29th St. New York 1, N.Y.

THE ASTROPHYSICAL JOURNAL

announces the publication in early summer of

A GENERAL INDEX, Volumes 76–100

Price: $5.00*

PREPUBLICATION ORDERS NOW ACCEPTED

Also available:

GENERAL INDEX, Volumes 1–25 .....$2.50
GENERAL INDEX, Volumes 26–50 .....$2.50
GENERAL INDEX, Volumes 51–75 .....$2.50

* Postage $0.15 per copy extra to foreign addresses.

THE UNIVERSITY OF CHICAGO PRESS

5750 ELLIS AVENUE CHICAGO 37 • ILLINOIS

Announcing . . .

Astrophysics

THE ATMOSPHERES OF THE SUN AND STARS

by LAWRENCE H. ALLER

Associate Professor of Astronomy, University of Michigan

A NEW WORK covering both the fundamentals and the major modern developments concerning the atmospheres of the sun and stars and solar-terrestrial relationships. A brief astronomical introduction is followed by a presentation of the background in physics necessary for a study of interstellar relationships—including atomic structure and spectra; gas laws and velocity distribution; ionization; excitation; dissociation of atoms and molecules; and selected aspects of radiation theory. In subsequent chapters these astrophysical principles are applied to the radiation of the sun and stars, to their continuous and dark-line spectra, to solar phenomena, and to solar-terrestrial relationships.

The book shows how each principle or important formula is put to use in solving some definite numerical problem concerned with the interpretation of the stars and nebulae.

CONTENTS:

SURVEY OF THE BASIC DATA. THE SPECTRA OF ATOMS AND MOLECULES. THE GAS LAWS AND THE EQUATIONS OF STATE; TURBULENCE. EXCITATION, IONIZATION, AND DISSOCIATION. THE EMISSION AND ABSORPTION OF RADIATION. THE RADIATION OF THE STARS. THE CONTINUOUS SPECTRA OF THE SUN AND STARS. THE FRAUNHOFER SPECTRUM. SOLAR PHENOMENA.

Approximately 450 pages, 117 illustrations, $12

PRE-PUBLICATION PRICE *(until April 15, 1953)*: $10.50

Order direct from

THE RONALD PRESS COMPANY 15 E. 26th St., New York 10